VÂNIA APARECIDA TERRA MALACHIAS

MECANISMOS DE AÇÃO DO ÓXIDO NÍTRICO EM MODELO EXPERIMENTAL DE IRRADIAÇÃO UVB NA PELE DE MURINOS

Londrina
2013

VÂNIA APARECIDA TERRA MALACHIAS

MECANISMOS DE AÇÃO DO ÓXIDO NÍTRICO EM MODELO EXPERIMENTAL DE IRRADIAÇÃO UVB NA PELE DE MURINOS

Tese apresentada ao Programa de Pós-Graduação em Patologia Experimental da Universidade Estadual de Londrina, como requisito à obtenção do título de Doutora em Patologia Experimental.

Orientadora: Profª Drª Alessandra Lourenço Cecchini Armani.

Londrina
2013

Catalogação na publicação elaborada pela Divisão de Processos Técnicos da Biblioteca Central da Universidade Estadual de Londrina

Dados Internacionais de Catalogação-na-Publicação (CIP)

M236m Malachias, Vânia Aparecida Terra.
Mecanismos de ação do óxido nítrico em modelo experimental de irradiação UVB na pele de murinos / Vânia Aparecida Terra Malachias. – Londrina, 2013.
138 f. : il.

Orientador: Alessandra Lourenço Cecchini Armani.
Tese (Doutorado em Patologia Experimental) – Universidade Estadual de Londrina, Centro de Ciências Biológicas, Programa de Pós-Graduação em Patologia Experimental, 2013.
Inclui bibliografia.

1. Patologia experimental – Teses. 2. Pele – Efeito da radiação – Teses. 3. Estresse oxidativo – Teses. 4. Radicais livres – Teses. 5. Óxido nítrico – Teses. 6. Células – Proliferação – Teses. 7. Camundongo como animal de laboratório – Teses. I. Armani, Alessandra Lourenço Cecchini. II. Universidade Estadual de Londrina. Centro de Ciências Biológicas. Programa de Pós-Graduação em Patologia Experimental. III. Título.

CDU 616-092

VÂNIA APARECIDA TERRA MALACHIAS

MECANISMOS DE AÇÃO DO ÓXIDO NÍTRICO EM MODELO EXPERIMENTAL DE IRRADIAÇÃO UVB NA PELE DE MURINOS

Tese apresentada ao Programa de Pós-Graduação em Patologia Experimental da Universidade Estadual de Londrina, como requisito à obtenção do título de Doutora em Patologia Experimental.

BANCA EXAMINADORA

_____
Orientadora: Profa Dra Alessandra Lourenço Cecchini Armani
Universidade Estadual de Londrina - UEL

_____
Profa Dra Leandra Naira Zambelli Ramalho
Universidade de São Paulo - USP

_____
Profa Drº Marco Andrey Cipriani Frade
Universidade de São Paulo - USP

_____
Profº Dr Rodrigo Cabral Luiz
Universidade Estadual de Londrina - UEL

_____
Profa Drº Rubens Cecchini
Universidade Estadual de Londrina - UEL

Londrina, 14 de junho de 2013.

AGRADECIMENTOS

À Drª. Alessandra Lourenço Cecchini Armani, pela imprescindível orientação durante a realização deste trabalho. Ao professor Dr. Rubens Cecchini, pelos vastos conhecimentos compartilhados.

À Drª. Leandra Ramalho, Dr. Marco Andrey Cipriani Frade, Dr. Rodrigo Ruiz pela parceria, colaboração, apoio e interesse pelo meu trabalho que contribuíram com a minha formação acadêmica. Ao Dr. Jair Tonon pela disponibilidade e troca de conhecimento.

À Dr[a]. Flávia Alessandra Guarnier pela colaboração e participação como membro da banca no exame de qualificação. Ao Jesus Antônio Vargas pela excelente assistência técnica prestada.

Aos meus pais Deonízia e Miguel, por terem me proporcionado minha formação, pelos bons exemplos e ensinamentos. Ao meu irmão, Paulo Henrique por toda assistência técnica e disposição. Ao meu companheiro Ronaldo, por estar sempre ao meu lado. Aos meus sogros, Diva e Airton por toda contribuição e dedicação. Agradeço à minha amiga Adazila Guimarães pelo grande incentivo, carinho e amizade.

Aos colegas da Pós-Graduação, Carolina Panis pela participação especial numa etapa deste trabalho e a Natália Ribeiro pelos agradáveis momentos na bancada. À Paula Gaspar, Vanessa Jacob Victorino, Fernanda Carolina de Campos, Renato Cardoso, e Pollyana Marinello pelos bons momentos compartilhados. Aos meus amigos e colegas da Iniciação-Científica e Mestrado, que participaram com dedicação e amizade deste trabalho, Fernando Pinheiro Souza Neto, Raissa Caroline, Carol Conchon, Thamara Nishida e Francielle Caroline Rodrigues.

Aos colegas Ângelo Augusto Chiachia Pasta, Jakeline Tiemy Guinoza Siraich, Thiago Antônio Moretti de Andrade pela parceria e amizade.

Ao corpo docente do Doutorado em Patologia Experimental, por ter contribuído para a minha formação científica.

Agradeço a todos que direta ou indiretamente contribuíram para a realização deste trabalho, para o meu crescimento pessoal e profissional.

“Se você não pode explicar algo de maneira simples é porque não compreende este algo bem o suficiente”

(Albert Einstein)

“Tudo concorre para o bem daqueles que amam a Deus”.

(Romanos 8, 28)

MALACHIAS, Vânia Aparecida **Terra. Mecanismos de ação do óxido nítrico em modelo experimental de irradiação UVB na pele de murinos**. 2013. 138 f. Tese (Doutorado em Patologia Experimental) - Universidade Estadual de Londrina, Londrina, 2013.

RESUMO

A irradiação UVB estimula a produção de radicais livres causando lesões oxidativas na pele que podem resultar na aceleração do envelhecimento e o desenvolvimento de doenças cutâneas malignas. O presente estudo avaliou o estresse oxidativo e nitrosativo na pele de camundongos após a irradiação UVB e determinou as espécies reativas formadas imediatamente, 6hs e 24hs após a radiação UVB. Além disso, demonstrou o mecanismo de ação do óxido nítrico (NO) na lesão cutânea e na modulação da proliferação celular. Ainda com o objetivo de estabelecer o modelo experimental de irradiação aguda por UVB eficiente para testes com antioxidantes avaliamos o mecanismo protetor da genisteína, neste modelo experimental. Neste estudo para que os níveis de NO fossem avaliados foi necessário adaptar e validar uma técnica por quimiluminescência (QL) utilizada anteriormente por outros autores em tempo real em rim e coração para amostras congeladas e a fresco de pele de murinos. A técnica descreve a reação entre o NO e H_2O_2-luminol. Durante a validação, utilizamos além da pele, músculo gastrocnêmio de ratos e dois sistemas químicos geradores de NO (Nitroprussiato de sódio- NPS e iodeto de potássio em meio ácido). Através do uso de cPTIO (inibidor de NO), foi confirmado que o NO é de fato a molécula que reage com H_2O_2-luminol durante a reação de QL, observado pela inibição da emissão de fótons em todos os sistemas estudados. Durante a reação do NO e H_2O_2-luminol, utilizamos também os inibidores histidina, manitol e superóxido dismutase (SOD), específico para $^1O_2$, radical hidroxil (OH) e ânion superóxido ($O_2^{\bullet}$), respectivamente e observamos que os resultados obtidos nos sistemas químicos e biológicos foram semelhantes aos descritos por outros autores. Conforme descrito as espécies emissoras de fótons, resultantes da reação entre o NO e H_2O_2-luminol, são o peroxinitrito ($ONOO^-$) ou oxigênio singlet ($^1O_2$). Concluímos que a reação rápida, sensível e específica do NO com H_2O_2-luminol por QL, acontece em sistema químico e biológico e pode ser utilizado para examinar o papel do NO em processos fisiopatológicos, ampliando a utilização deste método para diferentes amostras à fresco e congeladas. Ainda neste estudo utilizamos outras metodologias descritas anteriormente através da reação de QL avaliamos o estresse oxidativo ou nitrosativo após a radiação aguda por UVB na pele pela formação de lipoperóxidos de membrana resultante da reação lipoperoxidativa iniciada por radicais livres e a capacidade antioxidante total (TRAP) do tecido. A atividade da enzima catalase (CAT) e níveis de glutationa reduzida (GSH) e oxidada (GSSG) foram analisadas por espectrofotometria. O estudo da modulação na proliferação celular foi realizado por imunohistoquímica através dos marcadores, PCNA, VEGF, Ki67, p53 e marcação da apoptose (Tunel). Os resultados mostraram a formação de lipoperóxidos de membrana na pele imediatamente após a radiação UVB, com níveis superiores após 24hs sendo que após 6hs não ocorreu lesão lipoperoxidativa. A redução da capacidade antioxidante total da pele foi observada

somente imediatamente após a radiação UVB. Quando os animais swiss foram tratados com desferroxamina (DFX, quelante de ferro inibindo formação $^{\bullet}OH$), histidina (inibidor $^{1}O_2$), AG e L-Name (inibidores de iNOS e cNOS, respectivamente), houve diminuição da formação de lipoperóxidos de membrana imediatamente após a radiação UVB. A redução da capacidade antioxidante total só não foi revertida com o tratamento com inibidores de NOS. Concluímos que imediatamente após a radiação UVB, diferentes espécies reativas, como o $^{\bullet}OH$, $^{1}O_2$ e NO participam do estresse oxidativo e nitrosativo na pele de camundongos swiss. A intensa lesão lipoperoxidativa após 24hs da UVB foi acompanhada por altos níveis de NO. Ainda neste tempo, houve redução da atividade da CAT e dos níveis de GSH, com aumento da GSSG, sugerindo acúmulo de H_2O_2. Este acúmulo resultou na reação entre H_2O_2 e NO gerando $ONOO^-$, que é a espécie reativa responsável pela nitração de proteínas, conforme observado pela intensa marcação de nitrotirosina neste tempo. A análise histológica dos camundongos hairless tratados com AG e L-Name mostrou preservação tecidual que pode ser confirmada pela diminuição dos lipoperóxidos de membrana, na marcação da nitrotirosina assim como nos níveis de NO e proporcionou o aumento da proliferação celular avaliada pelo aumento dos marcadores PCNA e VEGF. Concluímos que após 24hs da radiação UVB, o NO é principal responsável pelo estresse nitrosativo na pele de camundongos hairless e swiss, bem como pela modulação da proliferação celular. O tratamento com genisteína (10 mg/kg) antes da radiação UVB mostrou pela análise histopatológica preservação tecidual sendo que a superfície epitelial permaneceu intacta. A ação protetora da Genisteína contra a lesão na pele após 24hs da radiação UVB, foi confirmada pela redução na formação de lipoperóxidos de membrana e na marcação da nitrotirosina embora os níveis de NO permanecessem elevados. Houve estimulação na proliferação celular avaliada pelo PCNA, VEGF, Ki67, p53 e diminui a apoptose. Estes resultados revelaram que a genisteína possui ação protetora contra o estresse nitrosativo na pele após 24hs da radiação UVB, provavelmente pela sua ação scavenger de H_2O_2 evitando a formação de $ONOO^-$. Neste estudo mostramos a importante participação do NO na patogenia da pele provocada pela radiação UVB e sugerimos este modelo experimental para a avaliação dos mecanismos protetores de substâncias antioxidantes.

Palavras-chave: Espécie reativa do oxigênio (ERO). Radicais livres. Radiação UVB. Estresse oxidativo. Proliferação celular. Óxido nítrico.

MALACHIAS, Vânia Aparecida Terra. **Mechanisms of nitric oxide action in experimental model of UVB irradiation in murine skin**. 2013. 138 f. Tese (Doutorado em Patologia Experimental) - Universidade Estadual de Londrina, Londrina, 2013.

ABSTRACT

UVB light stimulates production of reactive species that are the main cause of skin lesions and result in accelerated aging and the development of malignant skin diseases. The aim of this study was to evaluate the oxidative and nitrosative stress after UVB irradiation in the skin of hairless mice and swiss, and to determine the reactive species formed in the skin immediately (0h), 6hs and 24hs after UVB radiation, demonstrating the important role of nitric oxide (NO) in the skin injury and the modulates on cell proliferation, as well as, the skin protects by the use of a known antioxidant, genistein, in this experimental model. To evaluate the lipoperoxidative lesion in hairless and swiss mice skin subjected to acute UVB radiation, a technique used was the chemiluminescence (CL) reaction, induced by tert-butyl hydroperoxide. Total antioxidant capacity (TRAP) was assessed by QL while the activity of the enzyme catalase (CAT) and reduced glutathione (GSH) and oxidized (GSSG) by spectrophotometry. The levels of nitric oxide (NO) to the skin was also investigated by QL, describes a system that NO reacts with luminol-H_2O_2. The study of cell proliferation was performed by immunohistochemistry using the markers, PCNA, VEGF, Ki67, p53 and apoptosis marking (Tunnel). The animals were treated (i.p.) with deferoxamine (DFX), iron chelator, to characterize the participation of the hydroxyl radical ($OH^{\bullet}$), histidine, "scavenger" of singlet oxygen ($^1O_2$), and aminoguanidine (AG) and L-name, inhibitors of iNOS and cNOS, respectively.The results showed the moderate formation of lipoperoxides in the skin immediately after UVB radiation, while after 24 hours there was a important lipid peroxidation, estimated by high light emission during the CL reaction. Six hours after UVB radiation the lipoperoxidative lesion was not observed. Immediately after UVB radiation, all the treatment of animals (DFX, histidine, L-NAME, AG) inhibited the light emission and decreased the total antioxidant capacity which was not reversed by treatment with NOS inhibitors (AG, L-NAME), indicating the ROS involvement. The lipoperoxidation observed 24 hours after UVB radiation was accompanied by high levels of NO. In addition, there was a reduction of CAT activity and GSH levels, with increases of GSSG levels, suggesting an accumulation of H_2O_2 and possible reaction with NO to generate ONOO-, a highly oxidizing specie, which can cause lipid peroxidation and nitrotyrosine formation. The impairment of cell proliferation was also observed. The protective action of Genistein against the skin lesion was demonstrated by the reduction in nitrotyrosine formation and lipid peroxidation as well as stimulated the cell proliferation and decreases apoptosis.In conclusion, immediately after UVB radiation differents reactive species, such as the $^{\bullet}OH$, $^1O_2$ and NO participates of the moderate oxidative and nitrosative stress observed in mice skin. After 24hs of UVB radiation, NO is mainly responsible for oxidative stress in hairless and swiss mice skin and nitrosative stress, as well as by modulation of cell proliferation. The Genistein has protective action against nitrosative stress in the skin, probably due to its action of H_2O_2 scavenger preventing the $ONOO^-$ formation . This study showed the

important role of NO in the pathogenesis of the skin caused by UVB radiation and suggest that the anti-nitrosative effect must be considered in photoprotection researches. The objective of this study was also validate the technique used to assess the NO levels by QL in the mice skin, for frozen and fresh samples, since the method has only been used previously in biological systems in real time. To validate the techinic was used muscle gastrocnemius rats, two chemical systems (NO donors) sodium nitroprusside (NPS solution) and potassium iodide in acid medium (KI-NaNO3/H2SO4 system) and specific inhibitors of NO, $^{1}O_2$, $^{\bullet}OH$, and superoxide anion ($O_2^{\bullet}$), cPTIO, histidine, mannitol and superoxide dismutase (SOD), respectively. cPTIO added in the mixture reaction, inhibithed the light emission of CL reaction in chemical and biological systems, confirming that NO is in fact the molecule that reacts with H_2O_2-luminol-CL system. As described by other authors, the light-emitting species, resulting from the reaction between NO and H_2O_2-luminol-CL system, are peroxynitrite (ONOO-) or $^{1}O_2$. Specific reactive species inhibitors added in the misture reaction, showed similar effects on the light emission of CL curves in the chemical system comparing to biological system and those previously described by other authors. We conclude that and H_2O_2-luminol-CL system is a fast, sensitive and specific method to assess the NO levels and can be used to examine the role of NO in pathophysiological processes, expanding the use of this method for in fresh and frozen differents samples.

Keywords: Reactive oxygen species (ROS). Free radicals. UVB radiation. Oxidative stress. Cell proliferation. Nitric oxide.

LISTA DE ILUSTRAÇÕES

LISTA DE ABREVIATURAS E SIGLAS

ABAP	2,2-azo-bis(2-amidinopropano diidroclorido)
AP-1	proteína ativadora 1
Bax	proteína pro-apoptótica
Bcl-2	proteína oncogênica que inibe apoptose
BHT	butilato de hidroxitolueno
CaM	Calmodulina
CGC	Guanilato ciclase solúvel
cGMP	Guanosina de 3', 51-monofosfato cíclica
CAT	catalase
COX-II	ciclooxigenase II
DNPH	dinitrofenil hidrazina
DTNB	ácido 5,5-ditiobis-2-nitrobenzóico
eNOS	óxido nítrico sintase endotelial
EROs	espécies reativas de oxigênio
ERNs	espécies reativas de nitrogênio
GSH	glutationa reduzida
GSH-Px	glutationa peroxidase
GSH-Rd	glutationa redutase
GSSG	glutationa oxidada
GT	glutationa total
HCl	ácido clorídrico
HCLO	ácido hipocloroso
H_2SO4	ácido sulfúrico
H_2O	água
H_2O_2	peróxido de hidrogênio
I CAM-1	molécula de adesão intercelular
IE	índice de estresse
IFN-γ	interferon gama
IL	interleucina
IκB	subunidade do NF- κB
iNOS	óxido nítrico sintase indutível
J	joule

K	constante de velocidade
KCl	cloreto de potássio
KH_2PO_4	fosfato monobásico de potássio
$L^{\bullet}$	radical de ácido graxo
$LOO^{\bullet}$	radical peroxil
$LO^{\bullet}$	radical alcoxil
LOOH	peróxido orgânico
MDA	dialdeído malônico
Mn-SOD	manganês superóxido dismutase
MPO	mieloperoxidase
mtDNA	ácido desoxi-ribonucléico mitocondrial
NaCl	cloreto de sódio
NAOH	hidróxido de sódio
$NACO_3$	carbonato de sódio
NA_2HPO	monoidrogenofosfato de sódio
NK	Natural Killer
NF- κB	fator nuclear Kapa B
NMF	fator natural de hidratação
N_2O_3	trióxido de dinitrogênio
N_2O_3	tetróxido de dinitrogênio
$NO^{\bullet}$	óxido nítrico
NOS	óxido nítrico sintase
NTB	ácido 2-nitro-5-tiobenzóico
$^1O_2$	oxigênio singlet
$^{\bullet}O_2^-$	ânion radical superóxido
$^{\bullet}OH$	radical hidroxil
$ONOO^-$	peroxinitrito
PCs	proteinas carbonílicas
PCA	ácido pirrolidino carboxílico
p21	proteína reguladora do ciclo celular
p53	gene supressor de tumor
QL	quimiluminescência
SOD	superóxido dismutase
SBCs	células queimadas do sol

TCA	ácido tri-cloro acético
TBARS	substâncias reativas ao ácido tiobarbitúrico
TNF-α	fator de necrose tumoral α
TRAP	capacidade antioxidante total
Ub	ubiquitina
URL	unidade relativa de luz
USOD	unidades de SOD
UV	ultravioleta

SUMÁRIO

1 INTRODUÇÃO

1.1 EFEITOS BIOLÓGICOS DA RADIAÇÃO ULTRAVIOLETA NA PELE

A exposição dos seres humanos à radiação ultravioleta (UV) causa grande preocupação devido aos vários relatos sobre os efeitos nocivos causados pela exposição solar. Estudos epidemiológicos revelam que pessoas que trabalham sob exposição solar apresentam maior incidência de alterações na pele, desde a formação de rugas até o desenvolvimento de câncer (HARRIS, 2005).

A radiação UV provoca reações fotoquímicas ao alcançarem a pele. As ondas de radiação penetram diretamente, interagindo com as células da epiderme e da derme (Figura 1). Inicialmente estas reações podem estimular a produção de melanina, cuja manifestação é visível sob a forma de bronzeamento da pele ou pode levar desde a produção de simples inflamações ou graves queimaduras até ao envelhecimento e o câncer (HARRIS, 2005; KVAM; DAHLE, 2003).

As manifestações da exposição aguda aos raios UV incluem eritema e queimadura solar. A exposição crônica é considerada um dos agentes mais importantes para o desenvolvimento de doenças cutâneas malignas e o envelhecimento (ARMSTRONG; KRICKER, 2001; BICKERS; ATHAR, 2006; PERES et al., 2011).

Os raios solares contêm a radiação ultravioleta A, B e C. Os raios UVC incidem num comprimento de onda entre 180 e 290 nm, os raios UVB entre 290 e 320 nm e os raios UVA entre 320 e 400 nm (Figura 1).

Os raios ultravioletas do tipo A e B (UVA e UVB) são os principais responsáveis pela maioria das lesões cutâneas devido à excessiva exposição à radiação solar (PODDA et al., 1998; SAIJA et al., 2000).

Embora exista muito mais UVA do que UVB no espectro solar, UVB é 1000 vezes mais eficaz em produzir eritema do que a UVA. A UVB requer de 2,0 a 5,0 J/cm^2, para produzir uma dose mínima eritematosa (1 MED), dependendo das diferenças entre espécies e padrões considerados individuais, como a cor da pele. O eritema atinge máxima intensidade de seis a 20 horas após a exposição (YING; PARRISH; PATHAK, 1974). Na pele de camundongos hairless uma dose única de

1.5 J/cm^2 equivale a 1 MED (MOORE et al., 2004).

Como regra geral, quanto menor for o comprimento de onda da radiação UV, maior é o efeito biológico.

Figura 1 - Penetração dos raios UV nas camadas da pele

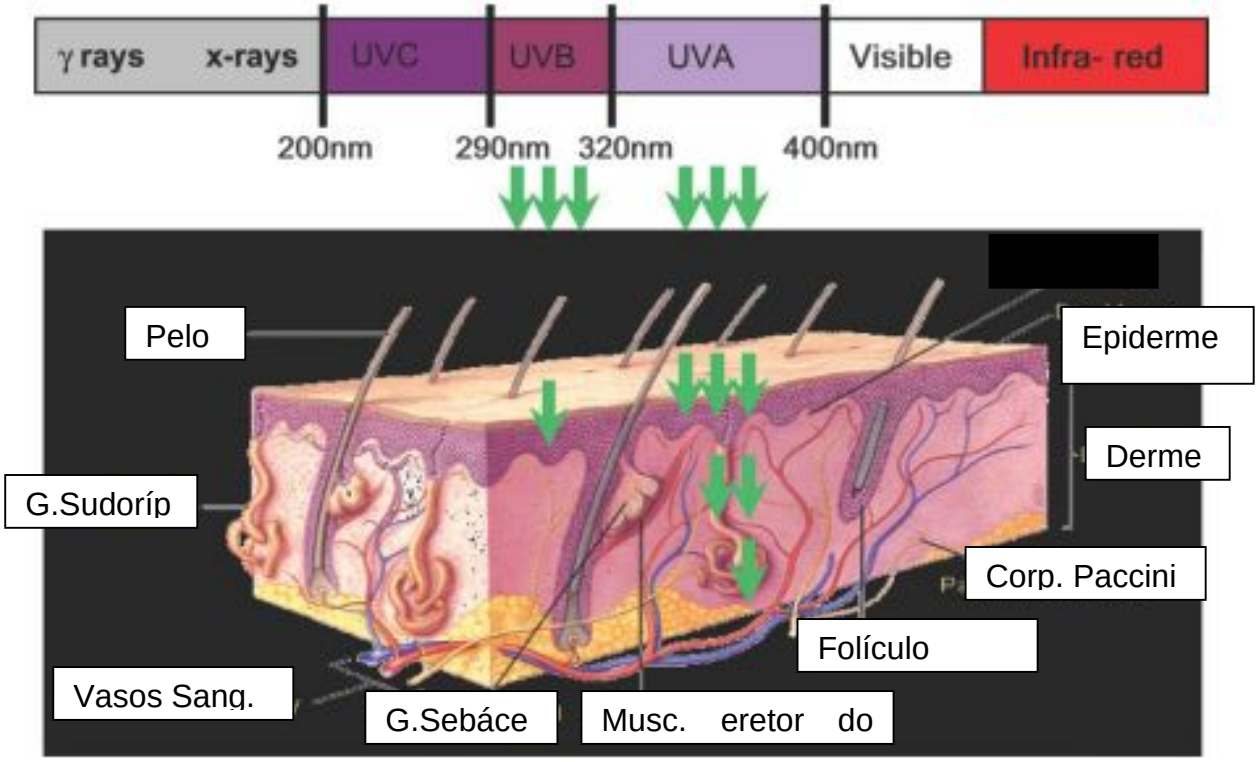

Fonte: Adaptado de Birch-Marchin e Swalwell (2010).

A radiação UVB, portanto, é considerada mais prejudicial à pele do que UVA, podendo provocar as queimaduras solares com conseqüente eritema, potente agente carcinogênico e mutagênico. É o principal componente da luz solar que causa lesões no DNA, e outras estruturas celulares resultando em processos inflamatórios, envelhecimento e o câncer de pele (IKEHATA et al., 2004; PODDA et al., 1998; SAIJA et al., 2000).

A radiação UVB inibe também a função das células natural killer (NK) e os processos de apoptose e lise celular. Esta alteração correlaciona-se diretamente com a carcinogênese em condições de desequilíbrio na expressão do gene p53 (CLYDESDALE; DANDIE; MULLER, 2001). O UVB pode, portanto, ser responsável pelo câncer na pele humana, como carcinomas de células basais e escamosas, até melanomas malignos (ARMSTRONG; KRICKER, 2001).

1.2 Efeitos Oxidativos Da Radiação Ultravioleta Na Pele

As espécies reativas do oxigênio (EROs) ou nitrogênio (ERNs) são fundamentais em diversos processos fisiopatológicos e bioquímicos, mantendo a sobrevivência e a homeostase celular, com um equilíbrio refinado entre sua formação e remoção. Porém, quando há alterações acentuadas neste equilíbrio, um estado pró-oxidante é gerado, levando, assim, ao chamado estresse oxidativo ou nitrosativo (GUARATINI; MEDEIROS; COLEPICOLO, 2007; TERRA et al., 2012b).

O estresse oxidativo/nitrosativo, portanto, é um fenômeno que ocorre quando há um desequilíbrio entre a produção EROs/ERNs e as defesas antioxidantes, podendo resultar tanto na diminuição destas defesas quanto no aumento da formação de radicais livres (HALLIWELL; GUTTERIDGE, 2007). O resultado deste desequilíbrio são as lesões oxidativas resultantes do ataque de radicais livres aos constituintes celulares, numa reação típica de oxi-redução. Os radicais livres reagem com lipídeos das membranas celulares, proteínas estruturais e enzimas e o próprio DNA. Todos os componentes celulares são susceptíveis à ação das espécies reativas do oxigênio e nitrogênio, porém os lipídeos das membranas biológicas (retículo endoplasmático, membranas mitocondriais ou plasmáticas) são os mais atingidos em decorrência da peroxidação lipídica ou lipoperoxidação (BICKERS; ATHAR, 2006; TERRA et al., 2012a, 2012b).

Durante a lipoperoxidação, ocorrem as reações em cadeia através da indução da peroxidação de ácidos graxos levando à formação de hidroperóxidos lipídicos, que na presença de Fe^{2+}, podem ainda ser oxidados a radical alcoxil ($LO^{\bullet}$), e peroxil ($LOO^{\bullet}$), vindo a sofrer quebra na ligação C-C seguinte e originar compostos intermediários, aldeídos de baixo peso molecular, dialdeído malônico (MDA), α-hidroxinonenal e hidrocarbonetos, como etano e n-pentano (CECCHINI; ARUOMA; HALLIWELL, 1990; OHKAWA; NOBUKO; YAGI, 1979), que podem atacar grupamentos amino de proteínas e fosfolipídios, modificando moléculas biológicas. Os aldeídos formados pela lipoperoxidação podem, ainda, interagir com o DNA formando aductos que têm sido associados ao câncer (HALLIWELL; GUTTERIDGE, 2007).

A peroxidação lipídica traz conseqüências homeostáticas graves para as membranas atacadas, refletidas, principalmente, na perda de sua integridade, devido à alteração na sua permeabilidade a íons e pequenas moléculas

e perda nas suas características de fluidez (HALLIWELL; GUTTERIDGE, 2007). Esta agressão acaba por interferir em mecanismos celulares importantes, incluindo sistemas enzimáticos, alterações na organização estrutural, expressão gênica, entre outros (CREMONESE; PEREIRA-FILHO; MAGALHAES, 2001).

Com relação às proteínas, quando há ação das EROs, suas estruturas secundárias e terciárias são rompidas, com subseqüente aumento de hidrofobicidade e perda de função (HALLIWELL; GUTTERIDGE, 2007; LINTON; DAVIES; DEAN, 2001).

A pele está continuamente exposta a uma combinação de fatores, tais como agentes químicos, físicos, muitos dos quais induzem a formação excessiva de EROs e ERNs (GUARATINI; MEDEIROS; COLEPICOLO, 2007; KOHEN, 1999; KOHEN; GATI, 2000).

Figura 2 - Fontes endógenas e exógenas de espécies reativas na pele, e mecanismos de defesa antioxidante

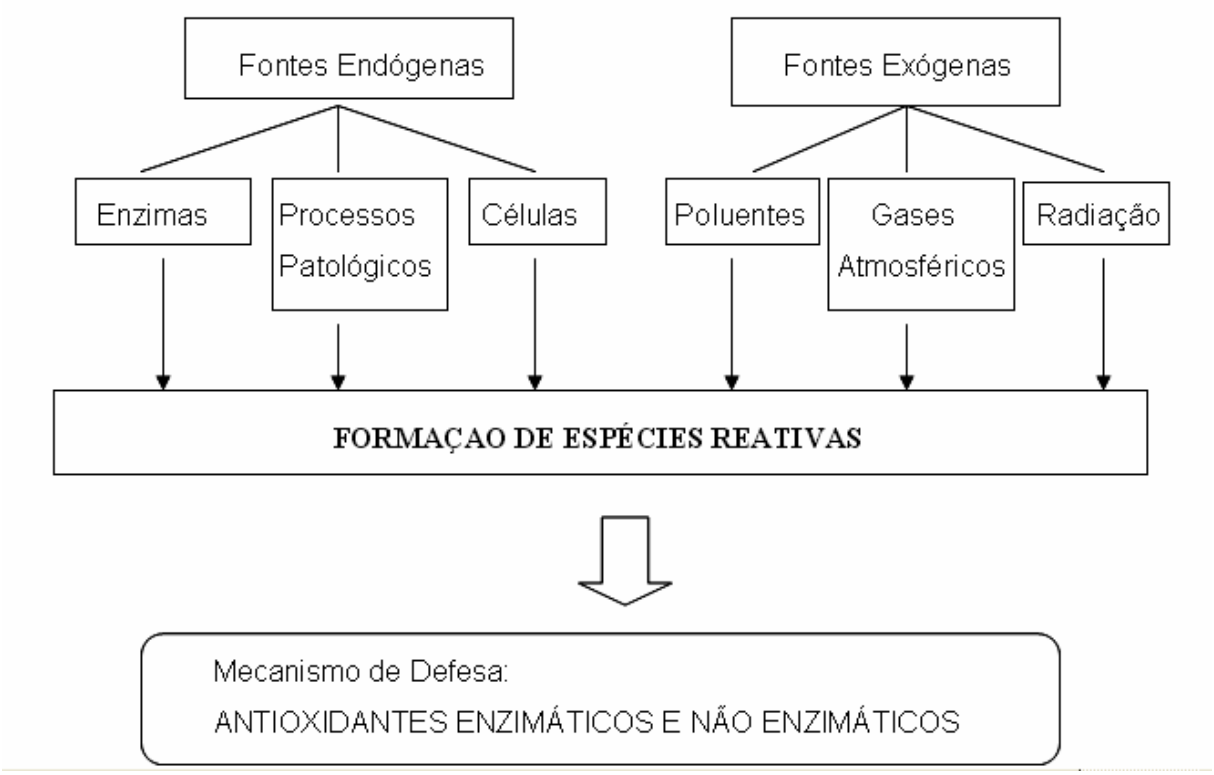

Fonte: Adaptado de Guaratini, Medeiros e Colepicolo (2007).

Dentre as agressões externas, a radiação UV é muito descrita como responsável pela maioria das lesões cutâneas devido excessiva exposição a radiação solar (ARMSTRONG; KRICKER, 2001; BICKERS; ATHAR, 2006).

A radiação UVA é considerada como principal fator extrínseco,

ligado ao processo do envelhecimento, através da formação de radicais livres na pele (YAAR; GILCHREST, 2007; YASUI; SAKURAI, 2000).

Peres et al. (2011) demonstraram que UVB provoca o envelhecimento, através do estresse oxidativo na pele pela formação radicais livres. Terra et al. (2012b) evidenciaram a formação tempo-dependente de espécies reativas responsáveis pela lesão oxidativa na pele, num modelo experimental de radiação aguda por UVB.

Embora os efeitos prejudiciais da radiação UVB na pele tenham sido relacionados durante muito tempo à formação direta de dímeros de pirimidina no DNA (WEI, 2002), tem sido demonstrado que as alterações no DNA também estão fortemente relacionadas com a formação de radicais livres, que podem causar danos oxidativos no DNA, levando a mutações e câncer (BEEHLER et al., 1992; PEAK; PEAK, 1982; ROSEN; PRAHALAD; WILLIAMS, 1996; WEI et al., 2002). As primeiras evidências experimentais in vitro, sugeriram que todo espectro da radiação UV (UVA,B,C) é capaz de gerar espécies reativas do oxigênio e resultar em dano oxidativo no DNA (WEI et al., 1997; ZHANG et al., 1997). A radiação UVB pode causar oxidação de resíduos de guanina no DNA num processo mediado por EROs (ICHIHASHI et al., 2003), bem como alterar os níveis de enzimas antioxidantes intracelulares (BICKERS; ATHAR, 2006; KOHEN, 1999; KOHEN; GATI, 2000).

1.3 Sistemas Antioxidantes da Pele

A pele, assim como todos os tecidos, possui uma rede de sistemas antioxidantes para manter o equilíbrio redox intracelular e combater o estresse oxidativo (SHINDO; WITT; PACKER, 1993).

Durante o processo de evolução do ser humano, vários mecanismos de defesas antioxidantes foram desenvolvidos (KOHEN; GATI, 2000). Na pele, as células possuem mecanismos enzimáticos de resposta rápida, bem como moléculas antioxidantes de baixo peso molecular para contrabalançar o efeito deletério causado pelo estresse oxidativo, como apresentado na figura 2 (GUARATINI; MEDEIROS; COLEPICOLO, 2007).

O sistema antioxidante cutâneo, portanto é formado por substâncias enzimáticas e não-enzimáticas. Dentre os antioxidantes enzimáticos, destacam-se a glutationa peroxidase (GSH-Px), a catalase (CAT) e a superóxido dismutase (SOD)

(KOHEN; FANBERSTEIN; TIROSH, 1997; SHINDO; WITT; PACKER, 1993). Estudos demonstraram a presença na epiderme dos principais antioxidantes enzimáticos, incluindo a GPx, glutationa redutase (GRx), SOD e CAT (SHINDO; WITT; PACKER, 1993).

As enzimas antioxidantes constituem o principal mecanismo de defesa intracelular, previnem as reações em cadeia dos radicais livres pela diminuição na concentração disponível destes para iniciar o processo oxidativo (FERREIRA; MATSUBARA, 1997).

A SOD contribui para um dos mecanismos antioxidantes mais eficientes, catalisando a dismutação do radical anion superóxido ($^{\bullet}O_2^-$) em peróxido de hidrogênio (H_2O_2) na presença de próton H^+ (HALLIWELL; GUTTERIDGE, 2007) e evita os danos que poderiam ser causados por este radical.

A CAT e a GSH-Px são as principais responsáveis pela remoção imediata de H_2O_2. A CAT encontrada em todos os órgãos do corpo, especialmente nos hepatócitos e eritrócitos, está presente em grandes concentrações nos peroxissomos e em baixas concentrações nas mitocôndrias, catalisando a decomposição específica de H_2O_2, gerando moléculas de água e oxigênio (O_2) (HALLIWELL; GUTTERIDGE, 2007).

$$2\ H_2O_2 \xrightarrow{CAT} 2H_2O + O_2$$

A GSH-Px, por sua vez, é fundamental no metabolismo de H_2O_2 e de outros peróxidos, pois catalisa reações de doação de elétrons, no qual se utiliza da glutationa reduzida (GSH) como agente redutor, formando a glutationa oxidada (GSSG) (ROVER et al., 2001).

$$H_2O_2 + 2\ GSH \xrightarrow{GPx} 2H_2O + GSSG$$

$$LOOH + 2\ GSH \xrightarrow{GPx} 2H_2O + GSSG + LOH$$

A GSH é um tripeptídeo formado pelos aminoácidos glicina, cisteína e ácido glutâmico. Sua capacidade redutora é determinada pelo grupamento tiol–SH presente na cisteína (MATSUBARA; MACHADO, 1991). Quando a GSH é oxidada pela reação da GSH-Px, há a interligação de duas moléculas do tripeptídeo por uma

ponte dissulfeto, com formação de GSSG. A queda nos níveis de GSH pode prejudicar as defesas celulares contra a ação deletéria dos radicais livres. As células íntegras mantêm uma razão GSH/GSSG alta. Para isso, a GSSG formada é reduzida novamente a GSH à custa de NADPH, pela ação da enzima glutationa redutase (GR) (HALLIWELL; GUTTERIDGE, 2007).

$$GSSG + NADPH + H^+ \xrightarrow{GR} GSH + NADP^+$$

GSH, portanto, é um mediador intracelular com uma importante ação direta na defesa contra intermediários reativos, com uma importante capacidade para conjugar com pro-oxidantes. Além disso, funciona como substrato para sistemas antioxidantes já que seu grupo tiol tripeptídio (SH) participa da regeneração do ácido ascórbico e do α-tocoferol (CARINI et al., 2000).

Na classe dos antioxidantes não enzimáticos, incluem-se um vasto número de compostos, sintetizados *in vivo* ou obtidos exogenamente, que previnem danos oxidativos por interações diretas ou indiretas com as EROs/ERNs (BIALY et al., 2002). Os antioxidantes de baixo peso molecular que protegem a pele contra as EROs, incluem o ácido ascórbico, GSH, α-tocoferol e ubiquinol (PODDA et al., 1998).

Dentre as substâncias endógenas, podemos ainda destacar alguns hormônios, como estradiol e estrógeno, que apresentam atividade antioxidante semelhante à vitamina E, devido, provavelmente, à sua porção fenólica, comum a ambas as moléculas (KVAM; DAHLE, 2003). O ácido lipóico, um cofator essencial em vários complexos enzimáticos, apresenta atividade antioxidante, podendo atuar como regenerador de formas oxidadas de glutationa, ascorbato e α-tocoferol. Além destes, a melanina, um pigmento formado pela oxidação e polimerização da tirosina, tem papel antioxidante, protegendo a pele principalmente contra $^{\bullet}O_2^-$ e $LOO^{\bullet}$ (KVAM; DAHLE, 2003). O ácido trans-urocanico e o ácido cis-urocânico, foram descritos como os principais antioxidantes naturais ($^{\bullet}OH$ scavenger) da epiderme (BARRESI et al., 2011; KAMMEYER et al., 1999).

1.3.1 Efeito da radiação UV no sistema antioxidante da pele e o uso de genisteína como antioxidante exógeno

Embora os danos causados a pele pela indução do estresse oxidativo possam ser controlados pela rápida eliminação das EROs através dos mecanismos antioxidantes eficientes da pele (KOHEN; FANBERSTEIN; TIROSHI, 1997; KOHEN; GATI, 2000), vários estudos sugeriram que as radiações UV são responsáveis pela diminuição de sistemas antioxidantes cutâneos, bem como pelo aumento de sistemas oxidantes, alterando assim o balanço redox celular e conseqüentemente a homeostasia cutânea (PERES et al., 2011; TERRA et al., 2012b). Diferentes doses de luz UV podem destruir completamente as lojas epidérmica de ascorbato, α-tocoferol, GSH, ubiquinol, SOD e CAT (SHINDO; WITT; PACKER, 1993).

Terra et al. (2012a) mostraram uma redução na concentração de GSH e aumento nos níveis de GSSG, na pele de camundongos swiss, correspondendo ao aumento no índice de estresse, (COLADO SIMÃO et al., 2005), depois de 24h da exposição à radiação UVB. Outros estudos atribuíram a redução nos níveis de GSH na pele como um mecanismo fotoprotetor (FONSECA et al., 2011; HANADA; GANGE; CONNOR, 1991; WHEELER et al., 1986).

Estudos revelaram que na pele de ratos, a distribuição da enzima CAT corresponde ao acúmulo de H_2O_2, indicando que na pele normal a CAT tem um importante papel no balanço redox (MURAMATSU et al., 2005). Terra et al. (2012a, 2012b), demonstraram a diminuição na atividade da CAT, 24h após a exposição à radiação UVB, na pele de camundongos swiss e hairless. Alguns estudos já haviam demonstrado diminuição na atividade da CAT neste mesmo tempo (FUCHS et al., 1989; JEON et al., 2003; VAYALIL; ELMETS; KATIYAR, 2003) e estes mesmos estudos sugeriram que a CAT é um dos mais sensíveis componentes da defesa antioxidante na pele.

O balanço redox que ocorre na pele após a irradiação UV, tem sido um importante parâmetro para compreensão dos sistemas antioxidantes endógenos e para a pesquisa por substâncias que minimizem os efeitos oxidativos na pele. (BARRESI et al., 2011; SAIJA et al., 2000; VAYALIL; ELMETS; KATIYAR, 2003; WEI et al., 2002).

Considerando que poucos tecidos no corpo estão sujeitos ao

estresse oxidativo como a pele (KOHEN; GATI, 2000), vários estudos sugerem o uso de substâncias antioxidantes como opção para diminuir os danos neste órgão mediados pela radiação UVB. O tratamento com chá verde contendo polifenóis preveniu a depledação da GPx, catalase e GSH em pele de camundongos hairless após a exposição aguda e crônica por UVB (VAYALIL; ELMETS; KATIYAR, 2003).

Os flavonóides são compostos que têm atraído vários estudos devido as suas propriedades antioxidantes. Foi reportado que a suplementação de isoflavonas (encontradas nos grãos de soja) na dieta diminui as lesões oxidativas no DNA em humanos, e também foi sugerido que este pode ser o possível mecanismo do efeito protetor destes compostos na prevenção ao câncer (DJURIC et al., 2001).

Estudos sugerem que o efeito antioxidante das isoflavonas é, parcialmente, devido aos efeitos sequestrador de radicais livres e quelador de metal, e depende da posição da hidroxila fenólica (ARORA; NAIR; STRASBURG, 1998).

A genisteína (4',5,7-triidroxisoflavona), uma isoflavona de grãos de soja, tem sido associada à prevenção ao câncer, doenças cardiovasculares e aumento da resposta imunológica (WATANABE; UESUGI; KIKUCHI, 2002).

A genisteína possui três grupo hidroxila com diferentes ações antioxidantes. A ação antioxidante da genisteína (4',5,7-triidroxisoflavona) contra radical peroxil está diretamente relacionada à presença das hidroxilas fenólicas nas posições C3' e C4', mas diferentemente de outros compostos fenólicos antioxidantes, ela não é consumida na reação (CAO et al., 1997).

Figura 3 - Estrutura química da genisteína

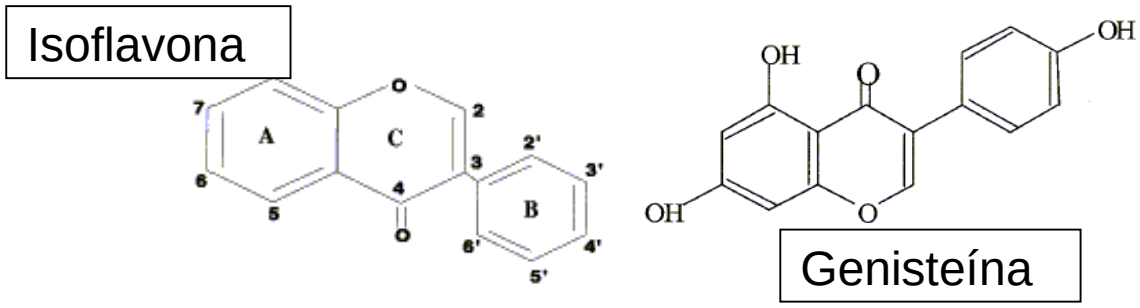

Fonte: Simão et al. (2006).

Estudos prévios demonstraram que a genisteína aplicada topicamente na pele de camundongos hairless expostos a irradiação UVB, age diretamente como sequestrador de H_2O_2 ou indiretamente pela inibição do

recrutamento de neutrófilos (WEI et al., 1997, 2002), podendo atuar também como sequestrador de outras espécies reativas do oxigênio e inibindo a reação de Fenton (LIU et al., 1998).

Em eritrócitos, a genisteína reduz a lesão pré-hemolítica, através da inibição da formação de lipoperóxidos na membrana do eritrócito (SIMÃO et al., 2006).

Neste estudo investigamos a ação protetora da genisteína contra o estresse nitrosativo provocado na pele após 24h da radiação UVB assim como o provável mecanismo protetor envolvido.

1.4 Espécies Reativas na Pele estimuladas pela Radiação UV

Pesquisadores demonstraram a geração de espécies reativas como o oxigênio singlet ($^1O_2$), $^{\bullet}O_2^-$, radical hidroxil ($^{\bullet}OH$), H_2O_2, peroxinitrito ($ONOO^-$), e óxido nítrico (NO) durante a foto exposição aos raios UV, principalmente *in vitro* (BICKERS; ATHAR, 2006; DELICONSTANTINOS; VILLIOTOU; STAVRIDES, 1996; HAKOZAKI et al., 2008; HECK et al., 2003; MASAKI; ATSUMI; SAKURAI, 1995; OGURA et al., 1991; VILE; TYRRELL, 1995).

De acordo com os estudos, podemos agrupar a formação de radicais livres na pele promovida pela radiação UV através de 5 principais mecanismos descritos a seguir:

1- As interações entre as ondas provenientes da radiação solar e a pele podem ocorrer por meio de ação direta da radiação sobre as estruturas celulares, como faz a UVB ou UVA (HARRIS, 2005). O $^1O_2$, uma espécie eletronicamente excitada, pode ser produzida por diversas reações químicas e fotoquímicas e devido a sua eletrofilicidade, reage com compostos insaturados, sulfetos e aminas, sendo os ácidos graxos insaturados, DNA e proteínas importantes alvos biológicos (Figura 4) (HALLIWELL; GUTTERIDGE, 2007). O dano oxidativo dependente de $^1O_2$ aos lipídios e proteínas, foi observado in vitro e em fibroblastos da pele humana submetidos aos raios UVA (VILE; TYRRELL, 1995).

2 - Os danos na pele, provocados pela radiação aguda por UVB, podem acontecer também de forma indireta, provavelmente resultante do aumento de radicais livres produzidos durante a resposta inflamatória imediata com eritema e infiltrado de leucócitos (CASAGRANDE et al., 2006). Os neutrófilos ativados por

citocinas pró-inflamatória, geram $^{\bullet}O_2^-$ por uma reação catalisada pela enzima NADPH oxidase. No neutrófilo, a SOD catalisa a dismutação do $^{\bullet}O_2^-$ em H_2O_2, a partir do qual podem ser gerados $^{\bullet}OH$ e ácido hipocloroso (HClO). O $^{\bullet}OH$ pela reação de Haber-Weiss/Fenton. O HClO é gerado a partir de uma reação catalisada pela mieloperoxidase (MPO), a partir do qual, podem ser formados derivados altamente tóxicos, as cloroaminas (Figura 4) (SHINDO; WITT; PACKER, 1993; VINTEN-JOHANSEN, 2004). Ainda durante as repostas inflamatórias o NO desempenha importante papel como componente vasodilatador e na modulação das respostas imunes na pele. O $NO^{\bullet}$ na presença de $^{\bullet}O_2^-$ resulta em $ONOO^-$, que pode provocar danos oxidativos na pele (Figura 4) (DELICONSTANTINOS; VILLIOTOU; STAVRIDES, 1996).

Wei et al. (2002) mostrou que H_2O_2 é parte da resposta da pele à exposição aguda por UVB e as espécies reativas podem ser gerados por queratinócitos e infiltração de neutrófilos. O $^{\bullet}OH$ foi descrito como uma importante espécie reativa de oxigênio responsável pela formação de radicais lipídicos na exposição da epiderme à luz UV (OGURA et al., 1991). Brenneisen et al. (1998) mostrou que a exposição das células da pele aos raios UVB induz uma liberação imediata de ferro lábil, o que pode catalisar a produção $^{\bullet}OH$ através de uma reação que requer Fe^{2+}, também conhecida como reação de Haber-Weiss ou reação de Fenton (KRUSZEWSKI, 2003).

3 - As espécies reativas podem ser formadas, ainda, indiretamente, por reações da luz com fotossensibilizadores endógenos cutâneos, como por exemplo, o ácido urocânico (BICKERS; ATHAR, 2006). Como resultado da ativação endógena pode ocorrer a produção do $^{\bullet}O_2^-$ ou $^1O_2$ (Figura 4) (MARTIN; BURCH, 1990). Substâncias exógenas aplicadas sobre a pele, na forma de cosméticos ou drogas fotossensibilizadoras ingeridas que atingem a pele, incluindo alguns fenotiazínicos (usado em tranqüilizantes), como também as fluoroquinolonas e os antibióticos (tetraciclinas), podem promover a geração de $^1O_2$, $^{\bullet}OH$ e outras espécies reativas de oxigênio, com efeitos nos queratinócitos da epiderme e células de Langerhans (Figura 4).

4 – Espécies reativas também podem ser geradas devido aos danos na mitocôndria pela radiação UV, produzindo $^{\bullet}O_2^-$, H_2O_2 e $^{\bullet}OH$ (BIRCH-MARTIN; SWALWELL, 2010).

5 - Outra situação é que apesar da luz UV não depositar energia

suficiente nas moléculas de água para ionizá-las, se H_2O_2 estiver disponível, a UVB pode causar fissão homolítica, gerando $^{\bullet}OH$, altamente reativo (Figura 4) (HALLIWELL; GUTTERIDGE, 2007).

$$H_2O_2 \longrightarrow {}^{\bullet}OH + {}^{\bullet}OH$$

6 - Outro mecanismo de formação de espécies reativas foi sugerido por Heck et al. (2003), quando identificaram uma catalase presente em queratinócitos capaz de formar EROs em resposta a radiação UV, em especial UVB. Usando cromatografia de troca iônica, afinidade metálica e exclusão de tamanho, uma proteína de 240 kDa e capacidade de gerar EROs foi isolada de cultura de queratinócitos previamente submetidos à irradiação UVB. A proteína exibiu grande absorção na extensão de 320 a 360nm com pico adicional entre 400 e 410 nm, sugerindo a presença do grupamento heme. Seqüenciamento pela cromatografia líquida iônica acoplada à espectrometria de massa identificou a proteína como catalase. Observações que os efeitos da luz UVB na catalase são altamente sensíveis ao pH e dependentes de oxigênio, mas que não requerem substratos adicionais, sugerem que as EROs podem ser formadas pela transferência de fótons derivados da água que subseqüentemente interagem com o oxigênio molecular (Figura 4).

Figura 4 - Mecanismos de **f**ormação de espécies reativas na pele provocada pela radiação UV

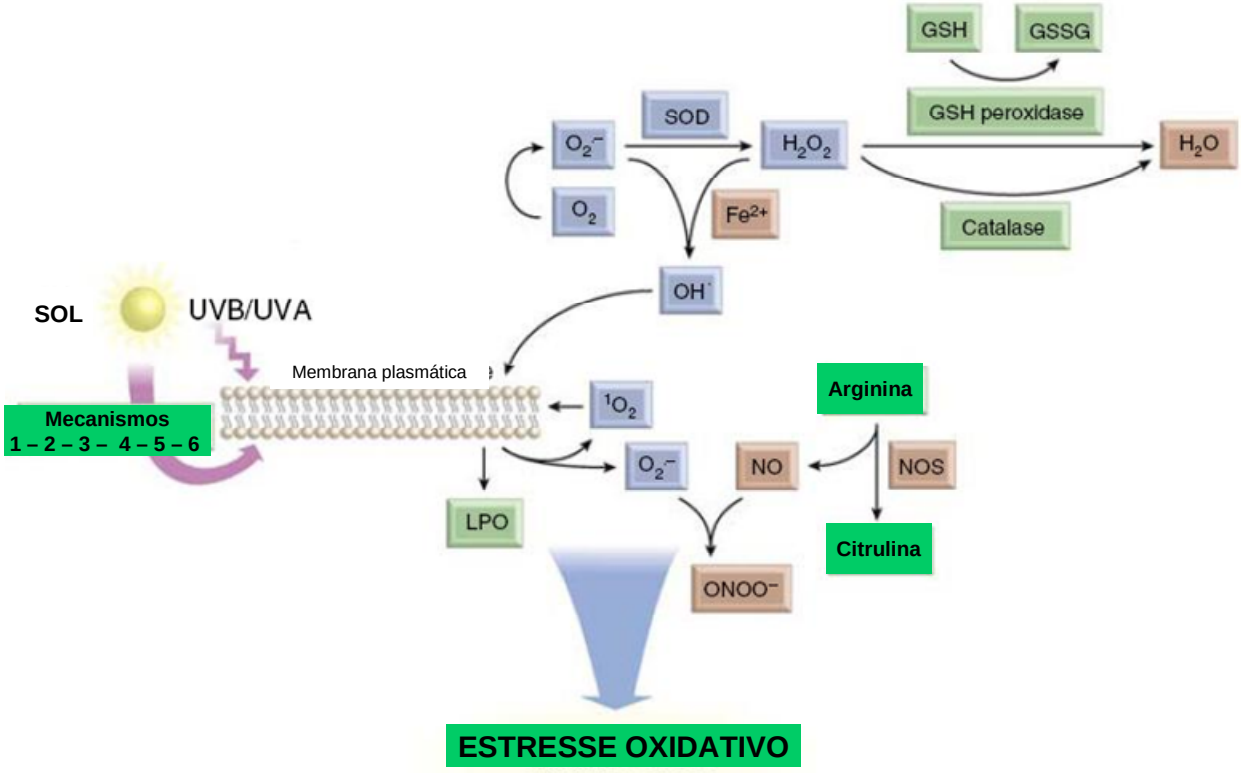

Fonte: Adaptado de Bickers e Athar (2006).

Os estudos realizados até agora revelaram, portanto, que a radiação UV promove estresse oxidativo na pele e que diferentes espécies são responsáveis pelo dano oxidativo na pele, no entanto ainda se fazem necessários estudos para determinação das espécies reativas formadas após diferentes tempos (tempo dependente) na pele após a irradiação UVB e a participação do NO na lesão da pele além do seu efeito sobre a proliferação celular, sendo objetivos do nosso estudo.

Terra et al. (2012b), demonstraram a participação do $^{\bullet}OH$, NO e do $^1O_2$ na lesão lipoperoxidativa da pele de camundongos swiss, imediatamente após a radiação UVB, utilizando desferroxamina, histidina e inibidores seletivos das enzimas responsáveis pela produção de NO (i.p). Desferroxamina, um forte quelante de ferro, é um importante composto utilizado para caracterizar a participação de $^{\bullet}OH$ na lesão celular oxidativa (GRONBERG et al., 2010; YIAKOUVAKI et al., 2006; ZHONG et al., 2004), assim como a histidina, um eficiente *scavenger* de $^1O_2$, tem sido utilizado para demonstrar o envolvimento do $^1O_2$ no estresse oxidativo em diferentes tecidos (GROSSMAN et al., 1998). Neste mesmo estudo os autores demonstraram também

que o NO é a principal espécie reativa responsável pela lesão lipoperoxidativa da pele, 24h após a radiação UVB (Figura 5).

Figura 5 - (1) Geração de espécies reativas na pele após 0h e 24hs da radiação UVB, observadas neste estudo. A radiação UVB gera diretamente (A) as EROS, $^1O_2$ e $^\bullet O_2^-$. (B) SOD converte $^\bullet O_2^-$ em H_2O_2. $^\bullet O_2^-$ e H_2O_2 podem ser convertidos numa espécie altamente reativa o radical hidroxil ($^\bullet OH$) numa reação catalizada pelo ferro (Fe^{2+}), conhecida por reação de Fenton e reação de Haber-Weiss. (C) Espécies reativas do nitrogênio (ERNS) são geradas como resultado da conversão da arginina a citrulina numa reação estimulada pela óxido nítrico sintase (NOS). Estas EROS e ERNS interagem com os lipídios da membrana plasmática e iniciam a lipoperoxidação. (2) Formação de radicais livres tempo dependente, depois da irradiação UVB. A peroxidação lipídica ocorre imediatamente após a radiação UVB e é mediada por várias espécies reativas tais como $^1O_2$ $^\bullet OH$ e NO. 24h após a radiação a espécie reativa predominante é o NO, provavelmente devido a expressão de iNOS.

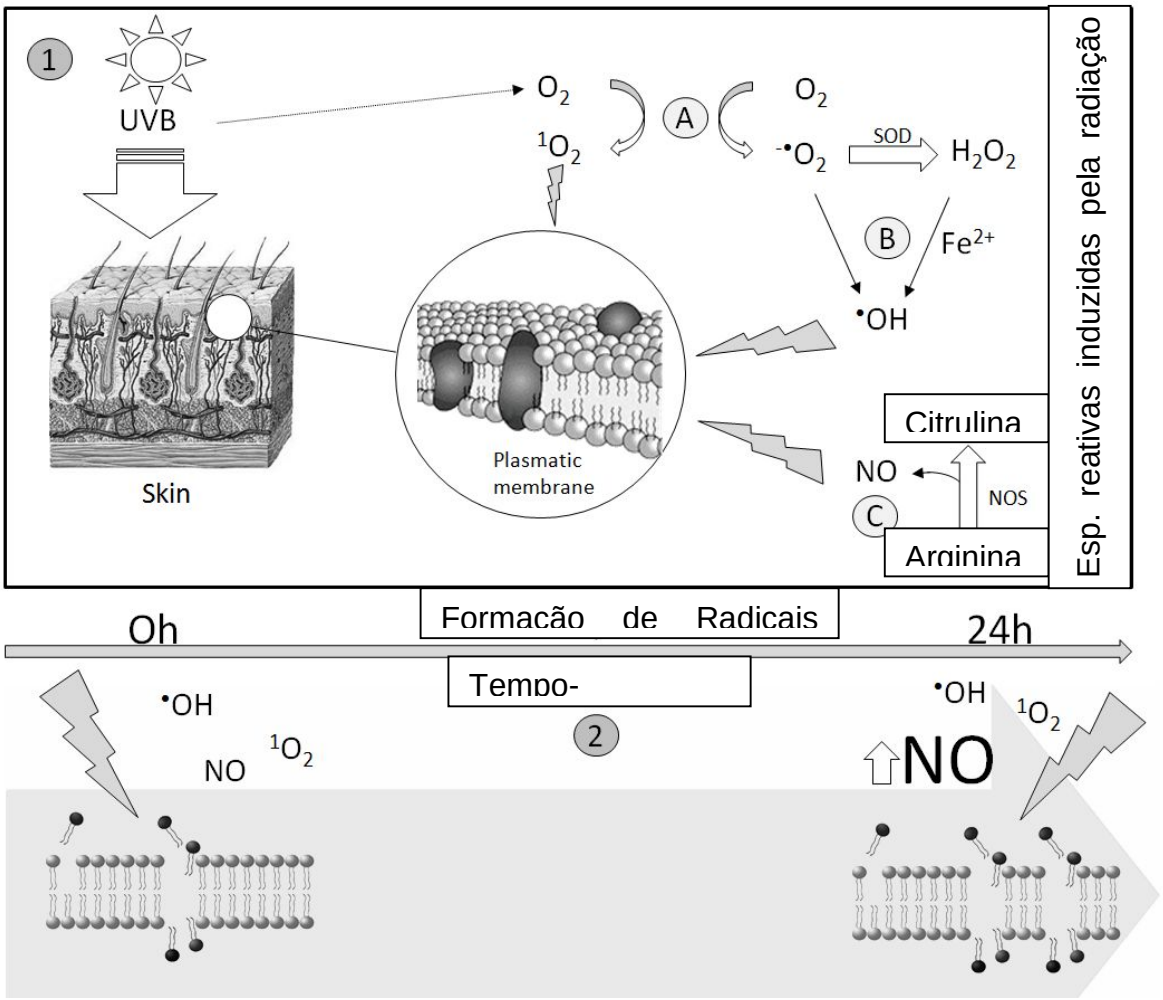

Fonte: Terra et al. (2012a).

Como neste trabalho a avaliação dos danos oxidativos/nitrosativos

na pele resultantes de níveis aumentados de NO devido à radiação UVB foi fundamental, segue abaixo uma revisão sobre alguns aspectos que envolvem o NO, importantes para compreensão deste estudo.

1.5 ÓXIDO NÍTRICO

Durante muitas décadas o NO, ou monóxido de nitrogênio, foi conhecido apenas por ser um gás poluente e nocivo, produzido pela combustão interna dos motores, causador das chuvas ácidas e poluição atmosférica, sendo alvo principalmente do estudo de ambientalistas e químicos (FUKUTO, 1995; FUKUTO; CHAUDHURI, 1995). Na década de 1980 foi identificado como um mensageiro intercelular ubíquo nos sistemas cardiovasculares, imunitário e nervoso. Em 1992, o NO foi chamado “a molécula do ano” pela revista *Science.* O Prêmio Nobel em Fisiologia e Medicina, em 1998, foi dado a Ferid Murad, Robert F. Furchgott e Louis J. Ignarro pela descoberta das propriedades de sinalização do NO (STANKEVICIUS et al., 2003).

A partir daí, o NO é tema de intensa pesquisa visando a compreensão de seu envolvimento em processos fisiológicos e fisiopatológicos. Vários livros e artigos de revisão foram publicados a respeito das diferentes funções do NO em sistemas biológicos, inicialmente no processo de hemostasia, sobre a vasodilatação, sinalização neuronal, atividade antimicrobiana e inibidor da agregação plaquetária (IGNARRO, 1990; LAVER; STEVANIN; READ, 2008), apresentando funções nos sistemas cardiovascular, reprodutor e imune (EGBRINK et al., 2005).

O NO e seus metabólitos também foram associados com várias condições patológicas desde a inflamação, aterosclerose, diabetes, doenças neurodegenerativas, acidentes vasculares cerebrais, lesão muscular após os eventos de isquemia e reperfusão (KHANNA; COWLED; FITRIDGE, 2005), doenças cardiovasculares (ANAYA-PRADO et al., 2002), caquexia associada ao câncer (BARREIRO et al., 2005), lesão celular na pele após a irradiação UVB (TERRA et al., 2012a; WANG et al., 2010), entre outras.

Considerando a dualidade de ação do NO, o conhecimento dos fatores que determinam a sua bioatividade, como a concentração, difusão desde o local de síntese e consumo em múltiplas reações, bem como, o tipo de exposição,

crônica ou aguda, parecem determinar o efeito global do NO num determinado sistema biológico (EGBRINK et al., 2005). Por exemplo, o NO pode ser citotóxico tanto para células eucariotas quanto para células procariotas (FREEMAN, 1994), ou também pode exercer um efeito protetor antioxidante devido à sua habilidade de seqüestrar o $^{\bullet}O_2^-$ (MILES et al., 1996).

1.5.1 Biossíntese do óxido nítrico

Em mamíferos, o NO é gerado pela ação da enzima óxido nítrico sintase (NOS) que existem sob três isoformas distintas: 2 constitutivas (cNOS e eNOS) e 1 induzível (iNOS). Apesar da enzima eNOS, inicialmente descoberta no endotélio vascular e a nNOS no sistema nervoso periférico, receberem o nome de acordo com tipo celular onde foram primeiramente descritas, sabe-se atualmente que as isoformas da NOS são expressas em vários tipos celulares, incluindo a iNOS (BIAN; MURAD, 2003).

Existem outras enzimas envolvidas na liberação ou na síntese de NO, tais como, nitrito redutases bacterianas e enzimas que agem sobre doadores de NO, além do NO poder ser gerado também em condições não enzimáticas nos sistemas biológicos, através dos estoques existentes nos tecidos (MOWBRAY et al., 2009; NAGASE et al., 1997). Neste estudo o enfoque será dado ao NO resultante da atividade da NOS, devido a sua relevante participação na lesão nitrosativa provocada pela radiação UVB.

A síntese do NO mediada pela enzima NOS, ocorre durante a transformação do aminoácido semi-essencial L-arginina em L-citrulina e óxido nítrico, utilizando oxigênio e a nicotinamida adenina dinucleotídeo fosfato (NADPH) como co-substratos (Figura 6) e como co-fatores a flavina mononucleotídeo (FMN), flavina adenina dinucleotídeo (FAD), tetra-hidrobiopterina (BH4), ferro protoporfirina IX (heme), cálcio (Ca^{2+})/calmodulina e possivelmente zinco (Figura 7). Algumas isoformas da NOS possuem o cofator adicional, a calmodulina. Na presença de elevada concentração de Ca^{2+}, a calmodulina liga-se a certas NOS, ativando-as. Esse processo está relacionado com as NOS constitutivas, ou seja, a endotelial e a neuronal. No entanto, a situação é diferente para a NOS induzida pelo estímulo imunológico ou inflamatório conhecida como iNOS, onde a atividade das mesmas é independente da presença de Ca^{2+} e da calmodulina (ALDERTON; COOPER;

KNOWLES, 2001; NATHAN, 1992).

Figura 6 - Síntese de óxido nítrico (NO)

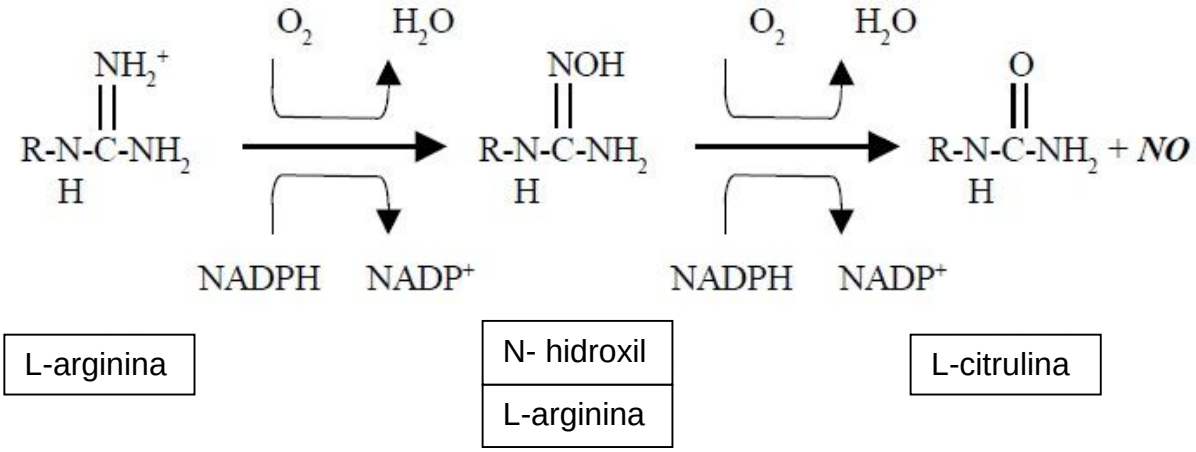

Fonte: Adaptado de Stankevicius et al. (2003).

Figura 7 - Esquema representativo da estrutura da NOS, mostrando as etapas da síntese de NO. Elétrons (e^-) são doados pela NADPH ao domínio redutase da enzima e prosseguem através dos carreadores redox FAD e FMN até o domínio oxigenase, onde interagem com o ferro do heme e com o BH_4 no sítio ativo para catalizar a reação do O_2 com a L-arginina, produzindo NO e citrulina. O fluxo de elétrons através do domínio redutase requer a ligação Ca^{2+}/Cam.

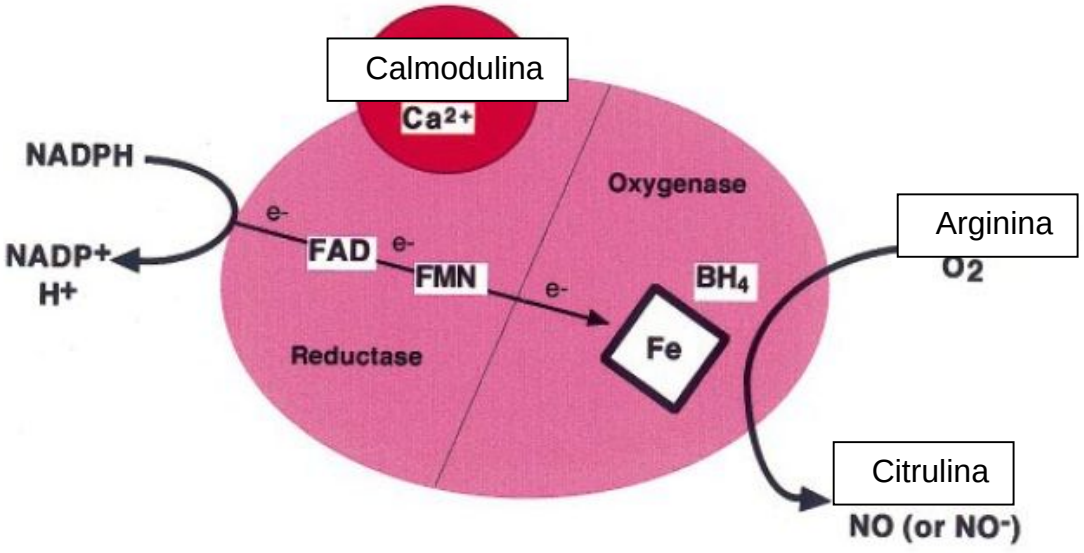

Fonte: Adaptado de Alderton, Cooper e Knowles (2001).

1.6 Reações Envolvendo Óxidos de Nitrogênio em Sistemas Biológicos

O NO é considerado um radical livre por apresenta um elétron desemparelhado na última camada de valência. Em sistemas biológicos as interações químicas do NO ocorrem por estabilização do elétron desemparelhado (IGNARRO, 1990).

Além disso, o NO em seu estado puro, sob condições normais de temperatura e pressão é um gás. Sua solubilidade é moderada em água (1,9mM a 25^{o} C), sendo muito mais solúvel em solventes apolares, como o hexano (0,13 M a 25^{o} C) (IGNARRO, 1990). Desta forma, quando presente em sistemas biológicos, o NO tende a se concentrar em ambientes lipofílicos, como membranas e domínios hidrofóbicos de proteínas e não é, portanto, armazenado em vesículas. Por outro lado não existe um receptor de membrana para o NO, podendo se difundir a longas distâncias. Um dos alvos melhor estudado é a atividade da enzima guanilato ciclase solúvel, que resulta em ações bem conhecidas como a vasodilatação e a neuromodulação (KERWIN; LANCASTER; FELDMAN, 1995).

O conhecimento da química do NO em sistemas biológicos é normalmente organizado em função dos efeitos diretos ou indiretos. Os efeitos diretos resultam de reações do NO com alvos moleculares (complexos metálicos ou espécies radicalares), resultando num efeito biológico enquanto os efeitos indiretos são mediados por produtos da reação de NO com O_2 ou $^{\bullet}O_2^-$, (IGNARRO, 1990; LIUDET; SORIANO; SZABO, 2000).

Os efeitos diretos estão relacionados pela atividade de cNOS, quando o NO é produzido em baixa concentração e equivale a menos do que 1 µM e os indiretos relacionados a expressão de iNOS e alta concentração de NO, mais do que 1 µM (EGBRINK et al., 2005; WINK; MITCHELL, 1998). Estudos indicam que a baixa produção de NO, direta ou transitória, exerce função homeostática/regulatória e antiinflamatória. No entanto, condições fisiológicas alteradas, como as que ocorrem durante a inflamação, podem resultar no aumento da iNOS e em altas concentrações de NO (KENDALL; MARSHALL; BARTOLD, 2001).

1.6.1 Efeitos diretos do óxido nítrico

Em geral a reação direta do óxido nítrico ocorre com outro radical

livre ou pela sua interação a um metal como o cobre, ferro e manganês, que são geralmente ligados a uma proteína. No primeiro caso, o resultado eventual é a formação de espécies diamagnéticas estáveis; no segundo caso, o elétron desemparelhado é dividido entre o óxido nítrico e o metal (KERWIN; LANCASTER; FELDMAN, 1995).

Reação com complexos metálicos

As mais reconhecidas reações de significância biológica envolvem o NO com metais de transição (livres ou em grupos prostéticos associados a proteínas. Esta reação ocorre principalmente entre o NO e o heme ferroso (Fe^{2+}) de algumas proteínas (Figura 6), resultando no deslocamento do Fe^{2+} para fora do anel porfirínico (COOPER, 1999). Esta alteração de conformação pode ativar ou inativar proteínas. Como exemplo, podemos citar a inibição da Catalase, pela formação de aductos nitrosilados, resultando na diminuição do consumo de H_2O_2 (FARIAS–EISNER et al., 1996). A ativação da guanilato ciclase, devido à interação direta do NO com núcleo heme da enzima, resultando no relaxamento do músculo liso, inibição da agregação plaquetária, inibição da adesão de leucócitos ao endotélio e na transdução de sinais no sistema nervoso (NATHAN; XIE, 1994).

Além disso, como de extrema importância podemos citar a reação com a oxi-hemoglobina que ocorre entre o NO e um complexo metálico ($Hb(Fe\text{-}O_2)$), uma das principais vias de remoção do NO em sistemas biológicos. Esta reação resulta na formação de nitrato (NO_3^-) e metahemoglobina (KIKUCHI et al., 1993a).

Reação com outras espécies radicalares

O NO age como um antioxidante quando reage com outras espécies radicalares como o $LO^{\bullet}$ e $LOO^{\bullet}$ (hidroperóxidos lipídicos), formados durante a peroxidação lipídica, funcionando, portanto como um terminador de cadeia (KERWIN; LANCASTER; FELDMAN, 1995).

1.6.2 Efeitos indiretos do NO

Os efeitos indiretos do NO ocorrem, quando esta espécie reativa é

capaz de interagir rapidamente com o O_2 e o $^{\bullet}O_2^-$, (IGNARRO, 1990; LIUDET; SORIANO; SZABO, 2000).

Reação com O_2

Segundo Liudet, Soriano e Szabo (2000), quando o NO é exposto a O_2, pode gerar uma variedade de ERNs com maior poder reativo do que NO ou O_2, individualmente. Em fase aquosa, o produto desta reação é o dióxido de nitrogênio (NO_2), que pode dimerizar formando tetróxido de dinitrogênio (N_2O_4) ou pode reagir com uma terceira molécula de NO para formar trióxido de dinitrogênio (N_2O_3) (equação 1-3). N_2O_3 e N_2O_4 reagem rapidamente com água, formando íons nitrito (NO_2^-) e nitrato (NO_3^-) (Equações 4 e 5) (IGNARRO, 1990).

$2NO + O_2$ ---------- $2NO_2^+$ (Equação 1)

$NO + NO_2$---------- N_2O_3 (Equação 2)

$NO_2 + NO_2$---------- N_2O_4 (Equação 3)

$N_2O_3 \xrightarrow{H_20}$----------$2NO_2 + 2H_2^+$ (Equação 4)

$N_2O_4 \xrightarrow{H_20}$---------- $NO_2^- + NO_3^- + 2H_2^+$ (Equação 5)

Baixas concentrações de NO, embora esta reação seja relativamente rápida, não possuem impacto biológico e o NO se difunde a distância consideráveis desde o seu local de síntese. Quando a concentração de NO pode atingir valores bastante elevados (acima de 1μM) a produção de N_2O_3 pode ser significativa. Portanto a concentração pode regular o seu tempo de meia vida: enquanto que para concentrações baixas não haverá auto-oxidação significativa de NO, este poderá difundir-se a longas distâncias; quando a concentração do gás é maior, o seu tempo de vida e a difusão são limitados (WINK; MITCHELL, 1998).

Reação com $^{\bullet}O_2^-$

A reação do NO com $^{\bullet}O_2^-$, resulta no $ONOO^-$ (Equação 6)

(IGNARRO, 1990).

$$NO + {}^{\bullet}O_2^- \text{ --------- } ONOO^- \text{------} NO_2 \text{ --------- } NO_3 \quad \text{(Equação 6)}$$

O valor aproximado de constante de reação para esta reação é de ($k = 6 \times 10^{10}\ M^{-1}s^{-1}$) (AITKEN et al., 2007). O $ONOO^-$ é uma espécie altamente oxidante e dada a sua potencial relevância no meio biológico enquanto mediador de ações atribuídas ao NO, interessa salientar que a sua produção, é controlada por diversos fatores inclusive as concentrações relativas dos dois reagentes. A concentração de O_2^- e o seu tempo de vida são muito baixas devido a atividade da SOD. A elevada velocidade de reação ($k = 5 \times l0^5\ M^{-1}.s^{-1}$) em condições fisiológicas de pH (7.0-7.4), entre a SOD e O_2^-, contribui para que esta enzima compita ativamente com o NO pela reação com O_2^- (HALLIWELL; GUTTERIDGE, 2007).

Estudos prévios *in vitro* demonstraram que o NO também pode reagir com H_2O_2 podendo resultar na formação de $ONOO^-$ (KIKUCHI et al., 1993a, 1993b; NORONHA-DUTRA; EPPERLEIN; WOOLF, 1993; RADI et al., 1991). Sabe-se que em condições de lesão celular ou na inflamação, além da grande produção de NO, existem grandes quantidades de ${}^{\bullet}O_2^-$ que é rapidamente dismutado para H_2O_2, sugerindo que a concentração de H_2O_2 no tecido possa ser muito maior do que a do ${}^{\bullet}O_2^-$, favorecendo a reação descrita (NORONHA-DUTRA; EPPERLEIN; WOOLF, 1993).

O $ONOO^-$ é uma espécie oxidante potente, com capacidade de oxidar tióis, iniciar a peroxidação lipídica, nitrar resíduos de tirosina, clivar o DNA e oxidar a guanosina (PRYOR; SQUADRITO, 1995). Desta forma, reação oxidativa nas bases do DNA promovida pelo $ONOO^-$, pode levar a mutagênese ou a morte celular por necrose ou apoptose (IGNARRO, 1990; KENDALL; MARSHALL; BARTOLD, 2001). A oxidação dos grupos tiol (SH) de GSH leva a diminuição do estado antioxidante (MARSHALL et al., 1999) da célula e ainda $ONOO^-$ pode catalizar a reação de peroxidação lipídica ocasionado lesões de membrana, desmielizações e oxidação de LDL (RADI et al., 1991; TERRA et al., 2012a). A reação de oxidação na mitocôndria pode levar à inibição dos complexos I, II e V, resultando na inibição da respiração celular, lesão de membrana com liberação do citocromo c e apoptose (BROWN, 1999).

$ONOO^-$ também é capaz de promover a nitração dos resíduos de tirosina das proteínas, levando mudanças na conformação e perda de função

(LAVER; STEVANIN; READ, 2008).

Tipicamente a nitração de proteínas consiste na adição eletrofílica de um equivalente NO_2^+ a resíduos de tirosina em proteínas. Como já mencionado anteriormente nas equações 1, o NO_2^+ resulta da reação do NO + O^2 ou da decomposição do $ONOO^-$ ou mais especificamente o $ONOO^-$ pode gerar um intermediário reativo, o íon NO_2^+, através da ligação com o ferro sérico (COOPER, 1999).

$$Fe^{3+} + ONOO^- \text{---------- } Fe^{2+}\text{-------}O^-\text{------ } NO_2^+ \text{ (Equação 10)}$$

Da reação de nitração dos resíduos de tirosina, resulta a formação do principal biomarcador de estresse nitrosativo em sistemas biológicos é a 3-nitrotirosina (3-NT), que já foi identificada em vários estudos patológicos (RADI, 2004)

A reversibilidade destas reações, liberando NO de aductos NO/heme, e da proteína tirosina nitrada (RADI, 2004), assegura significante importância fisiológica (VILLALOBO, 2006).

1.7 Participação do Oxido Nítrico na lesão Oxidativa/Nitrosativa da Pele Provocada pela UVB.

Praticamente todas as células humanas estudadas até agora têm a capacidade de produzir NO. A maioria dos tipos celulares residentes na pele produz NO em resposta à estimulação adequada. Queratinócitos (ARANY et al., 1996), células de Langerhans (QURESHI et al., 1996) fibroblastos dérmicos (WANG et al., 1996), melanócitos (ROCHA; GUILLO, 2001), e células de melanoma, (TSATMALI et al., 1999) expressam iNOS, após estimulação por citocinas inflamatórias.

Estudos realizados sobre o efeito do NO na pele após a irradiação UVB eram controversos. Alguns atribuíram um efeito protetor para NO contra a peroxidação lipídica (GONZALEZ-MAGLIO et al., 2005; LEE et al., 2000) e ao processo de apoptose (BHOWMICK; GIROTTI, 2011; WELLER et al., 2003), enquanto outros demonstraram a relação entre níveis aumentados do NO e a morte por apoptose (SEN et al., 2008; WANG et al., 2010). A formação de NO e O_2^- imediatamente após a radiação UVB foi demonstrado *in vitro* em células de

queratinócitos (HaCat) (AITKEN et al., 2007) ou *in vivo*, na epiderme (WU et al., 2010). Os autores relataram que estes radicais livres podem reagir rápida e imediatamente entre si e formando $ONOO^-$ (AITKEN et al., 2007), sendo apontado como o principal responsável pelo estresse oxidativo/ nitrosativo na pele após a radiação UVB em células endoteliais humanas (DELICONSTANTINOS; VILLIOTOU; STAVRIDES, 1996) em queratinócitos e na epiderme de camundongos (WU et al., 2010).

Recentemente foi demonstrada a relação entre níveis aumentados do NO com a peroxidação lipídica e a nitração de proteínas (formação de nitrotirosina) na pele após 24hs da radiação UVB (TERRA et al., 2012b). Os autores para esclarecer os relatos contraditórios encontrados na literatura científica até o momento, utilizando inibidores seletivos para iNOS e cNOS (AG e L-Name respectivamente), demonstraram a relação entre níveis aumentados do NO (TERRA et al., 2012a, 2012b; WANG et al., 2010) com a formação de peróxidos lipídicos e nitrotirosina na pele (TERRA et al., 2012a, 2012b), assim como a relação do NO com a morte celular por apoptose havia sido relatada anteriormente (SEN et al., 2008). O mecanismo da morte celular por apoptose descreve a S-nitrosação do gliceraldeído-3-fosfato desidrogenase (GAPDH), que inativa sua atividade catalítica, localizando-se no núcleo e mediando a morte celular (SEN et al., 2008).

Os autores demonstraram que após 24h da irradiação, UVB induziu a expressão da iNOS com um nível máximo de mRNA na pele de camundongos hairless (GONZALEZ-MAGLIO et al., 2005).

Imediatamente após a irradiação UVB o NO e outras espécies são responsáveis pela lipoperoxidação de membrana das células da pele. Neste tempo é provável que ocorra a ativação da enzima óxido nítrico sintase constitutiva (cNOS), pela elevação intracelular de Ca^{2+} e geração de NO (TERRA et al., 2012a; WANG et al., 2010). Outros relatos apontam a existência de estoques naturais na pele de NO, que são liberados poucas horas após a irradiação UVB, independente da participação das enzimas sintases na pele humana (MOWBRAY et al., 2009).

Neste estudo foi evidenciado ainda a relação dos níveis aumentados do NO com a inibição da proliferação celular na pele submetida à radiação UVB (TERRA et al., 2012b).

1.8 NO COMO MODULADOR DA PROLIFERAÇÃO CELULAR

O NO pode regular diversas funções fisiológicas incluindo a proliferação celular. A sua ação reguladora depende da sua concentração. Embora nem todos os detalhes sejam compreendidos, a ação citostática do NO sobre a proliferação celular em altas concentrações tem sido descrita, assim como a ação estimuladora sobre a proliferação celular em baixas concentrações de NO (TERRA et al., 2012a; VILLALOBO, 2006).

Estudos principalmente in vitro, demonstraram que este perfil paradoxal depende exclusivamente da concentração de NO. Desta forma, houve inibição da proliferação das células da retina, em condições de altos níveis de NO (GOUREAU et al., 1993; YILMAZ et al., 2000). A suplementação exógena de NO, em altas concentrações de NO, inibiu a proliferação de fibroblastos (DU et al., 1997) e queratinócitos (FRANK et al., 2000; KRISCHEL et al., 1998) enquanto que baixas concentrações de NO levou à estimulação da proliferação destas células. Os mecanismos moleculares que expliquem a ação proliferativa do NO em baixas concentrações ainda não são totalmente compreendidos.

Estudos demonstraram que a ação inibitória do NO sobre a proliferação celular, envolvem a regulação da expressão de iNOS por citocinas como o interferon-y (IFN-y), o fator de necrose tumoral-α (TNF-α), a interleucina 1 (IL-1), ou o lipopolissacarídeos (LPS), levando a produção de altas quantidades de NO, consequentemente inibindo a proliferação celular, de linfócitos, células musculares lisas vasculares, células hepáticas (VILLALOBO, 2007) (Figura 8). Em fibroblastos senescentes, a indução da iNOS pelo TNF-α, IFN-y e interleucina 1β (IL-1β) inibiu a proliferação celular (GANSAUGE et al., 1997).

Figura 8 - Regulação da expressão iNOS sobre a proliferação celular. A interação de citocinas como por exemplo LPS e IFN-y com receptores na célula gera eventos de sinalização conduzem a expressão de iNOS e subsequente produção de grandes quantidades de NO, que inibem a proliferação celular.

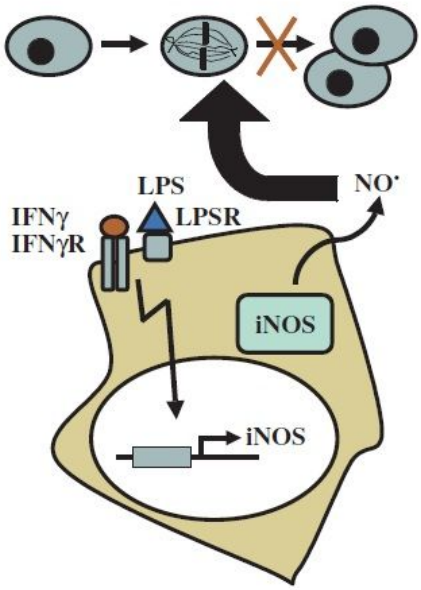

Fonte: Villalobo (2007).

O envolvimento do óxido nítrico sobre a inibição da proliferação celular foi descrito pela sua capacidade de parar o ciclo celular na fase de transição G1/S (VILLALOBO, 2006) (Figura 9)

Figura 9 – Mostra a ação inibitória de NO na fase de transição G 1 / S, sobre os alvos principais que afetam a expressão e / ou atividade de diferentes componentes relevantes para a progressão do ciclo celular.

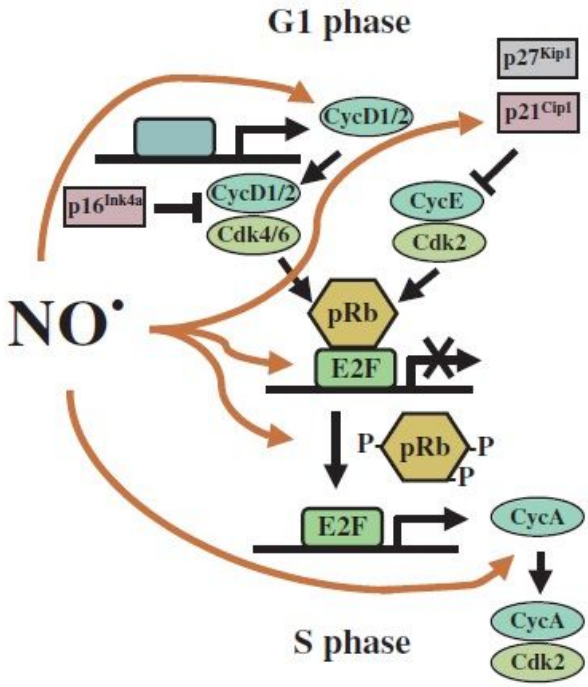

Fonte: Villalobo (2006).

Apesar da inibição sobre a proliferação celular em altas concentrações de NO ser o maior efeito exercido em vários tipos de células (normais e tumorais), existe um significante número de estudos descrevendo sua ação estimulatória sob altos níveis de NO, quando esta molécula é liberada endogenamente ou por suplementação exógena (VILLALOBO, 2006).

Bhowmick e Girotti (2011), utilizando células tumorais em condições moderadas de NO, observaram um efeito estimulador do crescimento celular, promotor de angiogênese e da expansão tumoral e anti-apoptótico.

O efeito estimulatório do NO sobre a proliferação celular descreve a ativação de receptores na membrana plasmática celular que levam a produção de NO através da expressão da iNOS, como os receptores do fator de crescimento endotelial vascular (VEGFR), receptor do fator de necrose tumoral (TNF-αR), receptores do interferon-y (IFN-yR) e de receptores de lipopolissacarídeos (LPSR) pelos seus respectivos ligantes extracelulares. Outros receptores também conhecidos por controlar a produção de NO, são os receptores de tirosina-quinase como o VEGFR e o fator de crescimento de fibroblasto (FGFR) e alguns receptores

o CD44v10, ativados por seus ligantes extracelulares VEGF, FGF e ácido hialurônico, respectivamente, levam ao aumento da concentração de Ca_2^+, resultando na formação do complexo Ca_2^+ /CaM, ativando eNOS e nNOS. Por outro lado o receptor de estrogênio 17β (17β-OestR), controla a expressão da eNOS com consequente produção de NO (VILLALOBO, 2007) (Figura 10).

Entre os poucos mecanismos sugeridos como responsáveis pela estimulação do NO sobre a proliferação celular, foi citada a ativação via MAPK, regulação da ciclooxigenase (COX-2) e a produção de espécies reativas do oxigênio como o $^{\bullet}O_2^-$ e H_2O_2 (VILLALOBO, 2007) (Figura 10).

Figura 10 - Resumo de alguns dos mecanismos moleculares e vias de sinalização que regulam a produção celular de NO e subsequente estimulação da proliferação celular, numa célula hipotética

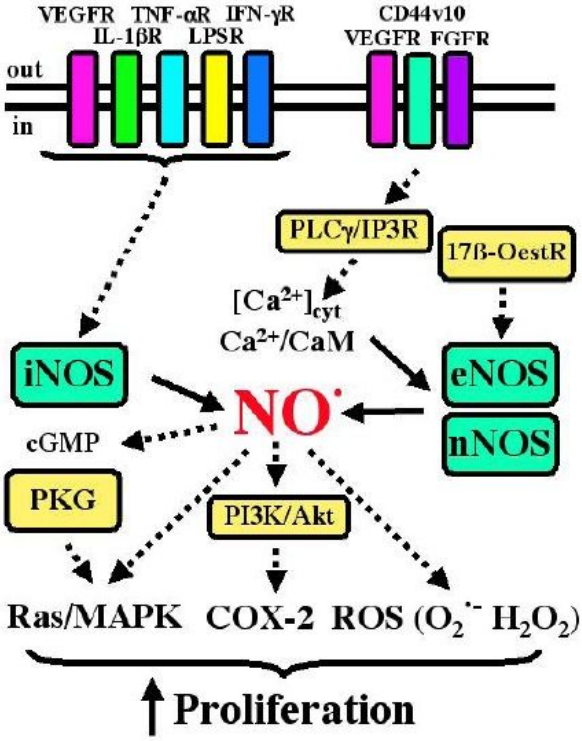

Fonte: Villalobo (2007).

Alguns estudos utilizaram o fator de crescimento do endotélio vascular (VEGF) como marcador e estimulador da proliferação celular frente a diferentes concentrações de NO, principalmente *in vitro.*

O VEGF é importante durante o processo de vasculogênese no desenvolvimento embrionário. A vasculogênese diminui progressivamente após o nascimento e é mínima na maioria dos tecidos adultos (GERBER et al., 1999). No

entanto, a expressão de VEGF é estimulada durante a angiogênese patológica, tal como ocorre em pacientes com isquemia do miocárdio ou na retina, no tecido inflamado (CARMELIET; COLLEN, 2000) e em carcinomas humanos (NICOL et al., 1997), sendo um potente fator da neovascularização tumoral (BATES et al., 2002).

Em pele de camundongos, o aumento da permeabilidade vascular induzida pelo VEGF foi relacionado com a produção local de NO, estimulada pela iNOS (FUJII et al., 1997). A ação inibitória do NO sobre a proliferação celular, foi demonstrada em células de coriocarcinoma, pela diminuição do VEGF (CHA et al., 2001). Ainda através da expressão do VEGF foi demonstrada a modulação da proliferação celular das células endoteliais do glomérulo renal pelo NO. Neste estudo o tratamento dos animais com inibidor de iNOS, levou a inibição da proliferação das células endoteliais (OSTENDORF et al., 2004). Em células de melanoma humano a resposta proliferativa, avaliada pelo VEGF é acompanhado pela super expressão da iNOS e conseqüente produção endógena do NO sendo que o tratamento com o inibidor de NOS (L-NAME) conteve a proliferação celular (TAO et al., 2005).

Terra et al. (2012a), observaram na pele de camundongos hairless a ação moduladora do NO sobre a proliferação celular após a irradiação UVB. Os resultados mostraram aumento nos níveis de NO assim como na imunoreatividade do VEGF, 6h e 24hs após a irradiação. O tratamento dos animais com AG resultou na diminuição dos níveis de NO, porém houve acentuado aumento na proliferação celular, como observado pela intensa marcação do VEGF e PCNA, sugerindo que baixas concentrações de NO possam estimular a proliferação celular mais intensamente do que altas concentrações de NO.

O antígeno nuclear de proliferação celular (PCNA), é uma proteína nuclear (36 kDa), que atua como cofator da enzima DNA polimeraze e que existe no núcleo de todas as células eucarióticas. PCNA é essencial para a síntese de ácido nucléico e desempenha um papel essencial nos processos de recombinação, replicação, reparo do DNA e na montagem da cromatina (MATHEWS et al., 1984; MIYACHI; FRITZLER; TAN, 1978). Portanto a expressão de PCNA está relacionado com o crescimento e proliferação celular. Nas células em divisão celular, a expressão desta proteína está muito aumentada na fase S do ciclo celular e diminuída na fase quiescente (JASKULSKI et al., 1988). Na clínica médica PCNA é utilizado para caracterizar a proliferação em populações celulares na epiderme humana de indivíduos saudáveis, nas lesões pré-malignas e malignas inclusive no

melanoma (GEARY; COOPER, 1992; KAWAHIRA, 1999). Estas investigações confirmaram que a distribuição da proteína PCNA está confinada na camada basal na epiderme de indivíduos saudáveis, podendo haver variação neste padrão, nas doenças cutâneas malignas.

PCNA foi descrita como um marcador de reparo do DNA e indiretamente, como um indicador de danos induzidos por UVB, na pele de camundongos e em queratinócitos (AFAQ et al., 2007; MOORE et al., 2004). AFAq et al. (2007), demonstraram que a irradiação UVB diminuiu a expressão da proteína PCNA em queratinócitos (HaCat) e que o tratamento com antioxidante, delfinidina, protegeu as células da apoptose induzida pela irradiação UVB, demonstrando expressão da PCNA pelas células com o tratamento.

Terra et al. (2012b), observaram que não ocorre imunoreatividade para PCNA na pele de camundongos hairless, após a irradiação UVB. Quando os camundongos hairless foram tratados com o inibidor de iNOS (AG), a marcação do PCNA foi evidente, confirmando o efeito modulador de baixos níveis de NO sobre a proliferação celular.

Wei et al. (2002), relatou a ação fotoprotetora da genisteína no modelo de pele reconstituída humana utilizando doses agudas de irradiação UVB (2,0 e 6,0 J/cm2). As amostras de pele tratadas com 3 concentrações de genisteína (10, 20 e 50 µM) 1 horas antes da irradiação UVB e analisadas 12 hs depois da radiação demonstraram que a genisteína preservou os mecanismos de proliferação e reparo celular avaliados pela aumentoimunoreatividade do PCNA e inibiu a formação de dímeros de piramidina, numa relação dose-dependente. Na pele irradiada e não tratada, houve aumento na formação de dímeros de piramidina e diminuição da imunoreatividade para o PCNA.

Ainda neste estudo nós utilizamos outro marcador da proliferação cellular, Ki67*,* para avaliar o efeito anti-nitrosativo da genisteína após 24h da irradiação UVB na pele de camundongos hairless. Ki67 é uma proteína nuclear de 359 kDa ou 320. A ausência de Ki67 em células quiescentes e a sua expressão universal em tecidos que proliferam revelou o seu potencial como marcador de proliferação celular (URRUTICOECHEA; SMITH; DOWSETT, 2005). El-Abaseri, Putta e Hansen (2006) relatou que alterações na expressão de Ki67 ocorrem paralelamente às alterações observadas na expressão de PCNA na pele de camundongos após UV, e que ambos estariam associados com a proliferação elevar

na epiderme.

1.9 Métodos de Análise dos níveis de NO e do Estresse Oxidativo/Nitrosativo na Pele Utilizados Neste Estudo

1.9.1 Detecção dos níveis de NO

Embora o elevado número de trabalhos dedicados ao estudo dos efeitos do NO, muito pouco se conhece sobre sua dinâmica de concentração, devido às dificuldades analíticas associadas à medição de uma espécie gasosa com tempo de vida reduzido em sistemas biológicos.

A alta instabilidade do NO sob tensões fisiológicas de O_2 e alta reatividade com as biomoléculas tornou a quantificação do NO um desafio, principalmente em sistemas biológicos devido a sua curta meia vida e baixas concentrações (ARCHER et al., 1995). Em sistemas biológicos o NO é facilmente oxidado a nitrito, com uma meia vida muito curta (< 6 sec.) (KELM et al., 1988), apesar que concentrações biologicamente ativas de NO (5nM-4uM) em soluções aquosas puras, a meia vida excede 500 segundos (LAVER; STEVANIN; READ, 2008).

Algumas metodologias são utilizadas para quantificar indiretamente o NO e seus metabólitos em vários tipos de amostras. São exemplos de métodos indiretos o uso de inibidores de NOS, L-arginina, doadores de NO, animais transgênicos, análises da expressão da isoformas de NOS e a quantificação de metahemoglobina ou de NO_2^- e NO_3^- pela reação de Griess. Contudo, estes ensaios fornecem evidências limitadas e por vezes, requerem interpretações complexas (KHANNA; COWLED; FITRIDE, 2005).

Kikuchi et al. (1993a) sugere que a reação do NO e oxi-hemoglobina, formando metemoglobina e NO_3^-, explorada para estimar a síntese de NO é um método pouco sensível.

A reação de Griess que estima os produtos da degradação do NO, ou seja, o NO_2^- e NO_3^- que reage com a sulfinilamida e N-(1-naftil)-etilenodiamina, formando um composto que pode ser detectado espectrofotometricamente a 540nm,

é considerado pouco específico para o NO. O NO_2 é um contaminante que pode ser encontrado na água e é produto do metabolismo de certas bactérias (ARCHER et al. 1995). Além disso, nitrocompostos análogos de L-arginina, tais como L-NAME, AG, e LNNA, interferem em ensaios de Griess (GREENBERG et al., 1995).

Os modelos transgênicos também podem gerar resultados duvidosos devido aos possíveis mecanismos compensatórios. Kanno et al. (2000), relatou que camundongos transgênicos deficientes de eNOS ou nNOS apresentavam expressão aumentada de iNOS, possivelmente para suprir a deficiência das isoformas constitutivas.

Neste estudo um dos objetivos foi determinar os níveis de NO na pele (fresca e congelada) pela primeira vez em condições fisiopatológicas através da detecção desta molécula por um método por quimiluminescência que descreve a reação do NO com o sistema H_2O_2-luminol, padronizado e utilizado por Kikuchi et al. (1993a, 1993b) na determinação os níveis de NO em tempo real, em rim perfundido.

Kikuchi et al. (1993a, 1993b) descreve a especificidade e sensibilidade da reação do NO com H_2O_2-luminol na reação de quimiluminescência, utilizando NO em forma de gás diluído em solução portanto sem interferentes, demonstrando que o método detecta de forma direta o NO em baixas concentrações (100fmol/l). Tsukada et al. (2003), ilustra a reação conforme figura 11.

Figura 11 - Reação de quimiluminescência entre o NO e H_2O_2-luminol

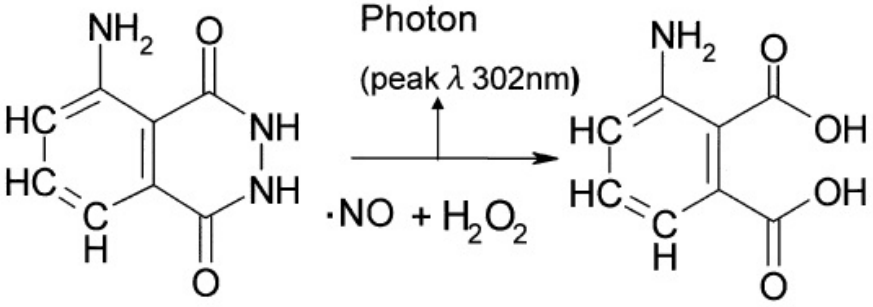

Fonte: Tsukada et al. (2003).

Como descrito por vários autores, a molécula analisada é de fato o NO, ou seja, a reação de quimiluminescência acontece entre o NO e o H_2O_2-luminol, porém desta reação, resulta a formação de outras espécies reativas emissoras de radiação responsáveis pela emissão de fótons (KIKUCHI et al., 1993b; NORONHA-DUTRA; EPPERLEIN; WOOLF, 1993; RADI et al., 1993; TSUKADA et al., 2003).

Para que esta hipótese pudesse ser comprovada, os autores utilizaram substâncias químicas doadoras de NO e inibidores específicos de radicais livres, apontando o $ONOO^-$ e $^1O_2$ como as espécies emissoras de fóton.

Kikuchi et al. (1993b), demonstrou a formação de $ONOO^-$, em tempo real durante a reação NO e H_2O_2-luminol em rim perfundido de ratos, acrescentando Mn-SOD durante a reação para excluir a possibilidade do O_2^-, ser o precursor do $ONOO^-$

Noronha-Dutra, Epperlein e Woolf (1993), utilizando nitroprussiato de sódio (NPS), como doador químico de NO, demonstrou que a reação entre o NO com H_2O_2, resulta na formação de $^1O_2$. Neste estudo, o uso de histidina (scavenger de $^1O_2$), revelou a formação do $^1O_2$ e o uso de manitol excluiu a presença de $^{\bullet}OH$ na mistura da reação de QL.

Tsukada et al. (2003) com o objetivo de estimar concentrações de NO, em tempo real pela reação com H_2O_2-luminol através da QL, em coração perfundido de ratos, construiu uma curva padrão de NO, trabalhando com concentrações de NO entre 1 a 400 pmol/l. A solução NO, utilizada para a construção da curva, foi obtida pela reação de redução do nitrito em meio ácido (ácido sulfúrico) preparado de acordo com a reação:

$$2KNO_2 + 2KI + 2H_2SO_4 \text{ ------ } 2NO + I_2 + 2H_2O + 2K_2SO_4$$

Para se obter 400pmol/l de solução de NO, utilizou-se 7.2ml de solução de 0.1 mmol/l KNO_2 + 1,8ml da solução de 0,1mol/l H_2SO_4 a 25ºC. Todas as soluções foram desgaseificadas com gás hélio.

Terra et al. (2012a, 2012b), com o objetivo de avaliar os níveis de NO na pele após a irradiação aguda por UVB, utilizaram a técnica baseada na quimiluminescência resultante da reação do NO, no sistema H_2O_2-luminol, desenvolvida por Kikuchi et al. (1993a, 1993b).

Para que pudéssemos utilizar a reação de QL para o NO com segurança, já que anteriormente a técnica foi utilizada apenas em sistemas biológicos em tempo real, adaptamos esta técnica para amostras a fresco e congeladas em 2 sistemas biológicos (pele de camundongos e músculo esquelético de ratos), utilizando conhecidos sistemas químicos doadores de NO (NPS e KI-$NaNO_3$/ H_2SO_4), e inibidores específicos de espécies reativas (manitol, histidina e

SOD), comparando os resultados obtidos com os descritos anteriormente na literatura.

1.9.2 Métodos de análise do estresse oxidativo/nitrosativo na pele

Modelos experimentais de irradiação por UV, *in vivo* ou *in vitro*, têm demonstrado a participação de EROs e ERNs e alterações no sistema antioxidante endógeno nas doenças cutâneas. Estes mesmos modelos experimentais são utilizados na avaliação das propriedades antioxidantes de fármacos. Todavia muitos dos resultados obtidos não são consistentes e ainda controversos, devido à falta de uma melhor padronização dos modelos e das técnicas de avaliação do estresse oxidativo na pele.

Normalmente a peroxidação lipídica no tecido cutâneo tem sido determinada pelo teste colorimétrico clássico, TBARS, ou seja, substâncias reativas ao ácido tiobarbitúrico. TBARS quantifica a presença de aldeídos de baixa massa molecular, como o MDA. Através desta técnica pesquisadores demonstraram não haver lipoperoxidação na pele após irradiação aguda por UVB atribuindo um efeito protetor aos mecanismos endógenos da pele, principalmente ao papel do óxido nítrico (NO) na pele (GONZALEZ-MAGLIO et al., 2005; LEE et al., 2000). Várias investigações utilizaram a técnica do TBARS como representante do dano lipoperoxidativo, porém a quimiluminescência (QL) mostrou-se um teste mais sensível (BARBOSA et al., 2003; GONZALEZ-FLECHA; LLESUY; BOVERIS, 1991; OLIVEIRA; CECCHINI, 2000). Procedimentos analíticos baseados em medidas de quimiluminescência caracterizam-se pela alta sensibilidade para detecção de radicais livres em baixas concentrações em soluções fisológicas. Este método torna a detecção possível mesmo em concentrações mínimas (atomol) (LAVER; STEVANIN; READ, 2008).

Luminescência é um termo empregado para descrever a emissão de radiação quando uma molécula ou átomo no estado excitado decai para o seu estado fundamental (DODEIGNE; THUNUS; LEJEUNE, 2000). Os vários tipos de luminescência são caracterizados em função da fonte de energia empregada para se obter o estado excitado. Na quimiluminescência, a energia de excitação é proporcionada por uma reação química, sendo a emissão de radiação observada

geralmente nas regiões do visível ou próximo do infravermelho (MERENYI; LIND; ERIKSEN, 1990).

Embora as duas técnicas (QL e TBARS), descritas acima, verifiquem a lesão oxidativa, não devem ser comparadas já que os produtos das reações avaliados por elas são diferentes. A QL avalia a formação de lipoperóxidos lipídicos, o que acontece num primeiro momento da reação de oxidação da membrana, enquanto TBARS quantifica a presença de aldeídos de baixa massa molecular como o MDA, que ocorre após a formação de hidroperóxidos lipídicos (TERRA et al., 2012b). Além disso, a reação de quimiluminescência reflete o estresse oxidativo prévio sofrido pelo tecido pela ação dos radicais livres, assim como, o consumo das defesas antioxidantes com conseqüente formação de hidrolipoperóxidos, responsáveis pela emissão de fótons (GONZALEZ-FLECHA; LLESUY; BOVERIS, 1991; GUARNIER et al., 2010; PERES et al., 2011).

Neste estudo, nós usamos a reação por quimiluminescência, iniciada por tert-butil hidroperóxido (GONZALEZ-FLECHA; LLESUY; BOVERIS, 1991), para analisar os níveis de hidroperóxidos, na pele de camundongos swiss e hairless, imediatamente, 6hs e 24hs após a irradiação UVB. Nossos resultados mostraram moderada emissão de fótons durante a reação de QL, imediatamente após a irradiação enquanto que após 24hs observou-se alta emissão de fótons, resultando numa lesão oxidativa mais intensa neste tempo. Em contraste, baixos níveis de substâncias reativas ao ácido tiobarbitúrico (TBARS), principalmente MDA foram observados tanto imediatamente quanto em 24hs após o UVB, indicando que a reação de liperoxidação na pele irradiada por UVB tende a formar hidroperóxidos lipídicos (TERRA et al., 2012). Este fenômeno pode ser explicado pela presença de antioxidantes que protegem a pele da desestabilização de membrana e propagação da cadeia de lipoperoxidação após a radiação UVB, como por exemplo, o ácido cis-urânico e trans urânico, dois componentes da epiderme que foram descridos como os maiores scavengers de radicais livres da pele (KAMMEYER et al., 1999).

Além disso, Wei et al. (2002), demonstrou que a formação de MDA reflete o efeito crônico, ou seja, a exposição repetida à radiação UVB na pele, além disso, o autor sugere a geração de H_2O_2 como marcador da resposta aguda da radiação UVB na pele. Nós sugerimos que a formação de hidroperóxidos lipídicos possa ser o marcador da resposta aguda da radiação UVB na pele (TERRA et al., 2012b).

O estresse oxidativo na pele pode ser avaliado também de maneira indireta através de possíveis desequilíbrios no sistema antioxidante, promovido pela irradiação UVB. Desta maneira, a avaliação do sistema antioxidante total por QL ou a determinação de uma enzima com atividade antioxidante como a CAT ou a SOD, além dos níveis de GSH e GSSG, através de técnicas espectrofotométricas, pode fornecer parâmetros importantes. Como já descrito anteriormente, nós evidenciamos o estresse oxidativo na pele após radiação UVB, também pelo desequilíbrio nas defesas antioxidantes, demonstrando a inversão na razão GSH/GSSG, levando a GSSG/GSH e pela diminuição na atividade da CAT (TERRA et al., 2012b).

A capacidade antioxidante total (TRAP) pode ser determinada por quimiluminescência e reflete o equilíbrio entre a ação conjunta de antioxidantes de baixa massa molecular e espécies oxidantes, portanto pode fornecer uma informação mais relevante do que a determinação da concentração isolada de um determinado antioxidante (GHISELLI; SERAFINI; NATELLA, 2000). Terra et al. (2012b), verificou diminuição das capacidade antioxidantes total na pele de camundongos swiss imediatamente após e 6h após a irradiação UVB enquanto que na pele de camundongos hairless a diminuição significativa ocorreu após 6h da radiação.

No nosso estudo demonstramos o balanço oxidativo na pele após 0, 6 e 24hs da irradiação aguda por UVB, pelas técnicas descritas, assim como a modulação da proliferação celular pelo NO por imunohistoquímica. Sugerimos a utilização deste modelo experimental e a utilização dos mesmos parâmetros de avaliação para demonstrar com segurança a atividade antioxidante de compostos naturais ou sintéticos.

Os resultados obtidos durante este estudo foram descritos conforme artigos em anexo, 2 publicados (Apêndice 1 e 2) e 2 submetidos (Apêndice 3 e 4).

2 JUSTIFICATIVA

O presente estudo apresenta a importante participação do NO na lesão da pele e na proliferação celular após a radiação UVB, avaliando resultados contraditórios apresentados anteriormente na literatura científica e garantindo o estudo dos mecanismos protetores das substâncias antioxidantes com maior eficácia e segurança podendo contribuir no avanço na pesquisa contra o envelhecimento e doenças cutâneas malignas.

3 OBJETIVOS

3.1 OBJETIVO GERAL

- Conhecer as principais espécies reativas envolvidas na lesão oxidativa/nitrosativa da pele após diferentes tempos da radiação UVB, bem como a participação do NO na modulação da proliferação celular, caracterizando um modelo experimental *in vivo*, que possibilite o estudo dos mecanismos protetores das substâncias antioxidantes garantindo maior eficácia e segurança nos resultados.

3.2 OBJETIVOS ESPECÍFICOS

- Investigar as principais espécies reativas envolvidas no estresse oxidativo e nitrosativo da pele de camundongos imediatamente, 6hs e 24hs após a radiação UVB.
- Investigar o efeito modulador do NO sobre a proliferação celular na pele após 24hs da radiação UVB.
- Caracterizar o modelo experimental em pele de camundongo hairless submetidos à radiação UVB, para que os parâmetros utilizados para avaliar o estresse oxidativo/nitrosativo e a proliferação celular, possam ser utilizados com segurança e eficácia na investigação do efeito e mecanismo protetor de diferentes substâncias antioxidante.
- Utilizar a genisteína, flavonoide com capacidade antioxidante reconhecida para avaliar sua ação protetora contra o estresse nitrosativo da pele após 24hs da radiação UVB, elucidando os mecanismos protetores envolvidos.
- Adaptar e validar a técnica que descreve a reação do NO com H_2O_2-luminol durante a reação de quimiluminescência

para amostras biológicas de pele, a fresco e congeladas, utilizando sistemas químicos doadores de NO (NPS e KI-$NaNO_3/H_2SO_4$) e os inibidores cPTIO, manitol, histidina e SOD, específicos para NO, $^{\bullet}OH$, $^1O_2$ e $^{\bullet}O_2^-$, respectivamente.

REFERÊNCIAS

AFAQ, F. et al. Delphinidin, an anthocyanidin in pigmented fruits and vegetables, protects human HaCaT keratinocytes and mouse skin against UVB-mediated oxidative stress and apoptosis. **Journal of Investigative Dermatology**, Baltimore, v. 127, p. 222-232, 2007.

AITKEN, G. R. et al. Direct monitoring of UV-induced free radical generation in HaCaT keratinocytes. **Clinical and Experimental Dermatology**, Oxford, v. 32, p. 722–727, 2007.

ALDERTON, W. K.; COOPER, C. E.; KNOWLES, R. G. Nitric oxide synthases: structure, function, and inhibition. **Biochemical Journal**, London, v. 357, p. 593-615, 2001.

ANAYA-PRADO, R. et al. Ischemia/reperfusion injury. **Journal of Surgical Research**, New York, v. 105, n. 2, p. 248-258, 2002.

ARANY, I. et al. Regulation of inducible nitric oxide synthase mRNA levels by differentiation and cytokines in human keratinocytes. **Biochemical and Biophysical Research Communications**, New York, v. 220, n. 3, p. 618-22, 1996.

ARCHER, S. L. et al. Preparation of standarts and measurement of nitric oxide, nitroxyl and related oxidation products. **Methods**, San Diego, v. 7, n. 1, p. 21-34, 1995.

ARMSTRONG, B. K.; KRICKER, A. The epidemiology of UV induced skin cancer. **Journal of Photochemistry and Photobiology: Biology B**, Lausanne, v. 63, p. 8-18, 2001.

ARORA, A.; NAIR, M.G.; STRASBURG, M. Antioxidant activities of isoflavones and their biological metabolities in a liposomal system. **Archives of Biochemistry and Biophysics**, New York, v. 356, n. 2, p. 133-141, 1998.

BARBOSA, D. S. et al. Decrease oxidative stress in patients with ulcerative colitis. **Nutrition**, Burbank, v. 19, n. 10, p. 837-842, 2003.

BARREIRO, E. et al. Both oxidtive and nitrosative stress are associated with muscle wasting in tumour-bearing rats. **Federation of European Bio-chemical Societies Letters**, Amsterdam, v. 579, n. 7, p.1646-1652, 2005.

BARRESI, C. et al. Increased Sensitivity of Histidinemic Mice to UVB Radiation Suggests a Crucial Role of Endogenous Urocanic Acid in Photoprotection. **Journal of Investigative Dermatology**, Baltimore, v. 131, n. 1, p.188-194, 2011.

BATES, D. O. et al. VEGF165b, an inhibitory splice variant of vascular endothelial growth factor, is down-regulated in renal cell carcinoma. **Cancer Research**, Baltimore, v. 62, n. 14, p. 4123-31, 2002.

BEEHLER, B. C. et al. Formation of 8-hydroxydeoxyguanosine within DNA of mouse keratinocytes exposed in culture to UVB and H_2O_2. **Carcinogenesis**, Oxford, v. 13, n. 11, p. 2003-2007, 1992.

BHOWMICK R.; GIROTTI A. W. Rapid upregulation of cytoprotective nitric oxide in breast tumor cells subjected to a photodynamic therapy-like oxidative challenge. **Photochemistry and Photobiology**, Lawrence, v. 87, n. 2, p. 378-386, 2011.

BIALY, T. L. et al. Dietary factors in the prevention and treatment of nonmelanoma skin cancer and melanoma. **Dermatologic Surgery**, New York, v. 28, n. 12, p. 1143, 2002.

BIAN, K.; MURAD, F. Nitric oxide (NO): biogeneration, regulation, and relevance to human diseases. Frontiers in Bioscience, Searington, v. 8, p. d264-278, 2003.

BICKERS, D. R.; ATHAR, M. Oxidative stress in the pathogenesis of skin disease. **Journal of Investigative Dermatology**, Baltimore, v. 126, p. 2565-2575, 2006.

BIRCH-MACHIN, M. A; SWALWELL, H. How mitochondria record the effects of UV exposure and oxidative stress using human skin as a model tissue. **Mutagênese**, Oxford, v. 25, n. 2, p. 101-107, 2010.

BRENNEISEN, P. et al. Central role of ferrous/ferric iron in the ultraviolet B irradiation-mediated signaling pathway leading to increased interstitial collagenase (matrix-degrading metalloprotease (MMP)-1) and stromelysin-1 (MMP-3) mRNA levels in cultured human dermal fibroblasts. **Journal of Biological Chemistry**, Baltimore, v. 273, n. 9, p. 5279-5287, 1998.

BROWN, G. C. Nitric oxide and mitocondrial respiration. **Biochemical et Biophysica Acta**, Amsterdam, v. 1411, n. 2-3, p. 351-369, 1999.

CARINI, M. et al. Fluorescent probes as markers of oxidative stress in keratinocyte cell lines following UVB exposure. **Farmaco**, Paris, v. 55, n. 8, p. 526-534, 2000.

CARMELIET, P.; COLLEN, D. Transgenic mouse models in angiogenesis and cardiovascular disease. **The Journal of pathology**, London, v. 190, n. 3, p. 387-405, 2000.

CASAGRANDE, R. et al. Protective effect of topical formulations containing quercetin against UVB-induced oxidative stress in hairless mice. **Journal of Photochemistry and Photobiology: Biology B**, Lausanne, v. 84, n. 1, p. 21-27, 2006.

CECCHINI, R.; ARUOMA, O. I.; HALLIWELL, B. The action of hydrogen peroxide on the formation of thiobarbituric acid-reactive material from microsomes or from DNA damage by bleomycin or o-phenanthroline. Artefacts in the thiobarbituric acid test. **Free Radical Research Communications**, New York, v. 10, n. 4/5, p. 245-258, 1990.

CHA, M. S. et al. Endogenous production of nitric oxide by vascular endothelial growth factor down-regulates proliferation of choriocarcinoma cells. **Biochemical and Biophysical Research Communications**, New York, n. 282, n. 4, p.1061-1066, 2001.

CLYDESDALE, G. J.; DANDIE, G. W.; MULLER, H. K. Ultraviolet light induced injury: Immunological and inflammatory effects. **Immunology and Cell Biology**, London, v. 79, n. 6, p. 547-568, 2001.

COLADO SIMÃO, A. N. et al. Genistein abrogates pre-hemolytic and oxidative stress damage induced by 2,2'-Azobis (Amidinopropane). **Life Sciences**, Oxford, v. 78, n. 11, p. 1202-1210, 2005.

COOPER, C. E. Nitric oxide and irons proteins. **Biochemica et Biophysica Acta**, Amsterdam, v. 1411, p. 290-309, 1999.

CREMONESE, R. V.; PEREIRA-FILHO, A. A.; MAGALHAES, R. Experimental cirrhosis induced by carbon tetrachloride inhalation: technical modifications and lipoperoxidation effects. **Arquivos de Gastroenterologia**, São Paulo, v. 38, n. 1, p. 40-47, 2001.

DELICONSTANTINOS, G.; VILLIOTOU, V.; STAVRIDES, C. J. Increase of particular nitric oxide synthase activity and peroxynitrite synthesis in UVB-irradiated keratinocyte membranes. **The Biochemical Society**, London, v. 320, p. 997-1003, 1996.

DJURIC, Z. et al. Effects of soy isoflavone supplementation on markers of oxidative stress in men and women. **Cancer Letters**, Amsterdam, v. 172, n. 1, p. 1-6, 2001.

DODEIGNE, C.; THUNUS, L.; LEJEUNE, A. Chemiluminescence as a diagnostic tool: a review. **Talanta**, Oxford, v. 51, n. 3, p. 415-439, 2000.

DU, M. et al. Promotion of proliferation of murine BALB , C3T3 fibroblasts mediated by nitric oxide at lower concentrations. **Biochemistry and molecular biology international**, Sydney, v. 41, n. 3, p. 625- 631, 1997.

EGBRINK, O. et al. Regulation of microvascular thromboembolism in vivo. **Microcirculation**, New York, v. 12, n. 3, p. 287-300, 2005.

EL-ABASERI, T. B.; PUTTA, S.;HANSEN, L. A. Ultraviolet irradiation induces keratinocyte proliferation and epidermal hyperplasia through the activation of the

epidermal growth factor receptor. **Carcinogenesis**, Oxford, v. 27, n. 2, p. 225-31, 2006.

FARIAS-EISNER, R. et al. The chemistry and tumoricidal activity of nitric oxide/hydrogen peroxide and the implications to cell resistence/susceptibility**. Journal of Biological Chemical**, Baltimore, v. 271, n. 11 p. 6144-6151, mar. 1996.

FERREIRA, A. L. A.; MATSUBARA, L. S. Radicais livres: conceitos, doenças relacionadas, sistema de defesa e estresse oxidativo. **Revista da Associação Médica Brasileira**, São Paulo, v. 43, p. 61-68, 1997.

FONSECA, Y. M. et al. Efficacy of marigold extract-loaded formulations against UV-induced oxidative stress. **Journal of Pharmaceutical Sciences**, Washington, v. 100, n. 6, p. 2182-2193, 2011.

FRANK, S. et al. Identification of copper o zinc superoxide dismutase as a nitric oxide regulated gene in human (HaCaT) keratinocytes: implications for keratinocyte proliferation. **The Biochemical Society**, London, v. 346, p. 719–728, 2000.

FREEMAN, B. Free radical chemistry of nitric oxide: looking at the dark side. **Chest**, Chicago, v. 105, n. 3, p. 79-84, 1994.

FUCHS, J. et al. Impairment of enzymic and nonenzymic antioxidants in skin by UVB irradiation. **Journal of Investigative Dermatology**, Baltimore, v. 93, p. 769-773, 1989.

FUJII, E. et al. Role of nitric oxide, prostaglandins and tyrosine kinase in vascular endothelial growth factor-induced increase in vascular permeability in mouse skin. **Naunyn-Schmiedeberg's Archives of Pharmacology**, Berlin, n. 356, n. 4, p. 475-80, 1997.

FUKUTO, J. M. Chemistry of nitric oxide: biologically relevant aspects. **Advances in Pharmacology**, San Diego, v. 34, p. 1-15. 1995.

FUKUTO, J. M.; CHAUDHURI, G. Inhibition of constitutive and inducible nitric oxide synthase: potential selective inhibition. **Annual Review of Pharmacology and Toxicology**, Palo Alto, Califórnia, v. 35, p. 165-194, 1995.

GANSAUGE, S. et al. Exogenous, but not endogenous, nitric oxide increases proliferation rates in senescent human fibroblasts. **Federation of European Biochemical Societies Letters**, Amsterdam, v. 410, p. 160-164, 1997.

GEARY, W. A.; COOPER, P.H. Proliferating cell nuclear antigen PCNA in common epidermal lesions. **Journal of Cutaneous Pathology**, Copenhagen, v. 19, p. 458-468, 1992.

GERBER, H. P. et al. VEGF is required for growth and survival in neonatal mice. **Development**, Cambridge, v. 126, p. 1149-1159, 1999.

GHISELLI, A.; SERAFINI, M.; NATELLA, F. Total antioxidant capacity as a tool to assess redox status: critical view and experimental data. **Free Radical Biology & Medicine**, New York, v. 29, p. 1106-1114, 2000.

GONZALEZ-FLECHA, B.; LLESUY, S.; BOVERIS, A. Hydroperoxide-initiated chemiluminescence: an assay for oxidative stress in biopsies of heart, liver, and muscle. **Free Radical Biology & Medicine**, New York, v. 10, p. 93-100, 1991.

GONZALEZ-MAGLIO, D. H. et al. Skin damage and mitochondrial dysfunction after acute ultraviolet B irradiation: relationship with nitric oxide production. **Photodermatology Photoimmunology and Photomedicine**, Oxford, v. 21, p. 311-317, 2005.

GOUREAU, O. et al. Differential regulation of inducible nitric oxide synthase by fibroblast growth factors and trans- forming growth factor β in bovine retinal pigmented epithelial cells: inverse correlation with cellular proliferation. **Proceedings of the National Academy of Sciences of the United States of America**, Washington, v. 90, p. 4276-4280, 1993.

GREENBERG, S. S. et al. Giles, nitro containing L-arginine analogs interfere with assays for nitrate and nitrite. **Life Sciences**, Oxford, v. 57, p. 1949-1961. 1995.

GRONBERG, A. et al. Antioxidants protect keratinocytes against M. ulcerans mycolactone cytotoxicity, **PLoS One**, San Francisco, v. 5, p. e13839, 2010.

GROSSMAN, N. et al. 780 nm low power diode laser irradiation stimulates proliferation of keratinocyte cultures: involvement of reactive oxygen species. **Lasers in Surgery and Medicine**, New York, v. 22, p. 212-218, 1998.

GUARATINI, T.; MEDEIROS, M. H. G.; COLEPICOLO, P. Antioxidantes na manutenção do equilíbrio redox cutâneo: uso e avaliação de sua eficácia. **Química Nova**, São Paulo, v. 30, p. 206-213, 2007.

GUARNIER, F. A. et al. Time course of skeletal muscle loss and oxidative stress in rats with Walker 256 solid tumor. **Muscle & Nerve**, New York, v. 42, p. 950-958, 2010.

HAKOZAKI, T. et al. Visualization and characterization of UVB-induced reactive oxygen species in a human skin equivalent model. **Archives of Dermatological Research**, Berlin, v. 300, p. 51-56, 2008.

HALLIWELL, B.; GUTTERIDGE, J. M. C. **Free radicals in biology and medicine**. 4. ed. New York: Oxford, 2007.

HANADA, K.; GANGE, R.W.; CONNOR, M.J. Effect of glutathione depletion on sunburn cell formation in the hairless mouse, **Journal of Investigative Dermatology**, Baltimore, v. 96, p. 838-840, 1991.

HARRIS, M. I. C. **Pele**: estrutura, propriedades e envelhecimento. 2. ed. São Paulo: SENAC, 2005.

HECK, D. et al. UVB light stimulates production of reactive oxygen species: unexpected role for catalase. **Journal of Biological Chemistry**, Baltimore, v. 278, p. 22432-22436, 2003.

ICHIHASHI, M. et al. UV-induced skin damage. **Toxicology**, Amsterdam, v. 189, p. 21-39, 2003.

IGNARRO, L. J. Biosynthesis and metabolism of endothelium-derived nitric oxide. **Annual Review of Pharmacology and Toxicology**, Palo Alto, v. 30, p. 535-560, 1990.

IKEHATA, H. et al. Mutation spectrum in sunlight exposed mouse skin epidermis: small but appreciable contribution of oxidative stress-mediated mutagenesis. **Mutation Research**, Amsterdam, v. 556, p. 11–24, 2004.

JASKULSKI, D. et al. Inhibition of cellular proliferation by antisense oligodeoxynucleotides to PCNA cyclin. **Science**, New York, v. 240, p. 1544-1546, 1988.

JEON, S. E. et al. Dietary supplementation of (+)-catechin protects against UVB-induced skin damage by modulating antioxidant enzyme activities. **Photodermatology Photoimmunology and Photomedicine**, Oxford, v. 19, p. 235-241, 2003.

KAMMEYER, A. et al. Urocanic acid isomers are good hydroxyl radical scavengers:a comparative study with structural analogues and with uric acid. **Biochimica et Biophysica Acta**, Amsterdam, v. 1428, p. 117-120, 1999.

KANNO, S. et al. Attenuation of myocardial ischemia/reperfusion injury by superinduction of inducible nitric oxide synthase. **Circulation**, Hagerstown, n. 23, p. 2742-2748, 2000.

KAWAHIRA, K. Immunohistochemical staining of proliferating cell nuclear antigen (PCNA) in malignant and non malignant skin diseases. **Archives of Dermatological Research**, Berlin, v. 291, p.413-418, 1999.

KELM, M. et al. Quantitative and kinetic characterization of nitric oside and EDRF released from culture endothelial cells. **Biochemical and Biophysical Research Communications**, New York, n. 154, p. 236-244, 1988.

KENDALL, H. K.; MARSHALL, R. I.; BARTOLD, N. P. M. Nitric oxide and tissue destruction. **Oral Diseases**, Copenhagen, v. 7, p. 2-10, 2001.

KERWIN, J. F.; LANCASTER, J. R.; FELDMAN, P. L. Nitric oxide: a new paradigm for second messengers. **Journal of Medicinal**, Washington, n. 27, p. 4343-4362, 1995.

KHANNA, A.; COWLED, P. A.; FITRIDGE, R. A. Nitric oxide and skeletal muscle reperfusion injury: current controversies (Research Review). **Journal of Sugical Research**, New York, v. 128, p. 98-107, 2005.

KIKUCHI, K. et al. Detection of nitric oxide production from a perfused organ by a luminol-H202 system. **Analytical Chemistry**, Washington, v. 65, p.1794-1799, 1993a.

KIKUCHI, K. et al. Real time measurement of nitric oxide produced ex vivo by luminol-H202 chemiluminescence method. **Journal of Biological Chemistry,** Baltimore, v 268, p. 23106-23110, 1993b.

KOHEN, R. Skin antioxidants: their role in aging and in oxidative stress-New approaches for their evaluation. **Biomedicine and Pharmacotherapy**, New York, v. 53, p. 181-192, 1999.

KOHEN, R.; FANBERSTEIN, D.; TIROSH, O. Reducing equivalents in the aging process. **Archives of Gerontology and Geriatrics**, Amsterdam, v. 24, p. 103-123, 1997.

KOHEN, R.; GATI, I. Skin low molecular weight antioxidants and their role in aging and in oxidative stress. **Toxicology**, Amsterdam, v. 148, p. 149-157, 2000.

KRISCHEL, V. et al. Biphasic effect of exogenous nitric oxide on proliferation and differentiation in skin derived keratinocytes but not fibroblasts. **Journal of Investigative Dermatology**, Baltimore, v. 111, p. 286-291, 1998.

KRUSZEWSKI, M. Labile iron pool: the main determinant of cellular response to oxidative stress. **Mutation Research**, Amsterdam, v. 531, p. 81-92, 2003.

KVAM, E.; DAHLE, J. Pigmented Melanocytes Are Protected Against Ultraviolet-A-Induced Membrane Damage. **Journal of Investigative Dermatology**, Baltimore, v. 121, p. 564-569, 2003.

LAVER, J. R.; STEVANIN, T. M.; READ, R. Chemiluminescence quantification of NO and its derivatives in Liquid Samples. **Methods in Enzymology**, New York, v. 436, p. 113-127, 2008.

LEE, S. C. et al. Protective role of nitric oxide-mediated inflammatory response against lipid peroxidation in ultraviolet B-irradiated skin. **British Journal of Dermatology**, Oxford, v. 142, p. 653-659, 2000.

LINTON, S.; DAVIES, M. J.; DEAN, R. T. Protein oxidation and ageing. **Experimental Gerontology**, New York, v. 36, p. 1503-1518, 2001.

LIU, Z. et al. Benzo(a)-pyrene enhances the formation of 8-hydroxyguanosisne by ultraviolet radiation in claf thymus DNA and human epidermoid carcinoma cells. **Biochemistry**, Washington, v. 37, p. 10307-10312, 1998.

LIUDET, L.; SORIANO, F. G.; SZABO, C. Biology of nitric oxide signaling. **Critical Care Medicine**, New York, v. 28, p. N37-N52, 2000.

MARSHALL, K. et al. The neuronal toxicity of sulfite plus peroxynitrite is enhanced by glutathione depletation: Implications for Parkinson's disease. **Free Radicals Biology and Medicine**, New York, v. 27, p. 515-520, 1999.

MARTIN, J. P.; BURCH, P. Production of oxygen radicals by photosensitization. **Methods in Enzymology**, New York, v.186, p. 635-645, 1990.

MASAKI, H.; ATSUMI, T.; SAKURAI, H. Detection of hydrogen peroxide and hydroxyl radicals in murine skin fibroblasts under UVB irradiation. **Biochemical and Biophysical Research Communications**, New York, v. 206, n. 2, p. 474-479, 1995.

MATHEWS, M. B. et al. Identity of the proliferating cell nuclear antigen and cyclin. **Nature**, London, v. 309, p. 374-376, 1984.

MATSUBARA, L. S.; MACHADO, P. E. A. Age-related changes of glutathione content, glutathione reductase and glutathione peroxidase activity of human erytrocytes. **Brazilian Journal of Medical and Biological Research**, São Paulo, v. 24, n. 5, p. 449-454, 1991.

MERENYI, G.; LIND, J.; ERIKSEN, T.E. Luminol chemiluminescence: chemistry, excitation, emitter. **Jounal of Bioluminescence and Chemiluminescence**, Sussex, v. 5, n. 1, p. 53-56, 1990.

MILES, A. M. et al. Modulation of superoxide-dependent oxidation and hydroxylation reactions by nitric oxide. **Journal of Biologycal Chemistry**, Baltimore, v. 271, p. 40-47, 1996.

MIYACHI, K.; FRITZLER, M. J.; TAN, E. M. Autoantibody to an nuclear antigen in proliferating cells. **Journal of Immunology**, Baltimore, v. 121, p. 2228-2233, 1978.

MOORE, J. O. et al. Effects of ultraviolet B exposure on the expression of proliferating cell nuclear antigen in murine skin. **Photochemistry and Photobiology**, Lawrence, v. 80, p. 587-595, 2004.

MOWBRAY, M. et al. Enzyme-independent NO stores in human skin: quantification and influence of UV radiation. **Journal of Investigative Dermatology**, Baltimore, v. 129, p. 834-842, 2009.

MURAMATSU, S. et al. Differentiation-specific localization of catalase and hydrogen peroxide, and their alterations in rat skin exposed to ultraviolet B rays. **Journal of Dermatological Science**, Amsterdam, v. 37, p. 151-158, 2005.

NAGASE, S. et al. A novel nonenxymatic pathway for the generation of nitric oxide by the reaction of hydrogen peroxide and D- or L-arginine, 233 (1997) 150-153, 1997.

NATHAN, C. Nitric oxide as a secretory product of mammalian cells. **FASEB Journal**, Bethesda, v. 6, p. 3051-3064, 1992.

NATHAN, C.; XIE, Q. W. Nitric oxide synthases: roles, tolls and controls. **Cell**, Cambridge, v. 78, p. 915-918, 1994.

NICOL, D. et al. Vascular endotelial growth factor expression is increased in renal cell carcinoma. **Journal of Urology**, Baltimore, v. 157, p. 1482-86, 1997.

NORONHA-DUTRA, A. A.; EPPERLEIN, M. M.; WOOLF, N. Reaction of nitric oxide with hydrogen peroxide to produce potentially cytotoxic singlet oxygen as a model for nitric oxide-mediated killing. **Federation of European Bio-chemical Societies Letters**, Amsterdam, v. 1, p. 59-62, 1993.

OGURA, R. et al. Mechanism of lipid formation following exposure of epidermal homogenate to ultraviolet light. **Journal of Investigative Dermatology**, Baltimore, v. 97, 1044-1047, 1991.

OHKAWA, H.; NOBUKO, O.; YAGI, K. Assay for lipid peroxidation in animal tissues by thiobarbituric acid reaction. **Analytical Biochemistry**, New York, v. 95, p. 351, 1979.

OLIVEIRA, F. J. D. A.; CECCHINI, R. Oxidative stress of liver in hamster infected with Leishmania (L) chagasi. **Journal of Parasitology**, Lawrence, v. 86, p.1067-1072, 2000.

OSTENDORF, T. et al. Inducible nitric oxide synthase-derived nitric oxide promotes glomerular angiogenesis via upregulation of vascular endothelial growth factor receptors. **Journal of the American Society of Nephrology**, Hagerstown, v. 15, p. 2307-2319, 2004.

PEAK, M. J.; PEAK, J. G. Solar-ultraviolet-induced damage to DNA. **Photo-Dermatology**, Copenhagen, v. 6, p. 1-15, 1982.

PERES, P. S. et al. Photoaging and chronological aging profile: understanding oxidation of the skin, **Journal of photochemistry and photobiology. B, Biology**, Lausanne, v. 103, p. 93-97, 2011.

PODDA, M. et al. UV-irradiation depletes antioxidants and causes oxidative damage in a model of human skin. **Free Radical Biology & Medicine**, New York, v. 24, p. 55-65, 1998.

PRYOR, W. A.; SQUADRITO, G. L. The chemistry of peroxynitrite: a product from the reaction of nitric oxide with superoxide**. American Journal of Physiology**, Washington, v. 268 p. 699-722, 1995.

QURESHI, A. A. et al. Langerhans cells express inducible nitric oxide synthase and produce nitric oxide. **Journal of Investigative Dermatology**, Baltimore, v. 107, p. 815-21, 1996.

RADI, R. et al. Peroxynitrite-induced luminol chemiluminescence. **Biochemical Journal**, London, v. 290, p. 51-57, 1993.

RADI, R. et al. Peroxynitrite-induced membrane lipid peroxidation: the cytotoxic potential of superoxide and nitric oxide. **Archives of Biochemistry and Biophysics**, New York, p. 288, p. 481-87, 1991.

RADI, R. Nitric oxide, oxidants, and protein tyrosine nitration. **Proceedings of the National Academy of Sciences of the United States of America**, Washington, v. 101 p. 4003-4008, 2004.

ROCHA, I. M.; GUILLO, L. A. Lipopolysaccharide and cytokines induce nitric oxide synthase and produce nitric oxide in cultured normal human melanocytes. **Archives of Dermatological Research**, Berlin, v. 293, p. 245-48, 2001.

ROSEN, J. E.; PRAHALAD, A. K, WILLIAMS, G. W. 8-Oxodeoxyguanosine formation in the DNA of cultured cells after exposure to H2O2 alone or with UVA irradiation formation in the DNA of cultured cells after exposure to H2O2 alone or with UVA irradiation. **Journal of Photochemistry and Photobiology. B, Biology**, Lausanne, 64, p. 117-122, 1996.

ROVER, L. J. et al. Sistema antioxidante envolvendo o ciclo metabólico da glutationa associado a métodos eletroanalíticos na avaliação do estresse oxidativo. **Química Nova**, São Paulo, v. 24, p. 112-119, 2001.

SAIJA, A. et al. In vitro and in vivo evaluation of caffeic and ferulic acids as topical photoprotective agents. **International Journal of Pharmaceutics**, Amsterdam, v. 199, p.39-47, 2000.

SEN, N. et al. Nitric oxide-induced nuclear GAPDH activates p300/CBP and mediates apoptosis. **Nature Cell Biology**, London, v. 10, p. 866-73, 2008.

SHAW, A. W.; VOSPER, A. J.; J. Chem. Soc. Faraday Trans. 1977, 8, 1239. Comut

SHINDO, Y.; WITT, E.; PACKER, L. Anti-oxidant defense mechanisms in murine epidermis and dermis their responses to ultraviolet light. **Journal of Investigative Dermatology**, Baltimore, v. 100, p. 260-265, 1993.

SIMÃO, A. N. C. et al. Genistein abrogates pre-hemolytic and oxidative stress damage induced by 2,2-azobis(amidinopropane). **Life Sciences**, Oxford, v. 78, n. 11, p. 1202-1210, 2006.

STANKEVICIUS, E. et al. Role of nitric oxide and other endothelium-derived factors. **Medivina**, Kaunas, v. 39, p. 4, 2003.

TAO, J. et al. Endogenous production of nitric oxide contributes to proliferation effect of vascular endothelial growth factor-induced malignant melanoma cells. **Clinical and Experimental Dermatology**, Oxford, v. 31, p. 94-99, 2005.

TERRA, V. A. et al. Nitric oxide is responsible for oxidative skin injury and modulation of cell proliferation after 24 hours of UVB exposures. **Free Radical Research**, London, v. 46, n. 7, p. 872-882, 2012a.

TERRA, V. A. et al. Time-dependent reactive species formation and oxidative stress damage in the skin after UVB irradiation. **Journal of Photochemistry and Photobiology B: Biology,** Lausanne, v. 109, p. 34-41, 2012b.

TSATMALI, M. et al. Alpha-MSH inhibits lipopolysaccharide induced nitric oxide production in B16 mouse melanoma cells. **Annals of the New York Academy of Sciences**, New York, v. 885, p. 474-76, 1999.

TSUKADA, Y. et al. Real-time measurement of nitric oxide by luminol-hydrogen peroxide reaction in crystalloid perfused rat heart. **Life Sciences**, Oxford, v. 72, p. 989-1000, 2003.

URRUTICOECHEA, A.; SMITH, I. E.; DOWSETT, M. Proliferation marker Ki-67 in early breast. **Journal of Clinical Oncology**, New York, v. 23, n. 28, p. 7212-20, 2005.

VAYALIL, P. K.; ELMETS, C. A.; KATIYAR, S. K. Treatment of green tea polyphenols in hydrophilic cream prevents UVB-induced oxidation of lipids and proteins, depletion of antioxidant enzymes and phosphorylation of MAPK proteins in SKH-1 hairless mouse skin. **Carcinogenesis**, Oxford, v. 24, p. 927-936, 2003.

VILE, F. G.; TYRRELL, R. M. UVA radiation-oxidative damage to lipids and proteins in vitro and in human skin fibroblasts is dependent on iron and singlet oxygen. **Free Radical Biology & Medicine**, New York, v. 18, p. 721-730, 1995.

VILLALOBO, A. Enhanced cell proliferation induced by nitric oxide. Dynamic Cell Biology, Baltimore, v. 1, p. 60-64, 2007.

VILLALOBO, A. Nitric oxide and cell proliferation. Federation of European Biochemical Societies Letters, Amsterdam, v. 273, p. 2329-2344, 2006.

VINTEN-JOHANSEN, J. Involvement of neutrophils in the pathogenesis of lethal myocardial reperfusion injury. **Cardiovascular Research**, London, v. 61, n. 3, p. 481-497, 2004.

WANG, L. et al. Nitric oxide synthase activation and oxidative stress, but not intracellular zinc dyshomeostasis, regulate ultraviolet B light-induced apoptosis. **Life Sciences**, Oxford, v. 86, p. 448-454, 2010.

WANG, R. et al. Human dermal fibroblasts produce nitric oxide and express both constitutive and inducible nitric oxide synthase isoforms. **Journal of Investigative Dermatology**, Baltimore, v.106, p. 419-427, 1996.

WATANABE, S.; UESUGI, S.; KIKUCHI, Y. Isoflavones for prevention of cancer, cardiovascular diseases, gynecological problems and possible immune potentiation**. Biomedicine & Pharmacotherapy**, New York, v. 56, n. 6, p. 302-312, 2002.

WEI, H. et al. Inhibition of ultraviolet light-induced oxidative events in the skin and internal organs of hairless mice by isoflavone genistein. **Cancer Letters**, Amsterdam, v. 185 p. 21-29, 2002.

WEI, H. et al. Singlet oxygen involvement in ultraviolet (254 nm) radiation-induced formation of 8-hydroxy-deoxyguanosine. **Free Radical Biology & Medicine**, New York, v. 23, n. 1, p. 148-154, 1997.

WELLER, R. et al. Autogous nitric oxide protects mouse and human keratinocytes from ultraviolet B radiation-induced apoptosis. **American Journal of Physiology. Cell Physiology**, Bethesda, v. 284, n. 5, p. 1140-48, 2003.

WHEELER, L. A. et al. Depletion of cutaneous glutathione and the induction of inflammation by 8-methxypsoralen plus UVA radiation, **Journal of Investigative Dermatology**, Baltimore, v. 87, p. 658-662, 1986.

WINK, D. A.; MITCHEL, J.B. Chemical biology of nitric oxide : insights into regulatory, cytotoxic and cytoprotective mechnisms of nitric oxide. **Free Radical Biology & Medicine**, New York, v. 25, n. 4-5, p. 434-456, 1998.

WU, S. et. al. Ultraviolet B light-induced nitric oxide/peroxynitrite imbalance in keratinocytes-implications for apoptosis and necrosis**. Journal of photochemistry and photobiology. B, Biology**, Lausanne, v. 86, p. 389-396, 2010.

YAAR, M.; GILCHREST, B. A. Photoageing: mechanism, prevention and therapy. **British Journal of Dermatology**, Oxford, v. 157, p. 874-887, 2007.

YASUI, H.; SAKURAI, H. Chemiluminescent detection and imaging of reactive oxygen species in live mouse skin exposed to UVA. **Biochemical and Biophysical**

Research Communications, **Biochemical and Biophysical Research Communications**, New York, v. 269, p. 131-136, 2000.

YIAKOUVAKI, A. et al. Caged-iron chelators a novel approach towards protecting skin cells against UVA-Induced necrotic cell death, **Journal of Investigative Dermatology**, Baltimore, v. 126, p. 2287-2295, 2006.

YILMAZ G. et al. Effect of nitric oxide on proliferation of human retina pigment epithelial cells. **Eye**, London, v. 14, p. 899-902, 2000.

YING, C. Y; PARRISH, J. A.; PATHAK, M. A. Additive erythemogenic effects of middle (280-320nm) and long (329-400nm) wave ultraviolet light. **Journal of Investigative Dermatology**, Baltimore, v. 63, p. 273-278, 1974.

ZHANG, B. S. et al. Induction of 8-hydroxy-20-deoxyguanosineby ultraviolet radiation in calf thymus DNA and HeLa cells. **Journal of Photochemistry and Photobiology. B, Biology**, Lausanne, v. 65, p. 119-124, 1997.

ZHONG, J. L. et al. Susceptibility of skin cells to UVA-induced necrotic cell death reflects the intracellular level of labile iron. **Journal of Investigative Dermatology**, Baltimore, v. 123, p. 771-780, 2004.

APÊNDICES

APÊNDICE 1 – Artigo 1: Time-dependent reactive species formation and oxidative stress damage in the skin after UVB irradiation.

Journal of Photochemistry and Photobiology B: Biology 109 (2012) 34–41

Contents lists available at SciVerse ScienceDirect

Journal of Photochemistry and Photobiology B: Biology

journal homepage: www.elsevier.com/locate/jphotobiol

Time-dependent reactive species formation and oxidative stress damage in the skin after UVB irradiation

V.A. Terra [a], F.P. Souza-Neto [a], R.C. Pereira [a], T.N.X. Silva [a], A.C.C. Costa [a], R.C. Luiz [a], R. Cecchini [b], A.L. Cecchini [a,*]

[a] Laboratory of Molecular Pathology, State University of Londrina, Brazil
[b] Laboratory of Pathophysiology and Free Radicals, State University of Londrina, Rodovia Celso Garcia Cid, PR-445, km 380, Campus Universitário, 86051-990 Londrina, PR, Brazil

ARTICLE INFO

Article history:
Received 18 October 2011
Received in revised form 17 January 2012
Accepted 19 January 2012
Available online 4 February 2012

Keywords:
Oxidative stress
Skin lipid peroxidation
Antioxidants
UVB irradiation
Reactive species
Nitric oxide

ABSTRACT

This study provides evidence that skin oxidative stress injury caused by UVB irradiation is mediated predominantly by reactive oxygen species immediately after irradiation and by reactive nitrogen species at later time points. Animals were pre-treated with free radical scavengers (deferrioxamine, histidine), α-tocopherol, or inhibitors of nitric oxide synthase (NOS) (L-NAME or aminoguanidine) or left untreated and subjected to UVB irradiation. α-Tocopherol inhibited the increase in lipid peroxidation, as evaluated by chemiluminescence at 0 h and 24 h after UVB irradiation. Immediately after UVB irradiation, lipid peroxidation increased moderately and was abolished by free radical scavengers but not by NOS inhibitors. Likewise, the reduction of antioxidant capacity was not reversed by NOS inhibitors. Nitric oxide augmentation was not observed at this time point. Twenty-four hours after irradiation, increased lipid peroxidation levels and nitric oxide elevation were observed and were prevented by NOS inhibitors. Low concentrations of GSH and reduced catalase activity were also observed. Altogether, these data indicate that reactive oxygen species (singlet oxygen and hydroxyl radicals) are the principal mediators of immediate damage and that reactive nitrogen species ($^{\cdot}NO$ and possibly $ONOO^-$) seem to be involved later in skin oxidative injury induced by UVB radiation. The reduced catalase activity and low level of GSH suggest that $^{\cdot}NO$ and H_2O_2 may react to generate $ONOO^-$, a very strong lipid peroxidant species.

1. Introduction

UVB light stimulates production of reactive species that are the main cause of the resulting skin lesions and result in accelerated aging [1] and the development of malignant skin diseases [2–4]. Exposure of skin cells to UVB induces an immediate release of labile iron [5], which can catalyze production of the highly toxic hydroxyl radical ($^{\cdot}OH$) via the Fenton reaction [6]. The strong iron chelator desferrioxamine (DFX) has been used to demonstrate the participation of $^{\cdot}OH$ in oxidative cell injury [7–9], while histidine (HIST), an efficient scavenger of singlet oxygen ($^1O_2$) [10], has been employed to show the involvement of that species as well. $^{\cdot}OH$ is the primary reactive oxygen species responsible for the formation of lipid radicals in the epidermis following exposure to UV light [11]. UVA-induced iron- and $^1O_2$-dependent oxidative damage to lipids and proteins has been observed *in vitro* and in human skin fibroblasts [12].

The reactive species $^1O_2$, $^{\cdot}OH$, hydrogen peroxide (H_2O_2), peroxynitrite ($ONOO^-$), and nitric oxide ($^{\cdot}NO$) have been demonstrated to be generated during UVB light-stimulated photosensitization [11–19]. Wei et al. [20] showed that H_2O_2 is part of the acute skin response to UVB exposure and can be generated by keratinocytes and infiltrating neutrophils. Recently, Mowbray et al. [22] have shown an enzyme-independent release of $^{\cdot}NO$ in human skin sweat a few hours after UVB irradiation. UV also induces iNOS expression, with the maximal mRNA level occurring 24 h postirradiation in hairless mice [23] and in human skin [24]. Although there is evidence that reactive species participates on UVB induced lipid peroxidation, some studies have also suggested that $^{\cdot}NO$ has a protective effect against lipid peroxidation after UVB irradiation [23,25].

The involvement of free radicals in the skin lesions induced by UVB irradiation is well-established, and while antioxidants have been used in an attempt to limit the damage, the choice of antioxidant is random, as the particular reactive species produced in this situation are not known. However, the skin is known to use a network of antioxidant systems to maintain the intracellular redox balance and counteract oxidative stress [26]. The skin has an endogenous antioxidant system comprising both antioxidant

* Corresponding author. Address: Department of General Pathology, Laboratory of Molecular Pathology, State University of Londrina, 86051-990 Londrina, PR, Brazil. Tel.: +55 43 3371 4521; fax: +55 43 3371 4267.
E-mail address: alcecchini@uel.br (A.L. Cecchini).

1011-1344/$ - see front matter © 2012 Elsevier B.V. All rights reserved.
doi:10.1016/j.jphotobiol.2012.01.008

enzymes and nonenzymatic antioxidants [26,27]. Ascorbic acid, α-tocopherol, uric acid, and glutathione are well-known non-enzymatic antioxidant molecules. Previous studies have also demonstrated the presence of several major enzymatic antioxidants, including glutathione peroxidase (GPx), glutathione reductase, superoxide dismutase (SOD), and catalase (CAT), in the epidermis [26]. Different doses of UV light can completely destroy the epidermal stores of ascorbate, glutathione, ubiquinol, α-tocopherol, superoxide dismutase, and catalase [26]. While antioxidants are not good markers of oxidative stress, they have been used to evaluate ROS-mediated skin lesions after UVB irradiation [20,28,4,29,30].

In this report, we intend to demonstrate that singlet oxygen, hydroxyl radicals, and nitric oxide are the reactive species that are produced immediately after UVB irradiation of murine skin and that $^{\bullet}NO$ becomes more relevant to the lesion 24 h after irradiation. We also determined the endogenous antioxidant balance immediately after UVB irradiation, which establishes the oxidative stress.

2. Materials and methods

2.1. Reagents

All chemicals were obtained from the Merck or Sigma laboratories.

2.2. Animals and UVB Irradiation

Male Swiss mice (20–25 g) were obtained from the Animal House of the Biological Sciences Center at Londrina State University and had access to water and food ad libitum. They were treated in accordance with the National Institute of Health guidelines for the welfare of experimental animals and with the approval of the Ethics Committee of the Londrina State University. The animals' backs were shaved with a Wahl's Panasonic ER389 Professional shaver without mechanical damage to the skin. The light source was a PHILIPS TL/12 40 W UVB fluorescent lamp, which emits radiation from 270 to 400 nm with an emission peak around 313 nm. The lamp was embedded in a 1.30 m × 0.43 m × 0.45 m box, into which the animals were placed in cages. Animals received a single dose (2.99 J/cm^2) of UVB radiation [31], and animals were sacrificed and dorsal skin samples and stored at −76 °C until use.

2.3. Drugs and treatments

Prior to UVB irradiation, the UV-0 h and UV-24 h groups were treated intraperitoneally (i.p.) 3 times every 8 h with aminoguanidine (AG; 50 mg/kg) [32] or NG-Nitro-l-arginine methyl ester (L-NAME 20 mg/kg i.p.) [33]. Post-irradiation, AG and LN were administered to the UV-24 h group every 8 h until the animals were sacrificed. The UV-0 h group animals were sacrificed and their skin removed immediately after irradiation. The UV-0 h group was treated with α-tocopherol (αT; 100 mg/kg i.p.) every 12 h beginning 3 days prior to UVB irradiation [34], and the skin was removed immediately after irradiation. The UV-24 h group was treated 1 day prior and 18 h after UVB irradiation with 1 dose of α-tocopherol (αT; 100 mg/kg i.p.) and the skin was removed 24 h post-irradiation. Desferrioxamine (DFO 60 mg/kg i.p.) [35] and L-histidine monohydrochloride (HIST 40 mg/kg) [36] treatments were performed 1 h prior to UVB irradiation, and the skin was removed immediately after the radiation.

2.4. Tissue preparation

The dorsal skin homogenates were prepared as described by Peres et al. [1]. Briefly, the skin samples were homogenized in an ULTRA-TURRAX homogenizer containing 10 mg/mL or 50 mg/mL of tissue in a buffer containing 30 mM KH_2PO_4/K_2HPO_4 and 120 mM KCl at pH 7.4. The 50 mg/mL supernatant was used for *tert*-butyl hydroperoxide-stimulated chemiluminescence, catalase activity, superoxide dismutase activity, and glutathione assays, while the 10 mg/mL supernatant was used for the thiobarbituric acid reactive substances (TBARS) assay and to determine the total radical antioxidant parameter (TRAP). The homogenate for the $^{\bullet}NO$ assay is described below. For the total protein carbonylation assay, the tissues (30 mg/mL) were processed specially according to the method of Reznick and Parker [37].

2.5. Lipid peroxide formation analysis

The reaction mixtures were placed in luminescence tubes containing 37.5% (w/v) of the skin supernatant and 3 mM tert-butyl hydroperoxide in a final volume of 1 mL. The tert-butyl hydroperoxide-initiated chemiluminescence (CL) reaction was measured using a GLOMAX TD/20 20 luminometer (Turner Designs) with a response range of 300–650 nm. The tubes were kept in the dark until the moment of the assay, which was carried out in a room kept at 28 °C [1,34,38–40]. The results were expressed in relative light units/g tissue (RLU/g tissue). The final lipoperoxidation products were analyzed by measuring the formation of thiobarbituric acid-reactive species (TBARS) as described by Oliveira and Cecchini [41]. Briefly, low molecular-weight aldehydes such as malondialdehyde (MDA) react with thiobarbituric acid (TBA) to generate a colored product that absorbs light at 532 nm. Carbonyl proteins were assayed using the method for detecting protein hydrazones followed by reaction with dinitrophenylhydrazine, according to Reznick and Parker [37]. $^{\bullet}NO$ was measured as described by Kikuchi et al. [42,43] with the following modifications. Mouse skin (5 mg/mL) was prepared by homogenization for 45 s intervals in 2 mM Na_2CO_3 buffer, pH 8.5 (previously degassed with N_2) using an ULTRA-TURRAX homogenizer (Marconi, Brazil) under N_2 bubbling to assure O_2-free medium. A tissue concentration of 0.250% (w/v) was used for all experiments related to investigating the role of $^{\bullet}NO$ in UVB-irradiated skin. Equal volumes of 360 uM luminol/3 mM desferrioxamine (DFO) and 200 mM H_2O_2 were mixed and incubated at room temperature under moderate agitation for 5 min. To initiate the chemiluminescence reaction, 50 μL of this mixture was added automatically to the luminometer chamber containing 40 μL of skin homogenate (0.250% (w/v)) and 760 μL of buffer. The chemiluminescence spectrum was recorded for 5 min using a GLOMAX TD/20 20 luminometer (Turner Designs, USA). The Origin v. 7.5 program was used to plot chemiluminescence curves that were analyzed using the area under the curve (AUC) to determine the amount of $^{\bullet}NO$ present in the sample. The results were expressed in relative light units/g tissue ($^{\bullet}NO$ RLU/g tissue).

2.6. Antioxidant activity analysis

Total radical antioxidant parameter (TRAP) was also detected by CL. Initially, light emission was measured in a reaction medium containing 2-azo-bis-(2-amidinopropane) and luminol, an alkoxyl-generating system. Then, another curve was measured in the presence of the standard antioxidant Trolox, a hydrosoluble vitamin E that hinders the curve peak due to its antioxidant activity. Finally, Trolox was replaced by the tissue homogenate, the peak hindering

time was determined in comparison with the Trolox standard, and the results were expressed in μM Trolox [1]. Superoxide dismutase (SOD) and catalase (CAT) activities were assayed spectrophotometrically, as previous described [44,45]. Briefly, SOD quantification was based on the inhibition of pyrogallol autoxidation in aqueous solution by SOD and CAT present in the skin homogenate and was determined using a standard H_2O_2 system. Final SOD results were expressed in USOD/mg protein. Catalase results were expressed as ABS per milligram protein per minute. The level of total glutathione (GST) was determined by titration with 5,5′-dithiobis-(2-nitrobenzoic acid), which was evidenced by yellow color formation. Oxidized glutathione (GSSG) was determined in the same manner in supernatant previously incubated with 4-vinylpyridine for 60 min at room temperature, according to the method described by Tietze [46]. Volumes of supernatant were adjusted for the assay with 50 mg/mL skin homogenate. The results were expressed in μM/mg protein. The stress index was calculated using the equation: SI = GSSG/(GSH-GSSG).

2.7. Protein concentration

Protein concentration was determined by the method of Lowry et al. [47] modified by Miller [48], except for the protein carbonyl protein content, where absorbance at 280 nm was used to determine the total protein in each sample. Bovine serum albumin (BSA) was used as a standard for both methods.

2.8. Statistical analysis

The results are shown as means ± SEM. Statistical comparisons of chemiluminescence results were made using the Student t test. Two-way ANOVA with the Bonferroni post-hoc test was used to analyze the lipid peroxidation and the entire chemiluminescence curve. Statistical analysis was performed using GraphPad Prism 4.0 and 5.0 (GraphPad, San Diego, CA).

3. Results

3.1. Lipid hydroperoxide measurement by the CL technique

Lipid hydroperoxide ($LOO^{\cdot}$) formation in Swiss mouse skin following UVB irradiation was evaluated, and the highest emission was observed for the UV-0 h and UV-24h groups (Fig. 1A). The entire curve was employed to perform statistical comparison by 2-way ANOVA ($p < 0.0001$) followed by the Bonferroni post-hoc test. The UV-0 h and UV-24 h curves showed 05 and 19 points, respectively, which were significantly different from that of the control. For the areas under the curves (AUCs), Student t test showed a significant increase in $LOO^{\cdot}$ immediately (UV-0 h; AUC: 15,590 ± 908.9; $p < 0.01$) and 24 h (UV-24 h; AUC: 18,720 ± 1552; $p < 0.001$) after irradiation compared with the control (AUC: 12,850 ± 532.6, $N = 10$). When the mice were treated with α-tocopherol (Fig. 1B), the lipid peroxidation decreased (AUC: αT-UV-0 h: 13,140 ± 655.4; αT-UV-24 h: 16,400 ± 853.6) and was not significantly different from that of the control group (αT-Control: 13,610 ± 987.0). Fig. 1C shows that the lipid peroxidation decreased to control levels when the UV-0 h group was treated with DFO (DFO-UV-0 h AUC: 13,410 ± 825.6), and treatment with HIST also decreased $LOO^{\cdot}$ formation (HIST-UV-0 h AUC: 12,630 ± 1172).

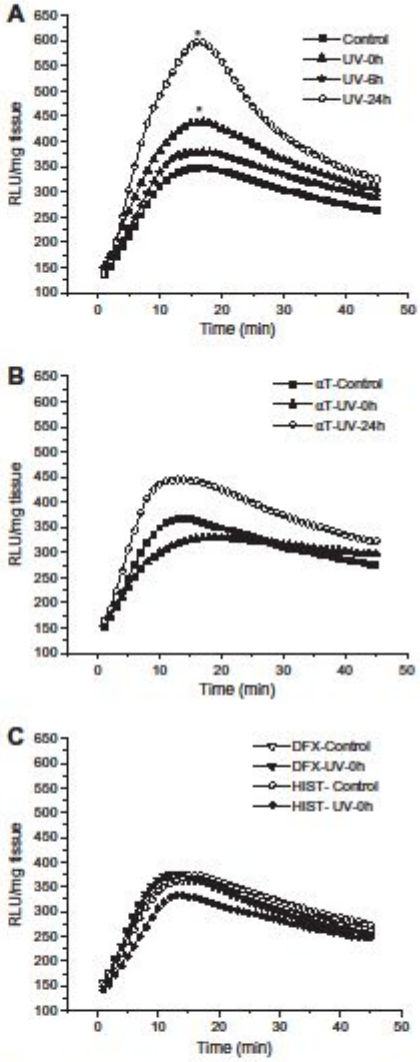

Fig. 1. (A) Levels of lipid hydroperoxides measured by chemiluminescence stimulated by *tert*-butyl hydroperoxide and expressed in relative light units (RLU). For comparison of the areas under the curves (AUCs), the student t test was used; $^{*}p < 0.01$, $^{*}p < 0.001$ for UV-0 h ($N = 7$) and UV-24 h ($N = 8$) compared with the control group ($N = 10$) (UV-6 h: $N = 6$). The entire curves were employed to perform statistical comparison by 2-way ANOVA ($p < 0.0001$) followed by the Bonferroni *post hoc* test. (B) Effect of the antioxidant α-tocopherol on lipid hydroperoxide levels expressed in RLU. αT (100 mg/kg) was administered as previously described (αT-control, $N = 8$; αT-UV-0 h, $N = 7$; αT-UV-24 h, $N = 8$). No statistically significant difference was detected. (C) Effect of Fe (III) chelator and a quencher of $^{1}O_2$ on lipid hydroperoxide levels of the AG-UV-0 h group and expressed in RLU. DFX (60 mg/kg) and HIST (40 mg/kg) were administered as previously described. No statistically significant difference was detected.

3.2. Nitric oxide quantification

The amount of $^{\cdot}NO$ was greater in the UV-24 h group (AUC: $58.0 \times 10^6 \pm 5.6 \times 10^6$; $p < 0.01$) than in the control group (AUC: $33.0 \times 10^6 \pm 6.8 \times 10^6$) (Fig. 2A). Fig. 2B shows the decrease in $^{\cdot}NO$ detection to control levels when the animals were treated with

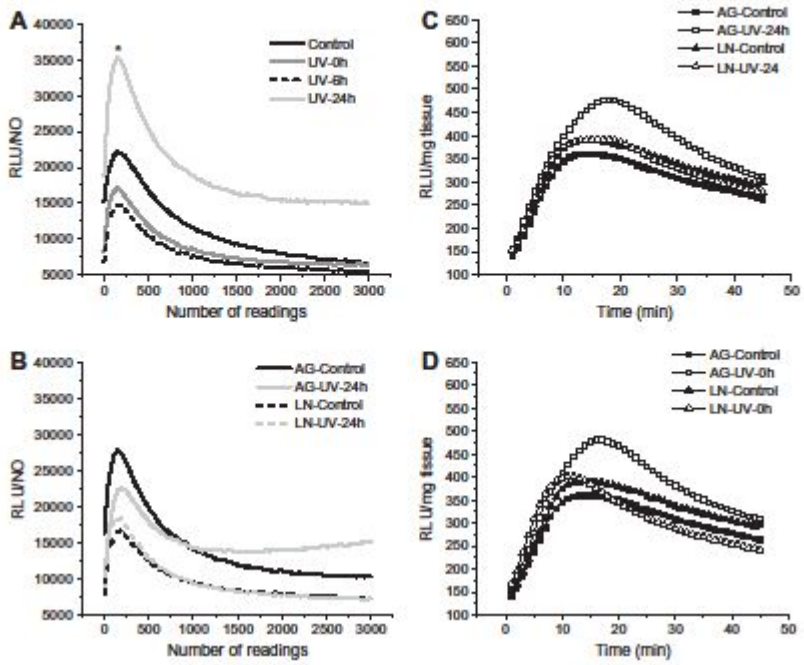

Fig. 2. (A) Nitric oxide quantification by luminol-H_2O_2-induced chemiluminescence. (B) Effect of specific iNOS and cNOS inhibitors AG (50 mg/kg) was administered as previously described (AG-Control, $N = 7$; AG-UV-24 h, $N = 7$). LN (20 mg/kg) was administered as previously described (LN-Control, $N = 7$; LN-UV-24 h, $N = 6$). No statistically significant difference was detected. (C) Effect of specific iNOS and cNOS inhibitors on lipid hydroperoxide levels expressed in RLU. AG (50 mg/kg) was administered as previously described (AG-Control, $N = 6$; AG-UV-24 h, $N = 6$). LN (20 mg/kg) was administered as previously described (LN-Control, $N = 5$; LN-UV-24 h, $N = 7$). No statistically significant difference was detected. (D) Effect of specific iNOS and cNOS inhibitors on lipid hydroperoxide levels and expressed as RLU. AG (50 mg/kg) and LN (20 mg/kg) were administered as previously described (AG-Control, $N = 6$; AG-UV-0 h, $N = 8$; LN-Control, $N = 5$; LN-UV-0 h, $N = 7$). No statistically significant difference was detected.

AG (AG-UV-24 h AUC: $48.3 \times 10^6 \pm 9.7 \times 10^6$; AG-Control AUC: $43.6 \times 10^6 \pm 5.7 \times 10^6$) or with LN (LN-UV-24 h AUC: $29.2 \times 10^6 \pm 4.6 \times 10^6$; LN-Control AUC: $28.4 \times 10^6 \pm 4.3 \times 10^6$).

Fig. 2C shows that lipid peroxidation decreased when the animals (UV-24 h) were treated with AG (AG-UV-24 h AUC: 15,210 ± 2057) or LN (LN-UV-24 h AUC: 14,370 ± 870.5), returning to control levels (AG-Control AUC: 13,350 ± 487.1; LN-Control AUC: 14,510 ± 992.0). Fig. 2D shows that lipid peroxidation also decreased when the UV-0 h group was treated with AG (AG-UV-0 h AUC: 16,540 ± 1366; AG-Control AUC: 13,350 ± 487.1) or with LN (LN-UV-0 h AUC: 13,610 ± 586.6; LN-Control AUC: 14,510 ± 992.0) but showed no significant differences.

3.3. Total radical antioxidant parameter (TRAP) analysis

TRAP decreased in the UV-0 h group (0.535 ± 0.033 μM Trolox; $p < 0.05$) compared with the control group (0.657 ± 0.046 μM Trolox) (Fig. 3). TRAP also decreased when the UV-irradiated groups were treated with AG (AG-UV-0 h: 0.435 ± 0.076 μM Trolox; $p < 0.05$) or LN (LN-UV-0 h: 0.664 ± 0.041 μM Trolox; $p < 0.05$). When the UV-0 h group was treated with α-tocopherol, the TRAP returned to control levels (αT-UV-0 h: 0.763 ± 0.075 μM Trolox.

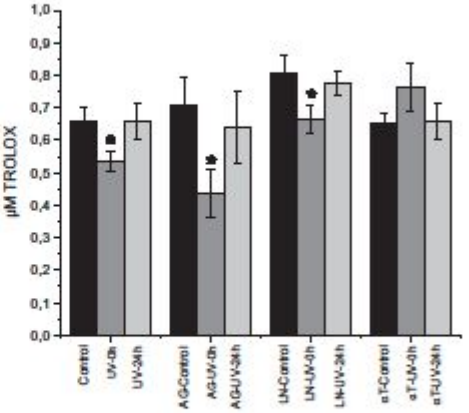

Fig. 3. Effect of UV irradiation on total antioxidant capacity (TRAP) in supernatants of mouse skin treated with or without iNOS inhibitor, cNOS inhibitor, or α-Tocopherol. Results are expressed in μM Trolox. *$p < 0.05$ compared with the control. These results represent means ± SE of 6 animals.

3.4. Determination of GSH, GSSG, and stress index

Reduced Glutathione (GSH) levels were lower in the UV-24 h group (8.742 ± 1.451 μM/mg protein; $p < 0.05$) than in the controls (14.67 ± 2.083 μM/mg protein) (Table 1). Oxidized glutathione (GSSG) was significantly decreased in the UV-0 h group

Table 1
Reduced glutathione (GSH) and oxidized glutathione (GSSG) concentrations and stress index (SI) in mouse skin exposed to acute UVB irradiation. Results are mean ± SEM.

Group	GSH (μM/mg protein)	GSSG (μM/mg protein)	Stress index (SI)	N
Control	14.67 ± 2.083	1.154 ± 0.078	0.100 ± 0.0147	10
UV-0 h	10.08 ± 1.092	0.627 ± 0.063*	0.071 ± 0.014	6
UV-24 h	8.742 ± 1.451*	1.696 ± 0.154**	0.258 ± 0.046*	7
αT-control	13.74 ± 1.265	2.350 ± 0.375	0.231 ± 0.054	6
αT-UV-0 h	14.97 ± 1.105	1.568 ± 0.241	0.122 ± 0.019	6
αT-UV-24 h	7.248 ± 1.100**	1.070 ± 0.175**	0.342 ± 0.085	8

* $p < 0.05$ compared with control.
** $p < 0.01$ compared with control.
* $p < 0.001$ compared with control.

Table 2
Lipid peroxidation measured by TBARS, levels of carbonyl proteins (PC) and antioxidant enzymes catalase and superoxide dismutase (SOD). Results are mean ± SEM.

GROUP	TBARS (nM MDA/mg protein)	PC (nM/mg protein)	SOD (USOD/mg protein)	CAT (ABS/min/mg protein)
Control	11.42 ± 1.04 $N = 12$	9.07 ± 0.52 $N = 07$	1.23 ± 0.13 $N = 17$	0.39 ± 0.01 $N = 15$
UV-0 h	9.26 ± 1.4* $N = 08$	10.48 ± 0.26 $N = 08$	1.17 ± 0.22 $N = 08$	0.41 ± 0.023 $N = 06$
UV-24 h	6.48 ± 1.10* $N = 07$	7.74 ± 0.31** $N = 06$	0.92 ± 0.05 $N = 06$	0.27 ± 0.01** $N = 07$

* $p < 0.05$ compared to control.
** $p < 0.01$ compared to control.

(0.627 ± 0.063 μM/mg protein; $p < 0.001$) and significantly increased in the UV-24 h group (1.696 ± 0.154 μM/mg protein; $p < 0.01$) compared with the control group (1.154 ± 0.078 μM/mg protein). However, the stress index (SI), which represents cellular oxidative stress, was significantly higher in the UV-24 h group (0.258 ± 0.046 SI; $p < 0.001$) than in the control group (0.100 ± 0.014 SI). Treatment with α-tocopherol decreased the GSSG levels in the UV-24 h group (1.070 ± 0.174 μM/mg protein; αT- Control: 2.350 ± 0.375 μM/mg protein; $p < 0.01$) but had no significant effect on SI.

3.5. Oxidative stress parameters and antioxidant enzyme activities

Table 2 shows the results of each analysis of the different groups in terms of protein oxidation (CP), lipid peroxide formation (TBARS), and antioxidant enzyme activities (CAT and SOD). TBARS was significantly decreased in the UV groups (UV-0 h: 9.26 ± 1.4 nM MDA/mg protein, UV-24 h: 6.48 ± 1.10 nM MDA/mg protein; $p < 0.05$) compared with the control group (11.42 ± 1.04 nM MDA/mg protein). CP decreased significantly in the UV-24 h group (7.74 ± 0.31 nM/mg protein; $p < 0.01$) compared with the control group (9.07 ± 0.52 nM/mg protein). Catalase, an enzymatic parameter, decreased significantly ($p < 0.001$) in the skin of the UV-24 h group (0.27 ± 0.010 ABS/min/mg protein) compared with that of the control group (0.39 ± 0.01). No changes were observed in SOD, another enzymatic parameter.

4. Discussion

Free radicals formed by UVB irradiation of cellular components may result in lipid peroxidation [49] and protein and DNA oxidation [37,50]. All cellular components are susceptible to the action of reactive oxygen species, but biological membranes are the most severely affected [50–52]. In this study, we used a very sensitive *tert*-butyl hydroperoxide-initiated chemiluminescence (CL) assay to analyze the levels of lipid hydroperoxides and antioxidant levels (variation in oxidative stress balance) in the skin of Swiss mice immediately and 24 h after UVB irradiation. Increasing CL is closely related to the oxidative stress previously endured by the tissue, and reflects the consumption of antioxidant defenses and formation of lipid hydroperoxides, leading to photon emission [1,34,38–40].

Our results showed increased CL levels immediately after irradiation (UV-0 h group), indicating moderate oxidative stress and a higher emission peak at 24 h after irradiation (UV-24 h group), indicating more severe oxidative stress. In contrast, low levels of thiobarbituric acid-reactive substances (TBARS), mainly malondialdehyde (MDA), were observed in both UV-0 h and UV-24 h groups, indicating that lipid peroxidation chain reaction in UVB-irradiated skin tends to form lipid hydroperoxides that do not undergo subsequent oxidation to aldehydes such as MDA. Accordingly, increasing CL levels were accompanied by TBARS impairment from 0 to 24 h. UVB-induced oxidative damage of cell membranes both *in vitro* and in vivo is currently assessed by measuring the formation of lipid peroxidation products such as MDA or TBARS. Both MDA and low molecular weight aldehydes demonstrated decreased lipid peroxidation after UVB irradiation as measured by the TBARS technique [23,25]. The TBARS levels were significantly decreased in the UV-0 h and UV-24 h groups as compared to the control group. However, it is well-established that the CL technique [66,67] can estimate the levels of skin lipid hydroperoxides formed during the early stages of cell damage [1,68], preceding the formation of low-molecular-weight aldehydes. Moreover, carbonyl proteins, which are formed in large amounts by reacting with MDA [69], either did not change or were reduced after UVB irradiation in the present study. This phenomenon could be explained by the presence of other antioxidants that protect the UVB-irradiated skin from membrane destabilization and lipid peroxide chain reaction, such as *trans*-urocanic acid and *cis*-urocanic acid, the 2 epidermal compounds that have been described as major natural free radical scavengers [57]. Thus, despite reduced TBARS levels, our evidence points toward the oxidative damage induced by UVB irradiation. This statement is reinforced by the reduced antioxidant capacity at 0 h and reduced GSH concentration in addition to the augmented levels of stress (GSSG/GSH) at 24 h after UVB irradiation, a phenomenon that is reverted by α-tocopherol treatment. The stress index reflects decreased GSH levels with a significant

increase in GSSG [40] as shown by our results at 24 h after irradiation. Other studies have reported decreased GSH levels as a photoprotective mechanism [25,59–61]. Glutathione is an intracellular mediator that is critical for cellular defense against reactive intermediates. In addition to its role as a substrate for glutathione-dependent antioxidant enzymes, this thioltripeptide participates in the regeneration of ascorbate and α-tocopherol and directly detoxifies reactive species via its ability to conjugate with pro-oxidants [55,56]. This time-dependent reduction in antioxidant profile, i.e., antioxidant capacity at 0 h and GSH at 24 h after irradiation, may reflect different species of radicals acting at different times (see below and Fig. 4).

If a chain-break antioxidant is an effective inhibitor of lipid peroxidation, it may also reduce CL. Our results show that pre-treatment of animals with α-tocopherol completely inhibited CL augmentation at 0 and 24 h after UVB irradiation. This result indicates that lipid peroxidation is a very important reaction in the initial and late phase of UVB oxidative damage of the skin. CL elevation at 0 h also depended on the consumption of antioxidant as demonstrated by a significant reduction in TRAP values. Indeed, pre-treatment of rats with α-tocopherol prevented the TRAP reduction induced by UVB irradiation at 0 h. Surprisingly, a reduction in antioxidant capacity at 24 h was not observed. This may be because of low-molecular-weight antioxidant mobilization from other tissues, as demonstrated in the models of tissue-specific oxidative damage [70]. Moreover, it may indicate that the reactive species associated with lipid peroxidation at 24 h are less sensitive to inhibition by α-tocopherol. If this true, the reactive species associated with oxidative damage are somehow different at 0 and 24 h.

The question to be addressed is this: is nitric oxide (•NO) involved in oxidative stress at 0 and 24 h after irradiation? To answer this question we evaluated •NO levels in the skin of rats by using a very sensitive CL method [42,43]. Rats were also pretreated with selective inhibitors of constitutive •NO synthase (cNOS) and inducible •NO synthase (iNOS), L-NAME and aminoguanidine, respectively. The results showed that •NO increased only at 24 h and was accompanied by CL elevation. Treatment with both L-NAME and aminoguanidine prevents $^{\bullet}NO$ and CL augmentation. These results indicate that $^{\bullet}NO$ plays an important role in UVB-induced peroxidation injury at 24 h after exposure. Increase in iNOS and cNOS levels after UVB irradiation have been reported [20,22,23]. Wu et al. [58] demonstrated that •NO produced high levels of $ONOO^-$, which enhances oxidative cell injury and apoptosis in irradiated cells.

Previous studies have shown that H_2O_2 reacts with •NO to form $ONOO^-$ [42,43,53,65]. Our studies showed that catalase activity is also decreased significantly in the UV-24 h group. In a study on the skin of newborn rats, Muramatsu et al. [62] showed that distribution of catalase corresponds to that of H_2O_2 accumulation, indicating the role of normal skin catalase as a marker of epidermal differentiation and its role in redox damage. The same study verified that catalase expression in the upper epidermal layers decreased 24 h after exposure to UVB [30,63,64]. These studies suggest that UVB impairs endogenous antioxidants and that catalase is one of the most sensitive components of these mechanisms [63]. Because our data strongly point $^{\bullet}NO$ as the main reactive species involved in oxidative damage of the skin via a delayed effect of UVB irradiation, the low levels of catalase and glutathione may cause H_2O_2 accumulation that can in turn react with •NO to generate peroxynitrite, which is largely responsible for the cell damage.

•NO did not increase immediately (UV-0 h) after UVB irradiation, which is in contrast to the significant increase in CL levels. Although L-NAME- and aminoguanidine-treated groups showed inhibition of CL increase at 0 h as compared to their corresponding

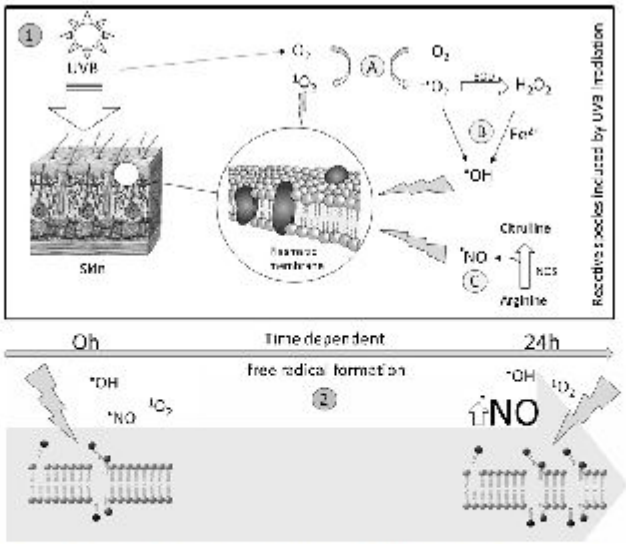

Fig. 4. General view of the time-dependent generation of reactive species in skin exposed to UVB radiation. (1) UVB irradiation directly generates (A) the reactive oxygen species (ROS) singlet oxygen ($^1O_2$) and superoxide anion ($^{\bullet-}O_2$). (B) Next, superoxide dismutase (SOD) converts $^{\bullet-}O_2$ into hydrogen peroxide (H_2O_2). Both $^{\bullet-}O_2$ and H_2O_2 may be converted into the highly reactive hydroxyl radical (•OH) by the iron (Fe^{2+})-catalyzed Haber–Weiss and Fenton reactions. (C) Similarly, reactive nitrogen species (RNS) are generated as a result of sequential reactions that begin with nitric oxide synthase (NOS)-mediated conversion of arginine to citrulline. These ROS and RNS interact with the lipid-rich plasma membrane and initiate lipid peroxidation. (2) Time-dependent free radical formation after UVB irradiation. The lipid peroxidation occurs immediately after UVB irradiation and is mediated mainly by nonspecific reactive species such as $^1O_2$, •OH, and •NO. Twenty-four hours post-irradiation, the predominant reactive species is •NO, probably due to the expression of iNOS.

control groups (LN-Control and AG-Control), the CL levels of the treated groups also did not differ from the UV-0 h group. In addition, L-NAME and aminoguanidine did not prevent the reduction of TRAP after UVB irradiation, indicating that $^{\bullet}NO$ is not part of the oxidative damage mechanism or plays a limited role in skin injury caused by UVB irradiation at 0 h (Fig. 4). Therefore, our hypothesis is that reactive oxygen species could play an important role in oxidative damage that occurs immediately after UVB irradiation. To address this hypothesis, animals were treated with histidine (HIST), a well-known quencher of singlet oxygen ($^1O_2$) [53], or desferrioxamine (DFX), an iron-chelating substance that prevents hydroxyl radical ($^{\bullet}OH$) production via the Fenton reaction [35]. DFX decreases lipid peroxidation in dermal fibroblasts exposed to UVB [5,54]. Ogura et al. [11] showed that in rat skin, superoxide anion ($^{\bullet}O_2^-$) is formed in the epidermis following exposure to UV light and $^{\bullet}OH$ is formed via the iron-mediated reaction. In the present study, DFX and HIST treatments restored the CL levels immediately after UVB irradiation. These results indicate that both hydroxyl radicals and singlet oxygen play an important role in oxidative cell injury immediately after UVB irradiation.

In conclusion, our results indicated that skin irradiation with UVB leads to immediate oxidative stress damage because of the decrease of antioxidant capacity and moderated increase in lipid peroxidation, mainly via reactive oxygen species such as hydroxyl radical and singlet oxygen. Moreover, the oxidative damage observed at 24 h after UVB irradiation might be provoked by a more severe lipid peroxidation most likely mediated by increased $^{\bullet}NO$ and reduced GSH levels and catalase activity. Reduced catalase activity and low GSH level at 24 h may favor the reaction between H_2O_2 and $^{\bullet}NO$, leading to peroxynitrite formation, which is a very efficient lipid peroxidant.

Acknowledgements

The authors would like to thank Jesus Antônio Vargas and Pedro S.R. DeonizioFilhofor excellent technical assistance and CAPES, CNPq, and FundaçãoAraucária for providing financial support.

References

[1] P.S. Peres, V.A. Terra, F.A. Guarnier, et al., Photoaging and chronological aging profile: understanding oxidation of the skin, J. Photochem. Photobiol. B 103 (2011) 93–97.
[2] B.K. Armstrong, A. Kricker, The epidemiology of UV induced skin cancer, J. Photochem. Photobiol. B 63 (2001) 8–18.
[3] M.A. Birch-Machin, H. Swalwell, How mitochondria record the effects of UV exposure and oxidative stress using human skin as a model tissue, Mutagenesis 25 (2005) 101–107.
[4] C. Barresi, C. Stremnitzer, V. Mlitz, et al., Increased sensitivity of histidinemic mice to UVB radiation suggests a crucial role of endogenous urocanic acid in photoprotection, J. Invest. Dermatol. 131 (2011) 188–194.
[5] P. Berneiser, J. Wenk, L.O. Klotz, et al., Central role of Ferrous/Ferric iron in the ultraviolet B irradiation-mediated signaling pathway leading to increased interstitial collagenase (matrix-degrading metalloprotease (MMP)-1) and stromelysin-1 (MMP-3) mRNA levels in cultured human dermal fibroblasts, J. Biol. Chem. 273 (1998) 5279–5287.
[6] M. Kruszewski, Labile iron pool: the main determinant of cellular response to oxidative stress, Mutat. Res. 531 (2003) 81–92.
[7] A. Yialouvaki, J. Savovic, A. Al-Qenaei, et al., Caged-iron chelators a novel approach towards protecting skin cells against UVA-Induced necrotic cell death, J. Invest. Dermatol. 126 (2006) 2287–2295.
[8] J.L. Zhang, A. Yialouvaki, P. Holley, et al., Susceptibility of skin cells to UVA-induced necrotic cell death reflects the intracellular level of labile iron, J. Invest. Dermatol. 123 (2004) 771–780.
[9] A. Gronberg, L. Zettergren, K. Bergh, et al., Antioxidants protect keratinocytes against M. ulceransmycolactonecytotoxicity, PLoS One 5 (11) (2010) e13839.
[10] N. Grossman, N. Schneid, 780 nm low power diode laser irradiation stimulates proliferation of keratinocyte cultures: involvement of reactive oxygen species, Lasers Surg. Medic. 22 (1998) 212–218.
[11] R. Ogura, M. Sugiyama, J. Nishi, N. Hamamaki, Mechanism of lipid formation following exposure of epidermal homogenate to ultraviolet light, J. Invest. Dermatol. 97 (1991) 1044–1047.
[12] F.G. Ville, R.M. Tyrrell, UVA radiation-oxidative damage to lipids and proteins in vitro and in human skin fibroblasts is dependent on iron and singlet oxygen, Free Radical. Biol. Med. 18 (1995) 721–730.
[13] J.P. Martin Jr., P. Burch, Production of oxygen radicals by photosensitization, Methods Enzymol. 186 (1990) 635–645.
[14] H. Masaki, T. Atsumi, H. Sakurai, Detection of hydrogen peroxide and hydroxyl radicals in murine skin fibroblasts under UVB irradiation, Biochem. Biophys. Res. Commun. 206 (1995) 474–479.
[15] G. Deliconstantinos, V. Villiotou, C.J. Stavrides, Increase of particular nitric oxide synthase activity and peroxynitrite synthesis in UVB-irradiated keratinocyte membranes, Biochem. J. 320 (1996) 997–1003.
[16] D. Heck, A.M. Vetrano, T.M. Mariano, J.D. Laskin, UVB light stimulates production of reactive oxygen species: unexpected role for catalase, J. Biol. Chem. 278 (2003) 22432–22436.
[17] D.R. Bickers, M. Athar, Oxidative stress in the pathogenesis of skin disease, J. Invest. Dermatol. 126 (2006) 2565–2575.
[18] K. Kabashima, M. Nagamachi, T. Honda, C. Nishigori, Prostaglandin E2 is required for ultraviolet B-induced skin inflammation via EP2 and EP4 receptors, Lab. Invest. 87 (2007) 49–55.
[19] T. Hakozaki, D. Akira, T. Yoshii, S. Toyokuni, et al., Visualization and characterization of UVB-induced reactive oxygen species in a human skin equivalent model, Arch. Dermatol. Res. 300 (2008) 51–56.
[20] H. Wei, X. Zhang, Y. Wang, et al., Inhibition of ultraviolet light-induced oxidative events in the skin and internal organs of hairless mice by isoflavone genistein, Cancer Lett. 185 (2002) 21–29.
[22] M. Mowbray, S. McLintock, R. Weerakoon, et al., Enzyme-independent NO stores in human skin: quantification and influence of UV radiation, J. Invest. Dermatol. 129 (2009) 834–842.
[23] M.D.H. Gonzalez, M.L. Paz, A. Ferrari, et al., Skin damage and mitochondrial dysfunction after acute ultraviolet B irradiation: relationship with nitric oxide production, Photodermatol. Photoimmunol. Photomed. 21 (2005) 311–317.
[24] A. Kuhn, K. Fehsel, P. Lehmann, et al., Aberrant timing in epidermal expression of inducible nitric oxide synthase after UV irradiation in cutaneous lupus erythematosus, J. Invest. Dermatol. 111 (1998) 149–153.
[25] S.C. Lee, J.W. Lee, J.E. Jung, et al., Protective role of nitric oxide-mediated inflammatory response against lipid peroxidation in ultraviolet B-irradiated skin, Br. J. Dermatol. 142 (2000) 653–659.
[26] Y. Shindo, E. Witt, D. Han, Enzymic and non-enzymic antioxidants in epidermis and dermis of human skin, J. Invest. Dermatol. 102 (1994) 122–124.
[27] K. Punnonen, A. Puntala, C.T. Jansen, M. Ahotupa, UVB irradiation induced lipid peroxidation and decreases antioxidant enzyme activities in human keratinocytes in vitro, Acta Derm. Venereol. 71 (1991) 239–273.
[28] A. Saija, D. Tomaino, A. Trombetta, et al., In vitro and in vivo evaluation of caffeic and ferulic acids as topical photoprotective agents, Int. J. Pharm. 199 (2000) 39–47.
[29] S. Ramachandran, N. Rajendra Prasad, S. Karthikeyan, Sesamol inhibits UVB-induced ROS generation and subsequent oxidative damage in culture human skin dermal fibroblasts, Arch. Dermatol. Res. 302 (2010) 733–744.
[30] P.K. Vayalil, C.A. Elmets, S.K. Katiyar, Treatment of green tea polyphenols in hydrophilic cream prevents UVB-induced oxidation of lipids and proteins, depletion of antioxidant enzymes and phosphorylation of MAPK proteins in SKH-1 hairless mouse skin, Carcinogenesis 24 (2003) 927–936.
[31] R. Casagrande, S.R. Georgetti, W.A. JVerri, et al., Protective effect of topical formulations containing quercetin against UVB-induced oxidative stress in hairless mice, J. Photochem. Photobiol. B 84 (2006) 21–27.
[32] M.A. Bowman, O.G. Simell, A.B. Peck, et al., Pharmacokinetics of aminoguanidine administration and effects on the diabetes frequency in nonobese diabetic mice, J. Pharmacol. Exp. 279 (1996) 790–794.
[33] A. Mehanna, D.C Vitorino, C. Panis C, et al., Cardiovascular and pulmonary effects of NOS inhibition in endotoxemic conscious rats subjected to swimming training, Life Sci. 81 (2007) 1301–1308.
[34] F.A. Guarnier, A.L. Cecchini, A.A. Suzukawa, et al., Time course of skeletal muscle loss and oxidative stress in rats with Walker 256 solid tumor, Muscle Nerve 42 (2010) 950–958.
[35] K. Takeshita, T. Takaja, H. Hirata, M. Ono, et al., In vivo oxygen radical generation in the skin of the protoporphyria model mouse with visible light exposure: an L-band ESR study, J. Invest. Dermatol. 122 (2004) 1463–1470.
[36] A.A. Farshid, E. Tamaddonfard, M.S. Belaskas, et al., Histopathological comparison of the effects of histidine and ketotifen in a rat model of colitis, Bull. Vet. Inst. Pulawy 53 (2009) 795–800.
[37] A.Z. Reznick, L. Packer, Oxidative damage to proteins: spectrophotometric method for carbonyl assay, Methods Enzymol. 233 (1994) 357–363.
[38] B. Gonzalez-Flecha, S. Llesuy, A. Boveris, Hydroperoxide-initiated chemiluminescence. an assay for oxidative stress in biopsies of heart, liver, and muscle, Free Rad. Biol. Med. 10 (1991) 93–100.
[39] D.S. Barbosa, R. Cecchini, M.Z. El Kadri, et al., Decrease oxidative stress in patients with ulcerative colitis supplemented with fish oil omega-3 fatty acids, Nutrition 19 (2003) 837–841.
[40] A.N. ColladoSimão, A.A. Suzukawa, M.F. Casado, F.A. Guarnier, et al., Genistein abrogates pre-hemolytic and oxidative stress damage induced by 2,2′-Azobis (Amidinopropane), Life Sci. 78 (2005) 1202–1210.
[41] F.J.A. Oliveira, R. Cecchini, Oxidative stress of liver in hamsters infected with Leishmania (L.) chagasi, J. Parasitol. 86 (5) (2000) 1067–1072.
[42] K. Kikuchi, T. Nagano, H. Hayakawa, et al., Detection of nitric oxide production from a perfused organ by a luminol-H_2O_2system, Anal. Chem. 65 (1993) 1794–1799.

[43] K. Kikuchi, T. Nagano, H. Hayakawa, et al., Real time measurement of nitric oxide produced ex vivo by luminol-H_2O_2-chemiluminescence method, J. Biol. Chem. 268 (1993) 23106–23110.
[44] S.A. Marklund, G. Marklund, Involvement of the superoxide anion radical in the autoxidation of pyrogallol and convenient assay for superoxide dismutase, Eur. J. Biochem. 47 (1974) 469–474.
[45] G. Cohen, D. Dembiec, J. Marcus, Measurement of catalase activity in tissue extracts, Anal. Biochem. 34 (1970) 30–38.
[46] F. Tietze, Enzymic method for quantitative determination of nanogram amounts of total and oxidized glutathione: applications to mammalian blood and other tissues, Anal. Biochem. 27 (1969) 502–522.
[47] O.H. Lowry, N.S. Rosenbrough, A.L. Farr, et al., Protein measurement with the folin phenol reagent, J. Biol. Chem. 193 (1) (1951) 265–275.
[48] G.L. Miller, Protein determination for large number of samples, Anal. Chem. 31 (5) (1959) 964.
[49] G. Aldini, P. Granata, C. Marinello, et al., Effects of UVB radiation on 4-hydroxy-2-trans-nonenal metabolism and toxicity in human keratinocytes, Chem. Res. Toxicol. 20 (2007) 416–423.
[50] W. Elberger, B. Vollmer, R. Amouroux, et al., Oxidative stress impairs the repair of oxidative DNA base modifications in human skin fibroblasts and melanoma cells, DNA Repair 7 (2008) 912–921.
[51] M. Perluigi, F.D. Domenico, C. Blarzino, et al., Effects of UVB-induced oxidative stress on protein expression and specific protein oxidation in normal human epithelial keratinocytes: a proteomic approach, Proteome Sci. 8 (2010) 13.
[52] M. Podda, M.G. Traber, C. Weber, et al., UV-irradiation depletes antioxidants and causes oxidative damage in a model of human skin, Free Radical. Biol. Med. 24 (1998) 55–65.
[53] A.A. Noronha-Dutra, M.M. Epperlein, N. Woolf, Reaction of nitric oxide with hydrogen peroxide to produce potentially cytotoxic singlet oxygen as a model for nitric oxide-mediated killing, FEBS Lett. 1 (1993) 59–62.
[54] K. Kitazawa, K. Iwasaki, Reduction of ultraviolet light-induced oxidative stress by amino acid-based iron chelators, Biochim. Biophys. Acta. 1473 (1999) 400–408.
[55] A. Ghiselli, M. Serafini, F. Natella, Total antioxidant capacity as a tool to assess redox status: critical view and experimental data, Free Rad. Biol. Med. 29 (11) (2000) 1106–1114.
[56] M. Carini, G. Aldini, M. Piccone, R.M. Facino, Fluorescent probes as markers of oxidative stress in keratinocyte cell lines following UVB exposure, Farmaco 55 (88) (2000) 526–534.
[57] A. Kammeyer, T.A. Eggelte, J.D. Bos, M.B.M. Teunissen, Urocanic acid isomers are good hydroxyl radical scavengers: a comparative study with structural analogues and with uric acid, Biochim. Biophys. Acta 1428 (1999) 117–120.
[58] S. Wu, L. Wang, A.M. Jacoby, et al., Ultraviolet B light-induced nitric oxide/peroxynitrite imbalance in keratinocytes–implications for apoptosis and necrosis, Photochem. Photobiol. 86 (2) (2010) 389–396.
[59] L.A. Wheeler, A. Aswad, M.J. Connor, N. Lowe, Depletion of cutaneous glutathione and the induction of inflammation by 8-methoxypsoralen plus UVA radiation, J. Invest. Dermatol. 87 (1986) 658–662.
[60] K. Hanada, R.W. Gange, M.J. Connor, Effect of glutathione depletion on sunburn cell formation in the hairless mouse, J. Invest. Dermatol. 96 (1991) 838–840.
[61] Y.M. Fonseca, C.D. Catini, F.T.M.C. Vicentini, et al., Efficacy of marigold extract-loaded formulations against UV-induced oxidative stress, J. Pharm. Sci. 100 (6) (2011) 2182–2189.
[62] S. Murasmatsu, Y. Suga, Y. Mizuno, et al., Differentiation-specific localization of catalase and hydrogen peroxide, and their alterations in rat skin exposed to ultraviolet B rays, J. Dermat. Sci. 37 (3) (2005) 151–158.
[63] J. Fuchs, M.E. Huflejt, L.M. Rothfuss, et al., Impairment of enzymic and nonenzymic antioxidants in skin by UVB irradiation, J. Invest. Dermatol. 93 (1989) 769–773.
[64] S.E. Jeon, S. Choi-Kwon, K.A. Park, et al., Dietary supplementation of (+)-catechin protects against UVB-induced skin damage by modulating antioxidant enzyme activities, Photoderm. Photoimmunol. Photomed. 19 (2003) 235–241.
[65] R. Radi, J.S. Beckman, K.M. Bush, B.A. Freeman, Peroxynitrite-induced membrane lipid peroxidation: the cytotoxic potential of superoxide and nitric oxide, Arch. Biochem. Biophys. 288 (1991) 481–487.
[66] A. Zamburlini, M. Maiorino, P. Barbera, et al., Measurement of lipid hydroperoxidesin plasma lipoproteins by a new highly-sensitive photon counting luminometer, Biochem. Biophys. Acta 1256 (2) (1995) 233–240.
[67] A. Zamburlini, M. Maiorino, P. Barbera, et al., Direct measurement by single photon counting of lipid hydroperoxides in human plasma and lipoproteins, Anal. Biochem. 232 (1) (1995) 107–113.
[68] J. Fossey, D. Lefort, J. Sorba, Free Radicals in Organic Chemistry, Wiley, New York, 1995.
[69] T. Grune, K.J. Davies, The proteasomal system and HNE-modified proteins, Mol. Aspects Med. 24 (4–5) (2003) 195–204.
[70] V.P. Palace, M.F. Hill, N. Khaper, P.K. Singal, Metabolism of vitamin A in the heart increases after a myocardial infarction, Free Radical. Biol. Med. 26 (11–12) (1999) 1501–1507.

APÊNDICE 2 – Artigo 2: Nitric oxide is responsible for oxidative skin injury and modulation of cell proliferation after 24h of UVB exposure

Free Radical Research, July 2012; 46(7): 872–882

ISSN 1071-5762 print/ISSN 1029-2470 online
DOI: 10.3109/10715762.2012.686036

informa
healthcare

ORIGINAL ARTICLE

Nitric oxide is responsible for oxidative skin injury and modulation of cell proliferation after 24 hours of UVB exposures

Vania Aparecida Terra[1], Fernando Pereira Souza-Neto[1], Raissa Caroline Pereira[1], Thamara Nishida Xavier Da Silva[1], Leandra Naira Zambelli Ramalho[3], Rodrigo Cabral Luiz[1], Rubens Cecchini[2] & Alessandra Lourenco Cecchini[1]

[1]*Laboratorio de Patologia Molecular, Universidade Estadual de Londrina. Rod. Celso Garcia Cid, PR-445, km 380, Londrina, PR, Brasil,* [2]*Laboratorio de Patofisiologia e Radicais Livres, Universidade Estadual de Londrina. Rod. Celso Garcia Cid, PR-445, km 380, Londrina, PR, Brasil, and* [3]*Departamento de Patologia e Medicina Legal, Universidade de São Paulo, Ribeirão Preto, SP, Brasil*

Abstract

Nitric oxide (NO) is produced by various mammalian cells and plays a variety of regulatory roles in normal physiology and in pathological processes. This article provides evidence regarding the participation of NO in UVB-induced skin lesions and in the modulation of skin cell proliferation following UVB skin irradiation. Hairless mice were subjected to UVB irradiation for 3 hours and the skin evaluated immediately, 6 and 24 hours postirradiation. The skin lipid peroxidation, and NO levels evaluated by chemiluminescence and inducible nitric oxide synthase (iNOS) and nitrotyrosine immunolabelling increased significantly 24 hours after irradiation and decreased under the treatment with aminoguanidine (AG). On the other hand, cell proliferation markers, PCNA and VEGF showed a strong labelling index when AG was used. The data indicate that NO mediates, at least in part, the lipid peroxidation and protein nitration and also promotes the down regulation of factors involved in cell proliferation. This work shows that the NO plays an important role in the oxidative stress damage and on modulation of cell proliferation pathways in UVB irradiated skin.

Keywords: nitric oxide, lipid peroxidation, oxidative stress, UVB skin irradiation, proliferation markers, iNOS, cell proliferation, modulation

Introduction

The skin is continuously exposed to chemical, microbiological and physical agents. Ultraviolet (UV) irradiation induces free radical formation, which provoke various skin changes, such as erythema, inflammation, photoaging and skin cancer [1–3]. UVB irradiation is related to induce elevation of nitric oxide (NO) [4] and superoxide radical (O_2^-) [5] in keratinocytes cells. Both of these free radicals can rapidly react with each other to form peroxynitrite ($ONOO^-$) [6], which are known to be responsible for oxidative/nitrosative stress and is cytotoxic, causing injury to the cell membrane [6]. Most cell types residing in the skin produce NO in response to the appropriate stimulation. Keratinocytes [7], Langerhans cells [8], dermal fibroblasts [9], melanocytes [10] and cells of melanoma [11] express inducible nitric oxide synthase (iNOS) upon stimulation with inflammatory cytokines. UV also induces iNOS expression with a maximised mRNA level at 24 hours postirradiation in hairless mice [12] and in human skin [13,14]. It has been demonstrated that ($^1O_2$) singlet oxygen, ($^\bullet OH$) hydroxyl radical and hydrogen peroxide (H_2O_2) are also generated in UVB light-stimulated photosensitisation [15–20]. Much evidence exists that UVB irradiation promotes oxidative stress in the skin; however, the reactive species involved remain unclear, particularly regarding the role of NO. Some studies have attributed a protective effect against lipid peroxidation [12,21] and resistance to the apoptotic process [22,23] to NO, while others have reported the participation of NO in oxidative lesions and apoptosis [24]. The activation of constitutive nitric oxide synthase (cNOS), which leads to an increase of NO, is triggered by the elevation of intracellular Ca^{2+}, and is most likely to occur in the first hours following UVB irradiation [24]. Recently, Mowbray et al. [25] have shown an enzyme-independent NO release followed by UVB exposure of human skin sweat, few hours after irradiation. The role of the late release of NO (24 hours after the end of irradiation) has not been elucidated. The increase in NO production following UVB skin exposure has been reported [24], but the relation between NO UVB production and the nitrosative stress (RNS) on cell membrane by UVB irradiation is not clear. These studies mainly used the TBARS technique and NOS expression as markers of oxidative and nitrosative stress, respectively. However, neither of these parameters can ensure reliable estimations of NO-mediated peroxidative damage or the modulation of signalling protein factors by NO. Furthermore, the majority of studies, if not all, have been conducted using resident skin cells in culture.

Thus, using the measurement of lipid peroxidation and NO levels by a very sensitive chemiluminescence techniques and evaluation of iNOS, nitrotyrosine, PCNA and VEGF by immunohistochemistry labelling, we showed

Correspondence: A. L. Cecchini, Laboratorio de Patologia Molecular, Universidade Estadual de Londrina, 86051-990 Londrina, Brasil. Tel: (+55-43) 3371-4521. Fax: (+55-43) 3371-4267. E-mail: alcecchini@uel.br

(Received date: 19 February 2012; Accepted date: 13 April 2012; Published online: 9 May 2012)

consistently the involvement of NO on oxidative and nitrosative stress injury and on cell proliferation pathways associated with VEGF and PCNA factors.

Materials and methods

Reagent

All the chemicals were obtained from Merck or Sigma Laboratories.

Animals, UVB irradiation and aminoguanidine treatment

Hairless mice HRS/J were obtained from University of São Paulo (USP), weighing 20–25 g, with access to water and food *ad libitum*. They were treated in accordance with the National Institutional of Health guidelines for the welfare of experimental animals and with the approval of the Research Ethics Committee of the Londrina State University. The irradiation chamber was adjusted with a PHILIPS TL/12 40W UVB fluorescent lamp, which emits irradiation from 270 to 400 nm with maximum peak around 313 nm. The mice were administered a single dose (2.46 J/cm^2) of UVB irradiation [26]. UVB output was measured using a Research Radiometer model IL-1700 (International Light, USA; calibrated by IL service staff) with a radiometer sensor for UV (SED005) and UVB (SED240), which detected that UVB was 73% of the total UV irradiation in the present experimental conditions. The UVB irradiation rate was 0.237125 mW/cm^2. The lamp was embedded in a 1.30 m × 0.43 m × 0.45 m box, in which the caged mice were placed 15 cm beneath the lamp. The groups were named UV-0h, UV-6h, UV-24h according to 0, 6 or 24 hours post UVB irradiation and AG-control, AG-UV-0h and AG-UV-24 for the animals pre-treated with aminoguanidine (AG). One square centimetre of dorsal skin was removed from each of the animals in the UVB irradiation treatment groups and processed for subsequent analysis. A control group that received the AG treatment but no irradiation was also included. Eight animals were used in each group and parameters were measured in triplicates. Dorsal skin samples were removed at 0 (UV-0h), 6 (UV-6h) and 24 (UV-24h) hours postirradiation and stored at −76°C until use. Freshly removed skin was tested to possible interference on the storage and no difference on the analysis was observed, so the samples were kept at −76°C until use. The UV-0h, UV-6h and UV-24h groups were treated three times every 8 hours with AG (AG; 50 mg/kg i.p.) [27], prior to UVB irradiation. Postirradiation, AG was administered once again in the UV-6h group and twice in the UV-24h group before the sacrifice.

Tissue preparation

The dorsal skin homogenates from control, irradiated (UV-0h, UV-6h; UV-24h) and AG treated mice were prepared as described by Peres et al. [28]. Briefly, the skins were homogenised in an Ultraturrax homogeniser containing 10 mg/ml or 50 mg/ml of tissue in 30 mM KH_2PO_4/K_2HPO_4 buffer and 120 mM KCl at pH 7.4. The supernatant (10 mg/ml) was used for *tert*-butyl hydroperoxide-stimulated chemiluminescence assay and also used to determine the total antioxidant capacity (TRAP). The supernatant (50 mg/ml) was used to determine the catalase activity and superoxide dismutase activity assays. The homogenate for the NO assay is described forward.

Lipid peroxidation measurement by tert-butyl hydroperoxide-initiated chemiluminescence

Reaction mixtures were placed in luminescence tubes containing 3% (w/v) of the skin supernatant and 3 mM *tert*-butyl hydroperoxide, in a final volume of 1 ml. The *tert*-butyl hydroperoxide-initiated chemiluminescence reaction was measured in a GLOMAX TD/20 20 luminometer (Turner Designs), with a response range of 300–650 nm. The tubes were maintained in the dark until assayed, which was performed in a room at 28°C [28–32]. The results were expressed in relative light units/g tissue (RLU/g tissue). The entire curve was used to determine the lipid peroxides present in the sample. For each mouse skin, a 45-min curve, where each point represented the differential smoothing of 45 readings, was obtained by interpolation. Peak-height (PH) and area under the curve (AUC) were extracted by integral calculus from each mouse curve, and were used to determine the lipid hydroperoxides present in the sample. The results are expressed in relative light units/g tissue (RLU/g tissue).

Nitric oxide quantification, a luminol-H_2O_2-induced chemiluminescence assay

NO was measured as described by Kikuchi et al. [33,34], with the following modifications. Hairless mouse skin (5 mg/ml) was prepared under N_2 bubbling to assure O_2 free medium in 2 mM NA_2CO_3 buffer, at pH 8.5, previously degassed by N_2 for 45 seconds periods of homogenisation using an Ultraturrax homogeniser (Marconi, Brazil). To investigate the role of NO in UVB irradiated skin, a tissue concentration of 0.250% (w/v) was adopted for all experiments. Equal volumes of 360 µM luminol/3 mM desferrioxamine (DFO) and 200 mM H_2O_2 were mixed and incubated at room temperature under moderate agitation for 5 minutes. To initiate the chemiluminescence reaction, 50 µL of this mixture were added automatically in the luminometer chamber containing at a final volume of 850 µL. The chemiluminescence spectrum was recorded for 5 minutes using a GLOMAX TD/20 20 luminometer (Turner Designs, USA). The Origin v. 7.5 program was used to plot chemiluminescence curves that were analysed using the peak height (PH) and AUC to determine the NO present in the sample. The results were expressed in relative light units/g tissue (NO RLU/g tissue). To prove the assay sensibility to NO quantification, 100 µM 2-(4-carboxyphenyl)-4,4,5,5-tetramethylimidazoline-1-oxyl-3-oxide (cPTIO), a specific scavenger of NO [35], was added immediately before the quantification of light emission in

chemical (standard NO solution) and biological (skin sample) analyses.

Standard NO solution

A solution of 400 pM NO was synthesized by nitrite reduction at acid pH [36]. For the reaction, 0.1 M H_2SO_4, 0.1 M KI and 0.1 mM $NaNO_2$ were used. The solution of 400 pM NO was diluted to a final concentration of 400 fM NO in 2 mM Na_2CO_3 buffer, pH 8.5, previously degassed by N_2 and chemiluminescence reading was performed in the same manner previously described.

Measurement of the total antioxidant capacity of skin (TRAP)

Total antioxidant capacity of supernatant skin homogenate prepared as described was measured by chemiluminescence, in a reaction medium containing 20 µM of 2-azo-bis-(2-amidinopropane) and 200 µM of luminol. After maximal emission was attained, 100 µL of tissue supernatant or 70 µL of trolox were added to the reaction medium. The time of total quenching was compared with trolox quenching and the results expressed in µM trolox [37].

Superoxide dismutase activity (SOD)

SOD activity was determined according to Marklund and Marklund [38], based on the inhibition of pyrogallol autoxidation in an aqueous solution of SOD. This oxidation is accompanied by a yellow colour formation in the reaction medium, monitored at 420 nm. Aliquots of supernatant skin homogenate (50 mg tissue/ml) diluted in Tris buffer with 1 N HCl and 5 mM EDTA, pH 8.0, were added to pyrogallol. The reaction was monitored continuously for 5 minutes. The autoxidation of pyrogallol alone was used as control. The amount of SOD that is able to inhibit 50% of pyrogallol autoxidation is defined as the enzymatic activity unit (U). Final SOD results were expressed in USOD/mg protein.

Catalase activity (CAT)

CAT activity was determined according to Cohen, Dembiec and Marcus [39], modified by Aebi [40]. The absorbance of a hydrogen peroxide (H_2O_2), in a 1 M HCl–Tris buffer, pH 8.0, was monitored at 240 nm. Aliquots of supernatant skin homogenate (50 mg tissue/ml) were added to the medium and the decrease in absorbance of hydrogen peroxide was monitored for 5 minutes. The results were expressed as ABS/mg protein/min. The decomposition of H_2O_2 is directly related to the decrease in absorbance.

Protein concentration

Protein was determined by the method of Lowry et al. [41], modified by Miller [42]. Both methods used bovine serum albumin (BSA) as standard.

Histological assessment

The skin samples preparations were submitted to immunohistochemical analysis. Nonspecific protein binding was blocked with normal serum (Vectastain Elite ABC Kit, Universal, Vector Laboratories Inc., Burlingame, CA, USA). The sections were then incubated with monoclonal primary antibodies specific for proliferating cell nuclear antigen (PCNA, clone PC10; DAKO A/S, Glostrup, Denmark, dilution 1:100), nitrotyrosine (clone HM11; Santa Cruz Biotechnology, Santa Cruz, CA, USA, dilution 1:100), vascular endothelial growth factor (VEGF, clone A20; Santa Cruz Biotechnology, dilution 1:100) and nitric oxide synthase (iNOS, clone ab15323; Abcam, Cambridge, UK, dilution 1:100), for 2 hours at room temperature (25°C) in a humid chamber. Following washes in PBS, biotinylated pan-specific universal secondary antibody (Vectastain Elite ABC Kit, Universal, Vector Laboratories Inc.). Next, the slides were incubated with the avidin–biotin-peroxidase complex (Vectastain Elite ABC Kit, Universal, Vector Laboratories Inc.) and developed with the Vector NovaRED kit (Vector Laboratories Inc.). The slides were counterstained by Harris haematoxylin, dehydrated and mounted with Permount (Biomeda, Foster City, CA, USA). As negative controls, all specimens were incubated with an isotope-matched control antibody under identical conditions. The preparations for each marker were evaluated randomly, at least 10 representative high-power fields (× 40). The immunolabelling percentage was evaluated by a ratio of unequivocal labelling located at nuclei (PCNA) for each 100 counted epithelial cells or percentage of labelled area (nitrotyrosine, VEGF and iNOS), using the Image J software.

Statistical analysis

The obtained values are presented as mean ± SEM. The student's *t*-test was used for statistical comparisons of the AUC and PH. Two-Way ANOVA and Bonferroni as *post-hoc* test, was used to analyse the lipid peroxidation entire chemiluminescence curve. Statistical analysis was performed using GraphPad Prism 4.0 and 5.0 (GraphPad, San Diego, CA). Histological assessments are reported as mean ± SD and statistical comparisons of the groups were performed using the Mann–Whitney test. Probability values less than 0.05 were considered statistically significant.

Results

Lipid peroxidation by tert-butyl hydroperoxide-initiated chemiluminescence

The formation of lipid peroxides (LOO) in hairless mouse skin following UVB irradiation was evaluated and the highest emission was observed on UV-0h and UV-24h.

The entire curves were employed to perform statistical comparison by two-way ANOVA ($p<0.0001$) followed the Bonferroni *post-hoc* test. It showed 20 points and 25 points significantly different to the UV-0h and UV-24h, respectively, compared to the control. Considering the AUC (Figure 1a), Student t-test showed a significant increase in LOO for the immediate irradiation at UV-0h (AUC: 5317 ± 180.4; $p<0.01$) and 24 hours after irradiation (UV-24h) (6965 ± 527.4; $p<0.0001$) when the groups were compared to the control (AUC: 4480 ± 140.6). All groups were treated with aminoguanidine and lipid peroxidation decreased (Figure 1b) in AG-UV-0h (AUC: 4940 ± 202.4) and AG-UV-24h (AUC: 5475 ± 255.9), to the point where it was no longer significantly different to the control group (AG-control) (AUC: 4903 ± 142.7). The PH analysis followed the AUC behaviour.

Nitric oxide quantification, a luminol-H_2O_2-induced chemiluminescence

Figure 2a shows the increase levels of NO in the UV-24h group (AUC: $41.0 \times 10^6 \pm 9.52 \times 10^6$; $p<0.01$) compared to the AUC of control group (AUC: $19.8 \times 10^6 \pm 1.9 \times 10^6$). Figure 2b shows the decrease in NO when the UV-24h group was treated with AG (AG-UV-24h) (AUC: $19.5 \times 10^6 \pm 2.7 \times 10^6$), returning to control levels (AG-control) (AUC: $15.4 \times 10^6 \pm 1.3 \times 10^6$). The AG-UV-0h remained unaltered with AG treatment when compared to non-treated mice (UV-0h; Figure 3a), and significantly increased (27.6×10^6; $p<0.01$) when compared to AG-control (Figure 3b). The PH analysis followed the AUC behaviour.

Figure 3a,b shows the biological (mouse skin sample = control) and chemical (standard NO solution) analysis quantification of NO by chemiluminescence, using cPTIO. When cPTIO was added to the reaction medium, photon emission decreased significantly in the biological and chemical analysis. Biological: C + cPTIO (AUC: $9.2 \times 10^6 \pm 0.4 \times 10^6$; $p<0.001$) compared to the control (AUC: $18.1 \times 10^6 \pm 0.4 \times 10^6$). Chemical: standard NO solution + cPTIO (AUC: $8.4 \times 10^5 \pm 0.7 \times 10^5$; $p<0.0001$) compared to the standard NO solution (AUC: $15.4 \times 10^5 \pm 1.8 \times 10^5$). The PH analysis followed the AUC behaviour.

Measurement of the TRAP

The total antioxidant capacity (Figure 4a) showed a significant decrease only on the UV-6h group (0.729 ± 0.077 µM trolox; $p<0.01$) when compared to control (1.000 ± 0.05695). When the UV-6h group was treated with AG (AG-UV-6h = 0.876 ± 0.832 µM trolox), the TRAP returned to control levels (AG-control: 0.9005 ± 0.1108).

The enzymatic parameters showed on Figure 4b, catalase decreased significantly ($p<0.01$) in the skin of

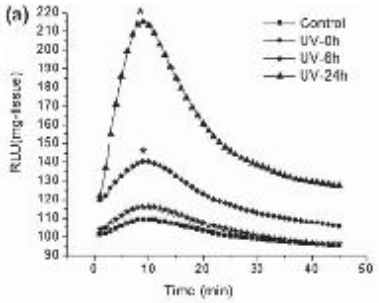

Statistical Analysis	Control X UV-0h	Control X UV-6h	Control X UV-24h
Two-way ANOVA	P < 0.0001	P = 0.0004	P < 0.0001
Bonferroni's Test	P < 0.0010 Points: 2 21	P > 0.0500	P < 0.0010 Points: 3 27
PH Student's t Test	P = 0.0011	P = 0.3875	P < 0.0001
AUC Student's t Test	P = 0.0026	P = 0.5820	P < 0.0001

Statistical Analysis	AG-Control X AG-UV-0h	AG-Control X AG-UV-6h	AG-Control X AG-UV-24h
Two-way ANOVA	P = 0.4245	P = 0.1014	P < 0.0001
Bonferroni's Test	P > 0.0500	P > 0.0500	P > 0.0500
PH Student's t Test	P = 0.4182	P = 0.3781	P = 0.0667
AUC Student's t Test	P = 0.8833	P = 0.7673	P = 0.0801

Figure 1. Lipid peroxides measured by chemiluminescence stimulated by *tert*-butyl hydroperoxide expressed in relative light units (RLU). (a) Lipid peroxide formation in mouse skin homogenate following UVB irradiation. (b) Effect of iNOS inhibitor (AG) on lipid peroxides levels; AG (50 mg/kg) was administered as previously described.

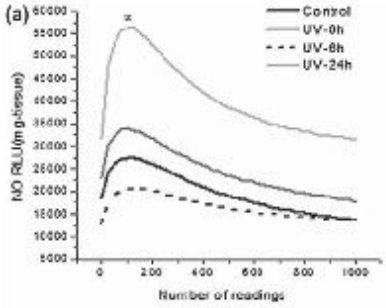

Statistical Analysis	Control X UV-0h	Control X UV-8h	Control X UV-24h
PH Student's t Test	P = 0.2212	P = 0.1736	P = 0.0146
AUC Students t Test	P = 0.1781	P = 0.3664	P = 0.0067

Statistical Analysis	AG-Control X AG-UV-0h	AG-Control X AG-UV-8h	AG-Control X AG-UV-24h
PH Student's t Test	P = 0.0107	P = 0.6387	P = 0.4335
AUC Student's t Test	P = 0.0083	P = 0.5404	P = 0.2615

Figure 2. Nitric oxide quantification by luminol-H_2O_2-induced chemiluminescence. (a) Quantification of NO in irradiated mouse skin homogenate. (b) Effect of iNOS inhibitor (AG) on NO production.

UV-6h (0.3018 ± 0.036 abs/mg protein) and remained low for the UV-24h (0.2909 ± 0.034 abs/mg protein) when compared to control (0.4339 ± 0.032). SOD activity did not change (control 0.8488 ± 0.075; UV-0h 0.6081 ± 0.061; UV-6h 0.7605 ± 0.103; UV-24h 0.6129 ± 0.097).

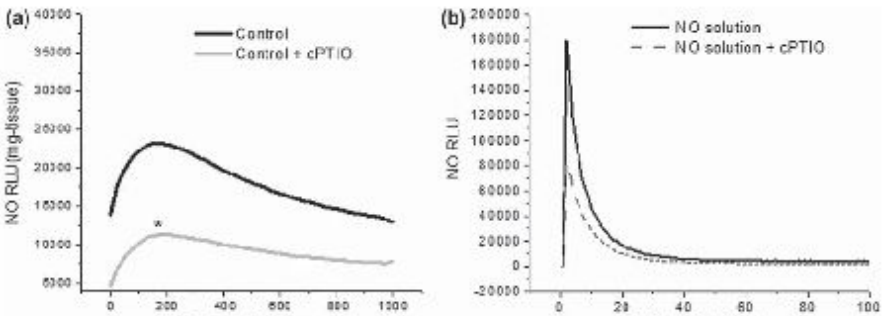

Statistical Analysis	Control X Control + cPTIO
PH Student's t Test	P = 0.0008
AUC Student's t Test	P = 0.0008

Statistical Analysis	NO solution X NO solution + cPTIO
PH Student's t Test	P = 0.0367
AUC Student's t Test	P = 0.0001

Figure 3. (a) Biological analysis of NO by luminol-H_2O_2-induced chemiluminescence. The mouse skin homogenate (control) was used and 100 µM cPTIO was added to the reaction medium and the emission was immediately quantified. (b) Chemical analysis of NO by luminol-H_2O_2-induced chemiluminescence. The standard NO solution at a final concentration of 400 fM NO was used and 100 µM cPTIO was added to the reaction medium and the emission was immediately quantified.

(a)

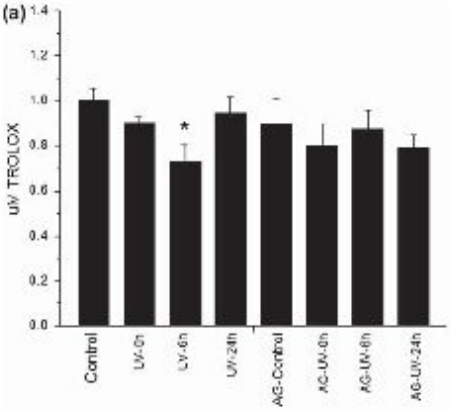

(b)

GROUP	SOD (USOD/mg protein) (number of animals)	CAT (ΔABS/mg protein) (number of animals)
Control	0.8488 ± 0.079 (12)	0.4339 ± 0.032 (11)
IR 3h	0.6081 ± 0.061 (6)	0.3411 ± 0.015 (5)
IR 6h	0.7605 ± 0.103 (7)	0.3018 ± 0.035* (7)
IR 24h	0.6125 ± 0.097 (6)	0.2939 ± 0.034* (5)

Figure 4. (a) Total antioxidant capacity (TRAP) in irradiated mouse skin measured by the chemiluminescence method. The results are the mean ± SEM; $p<0.01$. (b) Antioxidant enzymes, catalase and superoxide dismutase (SOD) of irradiated mice skin. The results are mean ± SEM; $^*p<0.05$ compared to control.

Histological assessment

Nitrotyrosine immunoreactivity (Figure 5a,b) was detected mostly in the dermal layer. The UV-0h (4.1% ± 0.36), UV-6h (6.0% ± 0.36) and UV-24h (15.86% ± 0.91) mice skin presented higher nitrotyrosine labelling when compared to control (0.5% ± 0.15), which diminished following AG treatment; AG-UV-0h (1.33% ± 0.21), AG-UV-6h (3.6% ± 0.25) and AG-UV-24h (7.57% ± 0.37). No significant finding was revealed in the control, AG-control (0.33% ± 0.21) groups (Figure 5b). The PCNA immunolabelling (Figure 6a,b) was almost absent in the control (0.28% ± 0.18), UV-0h (0.33% ± 0.21), UV-6h (0.33 ± 0.21) and UV-24h (0.41% ± 0.20) mice skin. The percentage of PCNA labelled area was increased in all AG-treated groups (AG-UV-0h (12.17% ± 0.47), AG-UV-6h (17.2% ± 0.86) and AG-UV-24h (6.28% ± 0.42)) (Figure 6b). VEGF labelling (Figure 7a,b) was increased in the UV-exposed mice with AG treatment (AG-UV-0h (12.33% ± 0.84), AG-UV-6h (23.8% ± 0.37) and AG-UV-24h (26.8% ± 0.67)) when compared to the control (0.07% ± 0.03) and to the groups that received only UV, UV-0h (0.4% ± 0.16), UV-6h (7.0% ± 0.57) and UV-24h (11.71% ± 0.68), but were not treated with AG (Figure 7b). The percentage iNOS labelled area was increased in the UV-24h group (7.3% ± 0.9), when compared to the control (0.5% ± 0.1). The AG treatment decreased the iNOS labelling in AG-UV-24h group (0.9% ± 0.2), compared to AG-control (0.7% ± 0.3) (Figure 8).

Discussion

UVB induces rapid release of NO and O_2^- in cultures of keratinocytes [5] or epidermis [6] and promptly react with each other in diffused controlled reactions ($k = 6 \times 10^{10}$ mmol^{-1} s^{-1}) leading to $ONOO^-$ production [5]. Peroxynitrite is an important mediator of free-radical-dependent toxicity [43,44], because of its strong oxidising properties towards different biomolecules, including protein and non-protein thiol [45] and membrane phospholipids [43].

In the skin, UVB light irradiation generates a cascade of cellular events in response to the induced damage, mediated by different signalling pathways [12]. Controversial studies concerning NO participation as a harmful or protective species in UV skin oxidative damage have been published. These studies mainly used the TBARS technique and NOS expression as a marker of oxidative and nitrosative stress evaluation, respectively [12–21]. In this study, a very sensitive *tert*-butyl hydroperoxide-initiated chemiluminescence assay was used to analyse the levels of lipidperoxidation in skin hairless mice on UVB irradiation. This assay indicates that the increase in chemiluminescence is closely related to the oxidative stress previously suffered by the tissue [28–32] leading to morphological changes, that is, UVB induces increase of lipid hydroperoxides formation, resulting in increased photon emission [28].

The NO levels were evaluated by a very sensitive and specific technique using a chemiluminescence measurement based on Kikushi et al. [33,34]. NO produced by chemical reaction (KI) showed a curve emission profile similar to that obtained using NO gas as obtained by other authors [33]. The skin sample produced low and wider curve profile possibly provoked by tissue and NO excess [33]. However, the PH and AUC of the light emission, resulting from the skin samples, increased in a dose dependent manner in respect to tissue concentration (data not shown). cPTIO, a specific NO scavenger [35], was used to provide more specificity on NO analysis. The scavenger decreased significantly the light emission in both the biological and chemical systems. Additionally, mice treated with AG an inhibitor of iNOS showed significant reduction on light emission as well as completely inhibit the induction of iNOS caused by UV irradiation. Altogether, these results confirm the specificity of the NO quantification. Our results showed a significant increase in lipid peroxidation immediately after skin UVB irradiation (UV-0h), which was reduced at 6 hours and achieved its highest value at 24 hours after irradiation. The identical profile of NO time course generation after UVB irradiation was observed. Treatment with AG significantly diminished the lipid peroxidation and NO levels in the UV-24h group besides marked reduction on iNOS labelling. Moreover,

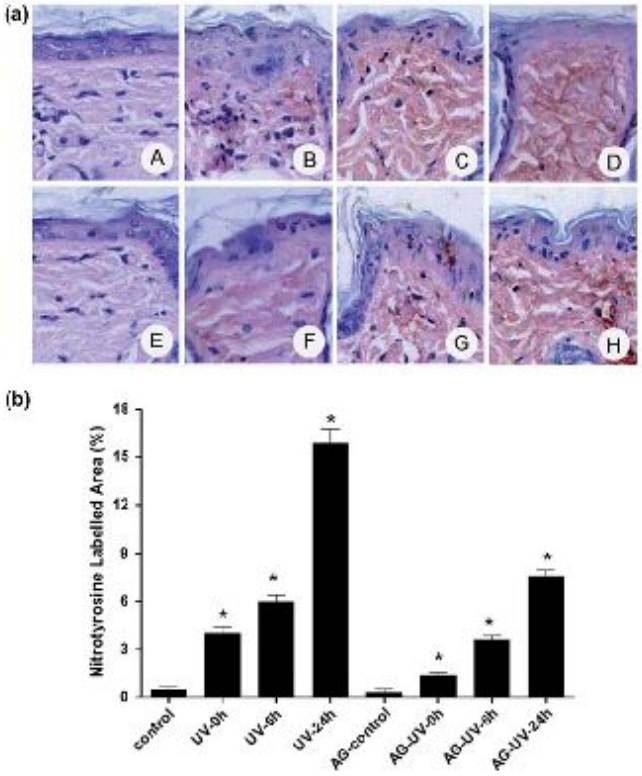

Figure 5. Immunohistochemical labelling of nitrotyrosine in UVB irradiated mice skin. (a) Photomicrographs of skin sections labelled with nitrotyrosine antibody: (A) control; (B) UV-0h; (C) UV-6h; (D) UV-24h; (E) AG-control; (F) AG-UV-0h; (G) AG-UV-6h; (H) AG-UV-24h. (b) Percentage of nitrotyrosine labelled area. The results are mean ± SEM; $*p < 0.001$ compared to the respective control.

nitrotyrosine arising mainly from $ONOO^-$ reaction with tyrosine protein [46], increased about 20-fold at 24 hours after UVB irradiation and was reduced by about 60% under AG treatment. These results indicated that NO produced by iNOS may react with O_2^- yielding $ONOO^-$, which mediated the skin oxidative and nitrosative damage 24 hours after UVB irradiation. In fact, the induction of iNOS is regulated through multiple signalling pathways and it can take hours to increase its expression [13]. In addition, Deliconstantinos et al. [47], showed that UVB radiation of keratinocytes increased NO and O_2^-, producing $ONOO^-$, a potent and noxious oxidant that initiates lipid peroxidation. Unlike that reported by Maglio et al. [12] and Lee et al. [21], our results indicated that the increase in iNOS postirradiation is a deleterious signalling pathway leading to lipid peroxidation and protein nitration in the skin of irradiated mice.

Immediately after skin UVB (UV-0h) irradiation, AG treatment was unable to inhibit NO generation, suggesting that NO production may be mediated by other sources at this time. NO is synthesized by a family of NO synthase enzymes, but its rapid release following UV exposure suggesting the existence of preformed stores, particularly nitrite and RSNOs, which can be directly mobilised by acute response to UV irradiation in the skin of *ex vivo* full-thickness human skin [48] as demonstrated an enzyme-independent nitric oxide formation [25]. More recently, another study indicated that UVB induced rapid increase of cNOS activity, which generated an imbalance between NO and $ONOO^-$, promoting apoptosis and skin damage [6]. Although NO levels did not decrease at UVB-0h, the analysis of the present results revealed that increased lipid peroxidation and nitrotyrosine levels were diminished by AG treatment. Since lipid and protein damage were inhibited by AG, it is reasonable to hypothesise that there is a small NO production in UV-0h group that is responsible, at least in part, for the oxidative and nitrosative damage at this time. More study will be necessary to determine the scale participation of the RNS and ROS in oxidative skin injury, immediately after skin UVB.

Lipid peroxidation levels observed in the control group, and at 6 hours after UVB irradiation were accompanied by the consumption of total antioxidant (TRAP) and decreased catalase activity, indicating that the antioxidant

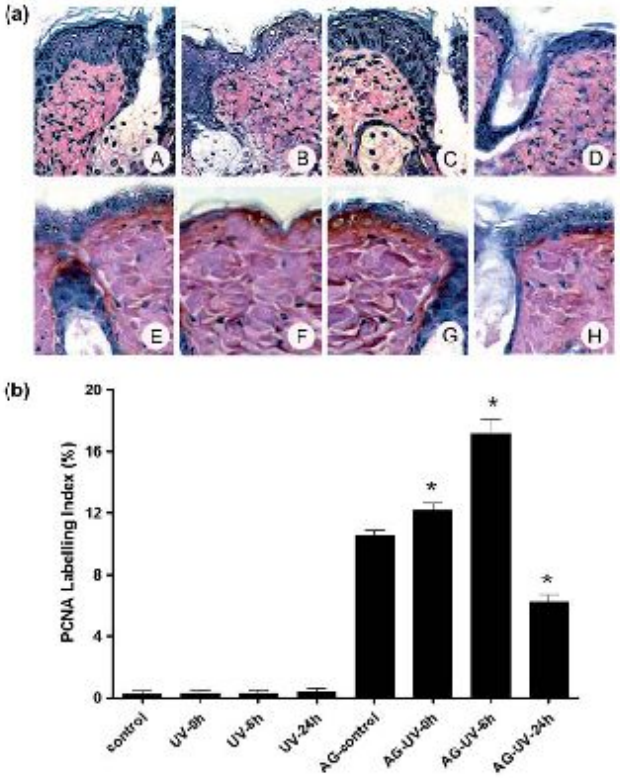

Figure 6. Immunohistochemical labelling of PCNA in UVB irradiated mice skin. (a) Photomicrographs of skin sections labelled with PCNA antibody: (A) control; (B) UV-0h; (C) UV-6h; (D) UV-24h; (E) AG-control; (F) AG-UV-0h (G); AG-UV-6h; (H) AG-UV-24h. (b) Percentage of PCNA labelled Area. The results are mean ± SEM; $*p<0.001$ compared to the respective control.

defences were able to mediate the reactive species yielded during this period. AG treatment inhibited TRAP consumption in the UV-6h group, probably due to the inhibition of NOS activity, which resulted in reduced NO production and a subsequent decrease in lipid peroxidation, returning to control levels as indicated by the chemiluminescence curve initiated by *tert*-butyl hydroperoxide. Previous studies suggested that UVB impairs endogenous antioxidant and that catalase is one of the most sensitive components of such mechanisms [49–52]. In UVB-24h, catalase activity is decreased, while TRAP returned to control levels. The antioxidant defences were not effective, as indicated by the great oxidative skin injury demonstrated in this time. The diminished catalase activity may play a role in this process. At physiological pH (7.0–7.4), O^{2-} is very rapidly dismutated to H_2O_2 ($K2 = 5 \times 10^5\ M^{-1}\ s^{-1}$) [53]. High levels of H_2O_2 are expected to react with NO, yielding ONOO_, a very strong lipid peroxidant. Evidence in support of this has been obtained *in vitro* for cell free systems [33,34]. In addition, NO is reported to react with O^{2-} to form $ONOO^-$ [19], which is a stronger oxidising species than H_2O_2 [25].

The histological analysis showed that in the UV-24h group (Figures 5, 6 and 7D) there is a thin or absent epithelial surface. Nevertheless, when treated with AG, the epithelial surface was preserved (Figures 5, 6 and 7H). PCNA is an active nuclear protein and serve as a marker of DNA repair and indirectly as an indicator of UVB induced damage [54,55]. Studies have demonstrated that UVB irradiation completely diminished PCNA protein expression in HaCaT cells and the treatment with delphinidin (antioxidant) significantly reversed UVB-induced PCNA inhibition, protecting the cells from UVB-induced apoptosis [55]. Our results showed that UVB irradiation completely abolished PCNA protein expression and treatment with AG reverses this condition. As PCNA indicates DNA repair [54,55] the decrease of its mark after UVB irradiation with the concomitant increase of NO and iNOS suggests that NO may modulate DNA repair. When AG was used, the PCNA labelling was evidenced again, supporting the evidence of NO participation on cell proliferation. The extensive range of NO-based signalling through *S*-nitrosylation has directly implicated *S*-nitrosylation in the regulation of numerous signalling pathways

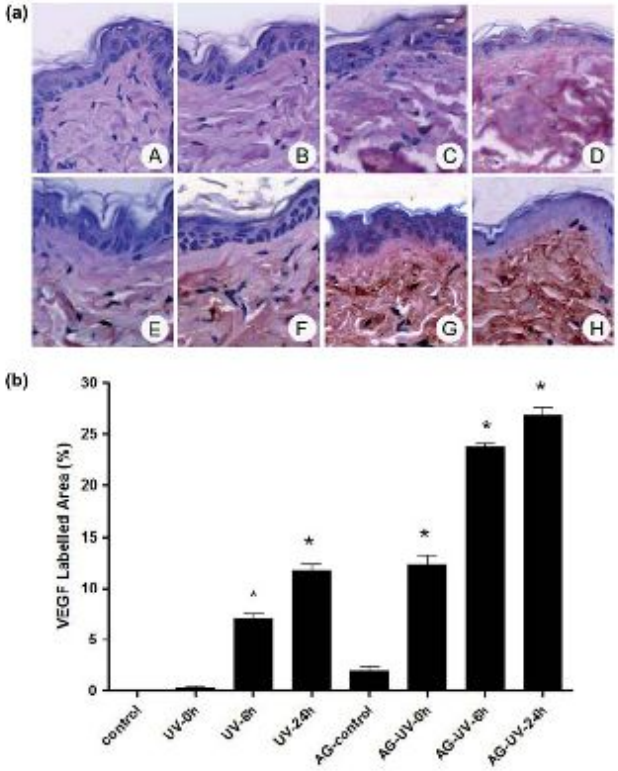

Figure 7. Immunohistochemical labelling of VEGF in UVB irradiated mice skin. (a) Photomicrographs of skin sections labelled with VEGF antibody: (A) control; (B) UV-0h; (C) UV-6h; (D) UV-24h; (E) AG-control; (F) AG-UV-0h; (G) AG-UV-6h; (H) AG-UV-24h. (b) Percentage of VEGF labelled area. The results are mean ± SEM; $^{*}p<0.001$ compared to the respective control.

in intact cellular systems [56–59]. Our results showed very low PCNA levels and very high nitrotyrosine labelled area with variation from 8- to 32-fold in all times after irradiation. Vascular endothelial growth factor (VEGF), which is the most potent growth factor of tumour neovasculature [60] and regulates vasculogenesis during embryonic development, progressively decreases postnatally and is minimal in most adult tissues [61]. However, VEGF expression is reinduced during pathologic angiogenesis, as occurs in patients with ischemic myocardium, in

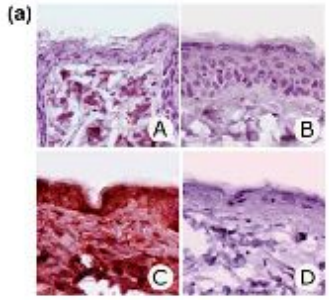

(b)

	NOS labeled Area (%) (number of animals)
Control	0.5 ± 0.1 [6]
AG-Control	0.7 ± 0.3 [6]
UV-24h	7.3 ± 0.9 * [6]
AG-UV-24h	0.9 ± 0.2 * [6]

Figure 8. Immunohistochemical labelling of iNOS in UVB irradiated mice skin. (a) Photomicrographs of skin sections labelled with iNOS antibody: (A) control; (B) AG-control; (C) UV-24h; (D) AG-UV-24h. (b) Percentage of iNOS labelled area. The results are mean ± SEM; $p<0.001$, *compared to control, $^{\#}$compared to AG-control.

inflamed tissue [62] and in human carcinomas [63]. These results consistently indicated that NO plays a very important role in the cell proliferation. In mouse skin, it was reported that increased vascular permeability induced by VEGF is mediated by local production of NO, produced by iNOS [64]. Our results indicated an increase in VEGF at 6 hours and 24 hours after UVB irradiation. Treatment with AG also resulted in an additional increase of cell proliferation markers (VEGF and PCNA), suggesting that those markers may suffer down regulation that is dependent on NO concentration in the milieu.

Taken together, these results indicate that the UVB irradiation effects are mainly mediated by NO, leading to oxidative and nitrosative skin injury after 24 hours postirradiation, as demonstrated by increased lipid peroxidation and nitrotyrosine labelling. Moreover, NO and other products from the oxidative process modulates PCNA and VEGF expression suggesting both direct and indirect NO involvement on cell lesion and proliferation. Additionally, in this study for the first time, the profile of nitric oxide levels in skin challenged by UVB irradiation was accomplished. Given that NO concentration is a critical factor underlying many different biological and pathological processes, our findings provide a better understanding of the mechanisms by which UVB exerts its deleterious effects on the skin in addition to mediating cell proliferation-related PCNA and VEGF.

Acknowledgements

Grant support was provided by the Coordenação de Aperfeiçoamento de Pessoal de Nível Superior – CAPES. The authors are very grateful to J. A. Vargas for his excellent technical assistance.

Declaration of interest

The authors state no conflict of interest. The authors alone are responsible for the content and writing of the paper.

References

[1] Podda M, Traber MG, Weber C, Yan L-J, Packer L. UV-irradiation depletes antioxidants and causes oxidative damage in a model of human skin. Free Radic Biol Med 1998;24:55–65.
[2] Ichihashi M, Ueda M, Budiyanto A, Bito T, Oka M, Fukunaga M, et al. UV-induced skin damage. Toxicology 2003;189:21–39.
[3] Nichols JA, Katiyar SK. Skin photoprotection by natural polyphenols: anti-inflammatory, antioxidant and DNA repair mechanisms. Arch Dermatol Res 2010;302:71–83.
[4] Yamaoka J, Kawana S, Miyachi Y. Nitric oxide inhibits ultraviolet B-induced murine keratinocyte apoptosis by regulating apoptotic signaling cascades. Free Radic Res 2004;38:943–950.
[5] Aitken GR, Henderson JR, Chang SC, McNeil CJ, Birch-Machin MA. Direct monitoring of UV-induced free radical generation in HaCaT keratinocytes. Clin Exp Dermatol 2007;32:722–727.
[6] Wu S, Wang L, Jacoby AM, Jasinski K, Kubant R, Malinski T. Ultraviolet B light-induced nitric oxide/peroxynitrite imbalance in keratinocytes-implications for apoptosis and necrosis. Photochem Photobiol 2010;86:389–96.
[7] Arany I, Brysk MM, Brysk H, Tyring SK. Regulation of inducible nitric oxide synthase mRNA levels by differentiation and cytokines in human keratinocytes. Biochem Biophys Res Commun 1996;220:618–622.
[8] Qureshi AA, Hosoi J, Xu S, Takashima A, Granstein RD, Lerner EA. Langerhans cells express inducible nitric oxide synthase and produce nitric oxide. J Invest Dermatol 1996;107:815–821.
[9] Wang R, Ghahary A, Shen YJ, Scott PG, Tredjet EE. Human dermal fibroblasts produce nitric oxide and express both constitutive and inducible nitric oxide synthase isoforms. J Invest Dermatol 1996;106:419–427.
[10] Rocha IM, Guillo LA. Lipopolysaccharide and cytokines induce nitric oxide synthase and produce nitric oxide in cultured normal human melanocytes. Arch Dermatol Res 2001;293:245–248.
[11] Tsatmali M, Manning P, McNeil CJ, Thody AJ. Alpha-MSH inhibits lipopolysaccharide induced nitric oxide production in B16 mouse melanoma cells. Ann NY Acad Sci 1999;885:474–476.
[12] Gonzalez Maglio DH, Paz ML, Ferrari A, Weill FS, Czerniczyniec A, Leoni J, Bustamante J. Skin damage and mitochondrial dysfunction after acute ultraviolet B irradiation: relationship with nitric oxide production. Photodermatol Photoimmunol Photomed 2005;21:311–317.
[13] Kuhn A, Fehsel K, Lehmann P, Krutmann J, Ruzicka T, Kolb-Bachofen V. Aberrant timing in epidermal expression of inducible nitric oxide synthase after UV irradiation in cutaneous lupus erythematosus. J Invest Dermatol 1998;111:149–153.
[14] Meeran SM, Katiyar N, Singh T, Katiyar SK. Loss of endogenous interleukin-12 activates survival signals in ultraviolet-exposed mouse skin and skin tumors. Neoplasia 2009;11:846–855.
[15] Martin JP Jr, Burch P. Production of oxygen radicals by photosensitization. Methods Enzymol 1990;186:635–645.
[16] Ogura R, Sugiyama M, Nishi J, Haramaki N. Mechanism of lipid formation following exposure of epidermal homogenate to ultraviolet light. J Invest Dermatol 1991;97:1044–1047.
[17] Masaki H, Atsumi T, Sakurai H. Detection of hydrogen peroxide and hydroxyl radicals in murine skin fibroblasts under UVB irradiation. Biochem Biophys Res Commun 1995;206:474–479.
[18] Heck D, Vetrano AM, Mariano TM, Laskin JD. UVB light stimulates production of reactive oxygen species: unexpected role for catalase. J Biol Chem 2003;278:22432–22436.
[19] Halliwell B, Gutteridge JM. Free radicals in biology and medicine. Oxford: University Press, New York; 2007.
[20] Hakozaki T, Date A, Yoshii T, Toyokuni S, Yasui H, Sakurai H. Visualization and characterization of UVB-induced reactive oxygen species in a human skin equivalent model. Arch Dermatol Res 2008;300:51–56.
[21] Lee SC, Lee JW, Jung JE, Lee HW, Chun SD, Kang IK, et al. Protective role of nitric oxide-mediated inflammatory response against lipid peroxidation in ultraviolet B-irradiated skin. Br J Dermatol 2000;142:653–659.
[22] Weller R, Schwentker A, Billiar TR, Vodovotz Y. Autologous nitric oxide protects mouse and human keratinocytes from ultraviolet B radiation-induced apoptosis. Am J Physiol Cell Physiol 2003;284:1140–1148.
[23] Bhowmick R, Girotti AW. Rapid upregulation of cytoprotective nitric oxide in breast tumor cells subjected to a photodynamic therapy-like oxidative challenge. Photochem Photobiol 2011;87:378–386.
[24] Wang L, Liu W, Parker SH, Wu S. Nitric oxide synthase activation and oxidative stress, but not intracellular zinc dyshomeostasis, regulate ultraviolet B light-induced apoptosis. Life Sci 2010;86:448–454.

[25] Mowbray M, McLintock S, Weerakoon R, Lomatschinsky N, Jones S, Rossi AG, Weller RB. Enzyme-independent NO stores in human skin: quantification and influence of UV radiation. J Invest Dermatol 2009;129:834–842.
[26] Casagrande R, Georgetti SR, Verri WA Jr, Dorta DJ, Santos AC, Fonseca MJV. Protective effect of topical formulations containing quercetin against UVB-induced oxidative stress in hairless mice. J Photochem Photobiol B 2006;84:21–27.
[27] Bowman MA, Simell OG, Peck AB, Cornelius J, Luchetta R, Look Z, et al. Pharmacokinetics of aminoguanidine administration and effects on the diabetes frequency in nonobese diabetic mice. J Pharmacol Exp Ther 1996;279:790–794.
[28] Peres PS, Terra VA, Guarnier FA, Cecchini R, Cecchini AL. Photoaging and chronological aging profile: understanding oxidation of the skin. J Photochem Photobiol B 2011;103: 93–97.
[29] Gonzalez-Flecha B, Llesuy S, Boveris A. Hydroperoxide-initiated chemiluminescence: an assay for oxidative stress in biopsies of heart, liver, and muscle. Free Rad Biol Med 1991;10:93–100.
[30] Oliveira FJ, Cecchini R. Oxidative stress of liver in hamster infected with *Leishmania (L.) chagasi*. J Parasitol 2000;86: 1067–1072.
[31] ColadoSimão AN, Suzukawa AA, Casado MF, Guarnier FA, Cecchini R. Genistein abrogates pre-hemolytic and oxidative stress damage induced by 2,2'-azobis (Amidinopropane). Life Sci 2005;78:1202–1210.
[32] Guarnier FA, Cecchini AL, Suzukawa AA, Maragno AL, Simão AN, Gomes MD, Cecchini R. Time course of skeletal muscle loss and oxidative stress in rats with Walker 256 solid tumor. Muscle Nerve 2010;42:950–958.
[33] Kikuchi K, Nagano T, Hayakawa H, Hirataj Y, Hirobe M. Detection of nitric oxide production from a perfused organ by a luminol-H_2O_2 system. Anal Chem 1993;65:1794–1799.
[34] Kikuchi K, Nagano T, Hayakawa H, Hirataj Y, Hirobe M. Real time measurement of nitric oxide produced ex vivo by luminol-H_2O_2 chemiluminescence method. J Biol Chem 1993;268:23 106–23110.
[35] Ederli L, Reale L, Madeo L, Ferranti F, Gehring C, Fornaciari M, et al. NO release by nitric oxide donors in vitro and in planta. Plant Physiol Biochem 2009;47:42–48.
[36] Tsukada Y, Yasutake M, Jia D, Kusama Y, Kishida H, Takano T, et al. Real-time measurement of nitric oxide by luminol-hydrogen peroxide reaction in crystalloid perfused rat heart. Life Sci 2003;72:989–1000.
[37] Repetto M, Reides C, Carretero MLG, Costa M, Griemberg G, Llesuy S. Oxidative stress in blood of HIV infected patients. Clin Chim Acta 1996;255:107–117.
[38] Marklund S, Marklund G. Involvement of the superoxide anion radical in the antioxidation of pyrogallol and a convenient assay for superoxide dismutase. Eur J Biochem 1974;47:469–474.
[39] Cohen G, Dembiec D, Marcus J. Measurement of catalase activity in tissue extracts. Anal Biochem 1970;34:30–38.
[40] Aebi H. Catalase in vitro. Methods Enzymol 1984;105:121–126.
[41] Lowry OH, Rosebrough NJ, Farr AL, Randall RJ. Protein measurement with the folin phenol reagent. J Biol Chem 1951; 193:265–275.
[42] Miller GL. Protein determination for large number of samples. Anal Chem 1959;31:964.
[43] Radi R, Beckman JS, Bush KM, Freeman BA. Peroxynitrite-induced membrane lipid peroxidation: the cytotoxic potential of superoxide and nitric oxide. Arch Biochem Biophys 1991;288:481–487.
[44] Villiotou V, Stavrides JC. Nitric oxide and peroxynitrite released by ultraviolet B-irradiated human endothelial cells are possibly involved in skin nitrosative stress promote fungal virulence. Curr Biol 1996;13:1963–1968.
[45] Radi R, Beckman JS, Bush K, Freeman BA. Peroxynitrite oxidation of sulfhydryls. J Biol Chem 1991;288:481–487.
[46] Radi R. Nitric oxide, oxidants, and protein tyrosine nitration. Proc Natl Acad Sci USA 2004;101:4003–4008.
[47] Deliconstantinos G, Villiotou V, Stavrides JC. Increase of particulate nitric oxide synthase activity and peroxynitrite synthesis in UVB-irradiated keratinocyte membranes. Biochem J 1996;320:997–1003.
[48] Paunel AN, Dejam A, Thelen S, Kirsch M, Horstjann M, Gharini P, et al. Enzyme-independent nitric oxide formation during UVA challenge of human skin: characterization, molecular sources, and mechanisms. Free Radic Biol Med 2005; 38:606–615.
[49] Fuchs J, Huflejt ME, Rothfuss LM, Wilson DS, Carcamo G, Packer L. Impairment of enzymic and nonenzymic antioxidants in skin by UVB irradiation. J Invest Dermatol 1989;93:769–773.
[50] Vayalil PK, Elmets CA, Katiyar SK. Treatment of green tea polyphenols in hydrophilic cream prevents UVB-induced oxidation of lipids and proteins, depletion of antioxidant enzymes and phosphorylation of MAPK proteins in SKH-1 hairless mouse skin. Carcinogenesis 2003;4:927–936.
[51] Jeon SE, Choi-Kwon S, Park KA, Lee HJ, Park MS, Lee JH, et al. Dietary supplementation of (+)-catechin protects against UVB-induced skin damage by modulating antioxidant enzyme activities. Photodermatol Photoimmunol Photomed 2003;19:235–241.
[52] Muramatsu S, Suga Y, Mizuno Y, Hasegawa T, Matsuba S, Hashimoto Y, et al. Differentiation-specific localization of catalase and hydrogen peroxide, and their alterations in rat skin exposed to ultraviolet B rays. J Dermatol Sci 2005;37: 151–158.
[53] Noronha-Dutra AA, Epperlein MM, Woolf N. Reaction of nitric oxide with hydrogen peroxide to produce potentially cytotoxic singlet oxygen as a model for nitric oxide-mediated killing. FEBS Lett 1993;1:59–62.
[54] Moore JO, Palep SR, Saladi RN, Gao D, Wang Y, Phelps RG, et al. Effects of ultraviolet B exposure on the expression of proliferating cell nuclear antigen in murine skin. Photochem Photobiol 2004;80:587–595.
[55] Afaq F, Syed DN, Malik A, Hadi N, Sarfaraz S, Kweon MH, et al. Delphinidin, an anthocyanidin in pigmented fruits and vegetables, protects human HaCaT keratinocytes and mouse skin against UVB-mediated oxidative stress and apoptosis. J Invest Dermatol 2007;127:222–232.
[56] Sen N, Hara MR, Kornberg MD, Cascio MB, Bae BI, Shahani N, et al. Nitric oxide-induced nuclear GAPDH activates p300/CBP and mediates apoptosis. Nat Cell Biol 2008;10: 866–873.
[57] Jaffrey SR, Erdjument-Bromage H, Ferris CD, Tempst T, Snyder SH. Protein *S*-nitrosylation: a physiological signal for neuronal nitric oxide. Nat Cell Biol 2001;3:193–197.
[58] Liu L, Yan Y, Zeng M, Zhang J, Hanes MA, Ahearn G, et al. Essential roles of S-nitrosothiols in vascular homeostasis and endotoxic shock. Cell 2004;116:617–28.
[59] de Jesús-Berríos M, Liu L, Nussbaum JC, Cox GM, Stamler JS, Heitman J. Enzymes that counteract nitrosative stress promote fungal virulence. Curr Biol 2003;13:1963–1968.
[60] Bates DO, Cui TG, Doughty JM, Winkler M, Sugiono M, Shields JD, et al. VEGF165b, an inhibitory splice variant of vascular endothelial growth factor, is down-regulated in renal cell carcinoma. Cancer Res 2002;62:4123–4131.
[61] Gerber HP, Hillan KJ, Ryan AM, Kowalski J, Keller GA, Rangell L, et al. VEGF is required for growth and survival in neonatal mice. Development 1999;126:1149–1159.
[62] Carmeliet P, Collen D. Transgenic mouse models in angiogenesis and cardiovascular disease. J Pathol 2000;190:387–405.
[63] Nicol D, Hii SI, Walsh M, Teh B, Thompson L, Kennett C, Gotley D. Vascular endothelial growth factor expression is increased in renal cell carcinoma. J Urol 1997;157:1482–1486.
[64] Fujii E, Irie K, Ohba K, Ogawa A, Yoshioka T, Yamakawa M, Muraki T. Role of nitric oxide, prostaglandins and tyrosine kinase in vascular endothelial growth factor-induced increase in vascular permeability in mouse skin. Naunyn Schmiedebergs Arch Pharmacol 1997;356:475–480.

APÊNDICE 3 - Artigo 3: Genistein prevents ultraviolet B radiation-induced nitrosative skin injury and promotes cell proliferation

Journal of Investigative Dermatology

Genistein prevents ultraviolet B radiation-induced nitrosative skin injury and promotes cell proliferation

Journal:	*Journal of Investigative Dermatology*
Manuscript ID:	Draft
Manuscript Type:	Original Article
Date Submitted by the Author:	n/a
Complete List of Authors:	Terra, Vania; Universidade Estadual de Londrina, Patologia Geral Frade, Marco Andrey; Universidade de São Paulo - Faculdade de Medicia de Ribeirão Preto, Clínica Médica - Divisão de Dermatologia Ramalho, Leandra; Universidade de São Paulo - Faculdade de Medicia de Ribeirão Preto, Departamento de Patologia e Medicina Legal Ramalho, Fernando; Universidade de São Paulo - Faculdade de Medicia de Ribeirão Preto, Departamento de Patologia e Medicina Legal Luiz, Rodrigo; Universidade Estadual de Londrina, Patologia Geral Souza-Neto, Fernando; Universidade Estadual de Londrina, Patologia Geral Andrade, Thiago; Universidade de São Paulo - Faculdade de Medicia de Ribeirão Preto, Clínica Médica - Divisão de Dermatologia Leite, Marcel; Universidade de São Paulo - Faculdade de Medicia de Ribeirão Preto, Clínica Médica - Divisão de Dermatologia Pasta, Angelo; Universidade de São Paulo - Faculdade de Medicia de Ribeirão Preto, Departamento de Patologia e Medicina Legal Costa, An Carolina; Universidade Estadual de Londrina, Patologia Geral Guedes, Flavia; Universidade de São Paulo - Faculdade de Medicia de Ribeirão Preto, Clínica Médica - Divisão de Dermatologia Rodrigues, Francielle; Universidade Estadual de Londrina, Patologia Geral Cecchini, Rubens; Universidade Estadual de Londrina, Patologia Geral Cecchini, Alessandra; Universidade Estadual de Londrina, Patologia Geral; Universidade Estadual de Londrina, Patologia Geral
Key Words:	Genistein, nitric oxide, proliferation markers, oxidative stress, UVB skin irradiation

Genistein prevents ultraviolet B radiation-induced nitrosative skin injury and promotes cell proliferation

V. A. Terra[1], M. A. C. Frade[4], L. N. Z. Ramalho[3], F. Ramalho[3], R. C. Luiz[1], F. P. Souza-Neto[1], T. A. M. Andrade[4], A.M.N. Leite[4], A.A.C. Pasta[1]; A. C. Conchon[1], F. A. Guedes[3], F.C. Rodrigues[1], R. Cecchini[2], A. L. Cecchini[1*]

[1]Laboratorio de Patologia Molecular, Universidade Estadual de Londrina . Rod. Celso Garcia Cid, PR-445, km 380, 86051-990, Londrina, PR, Brasil.
[2]Laboratorio de Patofisiologia e Radicais Livres, Universidade Estadual de Londrina. Rod. Celso Garcia Cid, PR-445, km 380, 86051-990, Londrina, PR, Brasil.
[3]Departamento de Patologia e Medicina Legal, Universidade de São Paulo, Ribeirão Preto, SP Brasil
[4]Departamento de Clínica Medica, Divisão de Dermatologia, Universidade de São Paulo, Ribeirão Preto, SP Brasil

Keywords
Genistein, nitric oxide, lipid peroxidation, oxidative stress, UVB skin irradiation, nitrotyrosine, proliferation markers.

***Corresponding author**

CORRESPONDING AUTHOR:
Alessandra Lourenço Cecchini

E-mail: alcecchini@uel.br;

Phone: +55 (43) 3371 45 29;

Fax: +55 (43) 3371 42 67;

Rodovia Celso Garcia Cid, PR445, km 380 Campus Universitário, Londrina, CEP 86051-990, Brazil

Abstract

Nitric oxide (NO) levels increase considerably after 24 h of exposure of skin to ultraviolet B (UVB) radiation, which leads to nitrosative skin injury. In addition, increased NO levels after exposure to UVB

radiation are associated with inhibition of cell proliferation. The search for preventive and therapeutic agents against UV radiation-induced skin lesions has become an important goal in dermatological research. However, the choice of antioxidants in current research often lacks a sufficient rationale because the photoprotective mechanisms of many antioxidants are not well understood and nitrosative-induced skin injury is often not considered. In this study, we determined the possible anti-nitrosative effects of genistein in the prevention of skin injury, and its effect on cell proliferation in a model of UVB-irradiated mouse skin. Genistein prevented skin injury and promoted cell proliferation via inhibition of protein nitration and lipid peroxidation even under conditions of high NO levels. These results reveal a novel photoprotective mechanism for genistein and indicate that anti-nitrosative effects should be taken into consideration in future studies on other photoprotective agents.

Introduction

Ultraviolet B (UVB) light stimulates the production of reactive oxygen species (Hakozaki *et al.*, 2008), which are the main cause of oxidative skin injury (Bickers and Athar, 2006). The free radical species generated by UVB exposure include the hydroxyl radical ($^{\bullet}OH$) (Kruszewski, 2003; Terra *et al.*, 2012 A), singlet oxygen ($^1O_2$) (Grossman and Schneid, 1998), superoxide radical ($O_2^{\bullet-}$) (Aitken *et al.*, 2007), and hydrogen peroxide (H_2O_2) (Masaki *et al.*, 1995; Wei *et al.*, 2002). Peroxynitrite ($ONOO^-$) and nitric oxide (NO) have been reported to be involved in oxidative skin injury induced by UVB radiation (Wu *et al.*, 2010; Wang *et al.*, 2010; Terra *et al.*, 2012 A, B). In a previous study, we showed that after 24 h of exposure to UVB radiation, development of skin lesions increased because of high levels of NO, which led to lipid peroxidation and nitrotyrosine formation, and cell proliferation decreased determined on the basis of the levels of markers of cell proliferation proliferating cell nuclear antigen (PCNA) and vascular endothelial growth factor (VEGF) (Terra *et al.*, 2012 A, B).

Development of preventive and therapeutic agents for skin lesions induced by UV radiation has become an important subject in dermatological research (Afaq *et al.*, 2006; Afaq e*t al.*, 2007). Among the compounds studied thus far, genistein (4',5,7-trihydroxyisoflavone), a soy isoflavone, has garnered significant attention from the scientific and medical communities because of its interesting biological effects, including chemoprevention against photocarcinogenesis (Wang *et al.*, 1998; Wei *et al.*, 1998; Moore *et al.*, 2006), prevention of photoaging (Kang *et al.*, 2003), and antiangiogenesis (Yu *et al.*, 2010). The exact

mechanism underlying genistein activity is still unknown, but its antioxidant properties have been proposed to mediate its protective effects (Kapiotis *et al.*, 1997; Wei *et al.*, 2002; Colado-Simão *et al.*, 2005; Zhan *et al.*, 2005; Izzo *et al.*, 2005; Holzbeierlein *et al.*, 2005).

Considering that the increase in NO levels associated with nitrosative damage is an important event in the formation of skin lesions 24 h after UVB irradiation (Terra *et al.*, 2012 A, B), we investigated the possible anti-nitrosative effect of genistein in the prevention of skin injury and in the modulation of cell proliferation.

Results

Oxidative stress and antioxidant parameters

Figure 1A and B shows that, compared to the control group (AUC, 4679 ± 155.3), the UV-control (6958 ± 527.1) and UV-GEN15 (6042 ± 267.1) groups showed a significant increase in lipid peroxide formation. Compared to the UV-control group, the UV-GEN10 group (AUC, 5712 ± 98.76) showed a decrease in the formation of lipid peroxides. No significant difference was observed in the TRAP between groups (Fig. 1C). The CAT activity significantly decreased in all UV-irradiated groups compared to that in the control group.

NO parameters

The NO levels were high in all UVB-irradiated groups (Fig. 2 A, B) (UV-GEN10, $34.6 \times 10^6 \pm 6.9 \times 10^6$; UV-GEN15, $46.5 \times 10^6 \pm 5.9 \times 10^6$; and UV-control $41.0 \times 10^6 \pm 9.52 \times 10^6$) compared to those in the control group; however, the NO levels in the UV-GEN10 group were similar to those in the control group. The percentage of iNOS-labeled area (Fig. 2C & D) was greater in the UV-Control (6.1% ± 0.4%), UV-GEN10 (4.9% ± 0.5%), and UV-GEN15 (4.7% ± 0.1%) groups than in the control (2.2% ± 0.5%). The UV-control (16.4% ± 1.3%) and UV-GEN15 (11.3% ± 1.7%) groups showed higher nitrotyrosine labeling than the control group (0.6% ± 0.14%, Fig. 2E). The nitrotyrosine labeling was not different in the UV-GEN10 (0.5% ± 0.12%) group compared to that in the control group, but it showed a significant reduction compared

to that in the UV-control (97%) group. The nitrotyrosine labeling was slightly reduced in the UV-GEN15 (31%) group compared to that in the UV-control.

Qualitative analyses of histological sections, p53, and apoptotic cells

Histopathological analysis of the tissues (Fig. 3A) showed that the epithelial surface was intact in control and UV-GEN10 groups, which showed appreciable tissue preservation. Nevertheless, a thin or absent epithelial layer was observed in UV-control and UV-GEN15 groups, which were characterized by the absence of clear limits between the stratum corneum and the stratum basale, with a slight flattening of the latter. Here, the disruption was deeper, with an increase in condensed nuclei, which indicated significant cell destruction.

The p53-positive cells were higher in the UV-control (93.92% ± 1.33%), UV-GEN10 (51.71% ± 4.91%), and UV-GEN15 (73.7% ± 5.7%) groups than in the control (13.2% ± 2.5%) group (Fig. 3B). Compared to the UV-control group, the UV-GEN15 group showed a slight reduction (21%), but the UV-GEN10 group showed the most significant reduction in p53-positive cells (55%). A representative image of p53 labeling is shown in Fig. 2C. The percentage of apoptotic cells (Fig. 3D) was higher in all UVB-irradiated groups, UV-Control (12.6% ± 0.93%), UV-GEN10 (3.6% ± 0.60%), and UV-GEN15 (7% ± 0.71%) than in the control (0.4% ± 0.3%). Compared to the UV-control group, the UV-GEN10 (71.4%) and UV-GEN15 (44.4%) groups showed a significant decrease in the percentage of apoptotic cells. A representative image of apoptotic cell labeling is shown in Fig. 3E.

Ki67, PCNA, and VEGF immunoreactivity

Ki67 immunolabeled cells (Fig. 4 A) were higher only in the UV-GEN10 (16.3% ± 2.1%) group than those in the control (12.9% ± 1.6%) group. A representative image of Ki67 labeling is shown in Fig. 4B. PCNA immunolabeling (Fig. 4 C) increased only in the UV-GEN10 (2.3% ± 0.5%) group compared to that in the control (0.2% ± 0.4%) group. Compared to the control (0.7% ± 0.3%) group, the UV-control (12.0% ± 1.00%) and UV-GEN10 (11.7% ± 2.6%) groups showed increased VEGF labeling (Fig. 4D). The percentage of VEGF-labeled area decreased (95%) in the UV-GEN15 group compared to that in the UV-control group.

Effect of genistein treatment on cell proliferation and cytotoxicity in HaCat cells

The results of the MTT assay (Fig. 5 A) showed that the cell viability in the UV-GEN3 (81.7% ± 1.2%) and UV-GEN10 (73.0% ± 1.6%) treatment groups was lower than that in the control (94.7% ± 1.5%) group. The cell viability was lower in the UV-GEN10 (15. 4% ± 0.5%) group than that in the UV-control (30.5% ± 1.2%). The neutral red assay (Fig. 5 B) showed that the cell viability was reduced only in the GEN10 (82.2% ± 2.0) group compared to Control (94.3% ± 2.6). In irradiated plates, the UV-GEN10 (40.40%± 2.3) group showed a decrease in cell viability when compared to UV-Control (75.3% ± 1.5).

Discussion

UVB light stimulates the production of various free radicals species that are responsible for oxidation of lipids, protein, and DNA, which result in skin lesions, accelerated aging, and development of malignant skin diseases (Armstrong and Kricker, 2001; Birch-Machin and Swalwell, 2005; Yaar and Gilchrest, 2007; Peres *et al.*, 2011). Antioxidants are used to prevent UV radiation-induced oxidative damage (Cao *et al.*, 1997; Afaq 2006; Huang *et al.*, 2008). However, antioxidants have been randomly selected in previous studies because the photoprotective mechanisms of many antioxidants are not well understood, and the nitrosative events have not been considered.

It is well known that after UVB irradiation, H_2O_2 accumulates in the skin via: (i) reduction in CAT activity (Kang *et al.*, 2003; Muramatsu *et al.*, 2005; Chiu *et al.*, 2009; Terra *et al.*, 2012 A, B) or (ii) rapid release of O^{2-} (Deliconstantinos *et al.*, 2006; Aitken *et al.*, 2007; Wu *et al.*, 2010), which is dismutated to H_2O_2 under physiological conditions (Noronha-Dutra *et al.*, 1993). Currently, the antioxidant capacity of genistein and its ability to inhibit H_2O_2 generation in the skin are thought to be the main mechanisms underlying prevention of UVB radiation-induced lesions. Wei *et al.*, (2002) showed that pretreatment of hairless mice with genistein significantly inhibited UVB radiation-induced H_2O_2 formation in the epidermis as well as in internal organs. In addition, Huang *et al.*, (2008) showed that genistein reduced H_2O_2 production in UVB radiation-exposed keratinocytes.

Previously, we showed that NO is important in the formation of skin lesions 24 h after exposure to nitrosative damage-inducing UVB irradiation (Terra *et al.*, 2012 A, B). Other studies have shown that NO reacts with H_2O_2 to form $ONOO^-$ (Radi *et al.*, 1991A; Noronha-Dutra *et al.*, 1993; Kikuchi K *et al.*, 1993 A; Kikuchi K *et al.*, 1993 B; Mowbray *et al.*, 2009;), which is considered a strong reactive species that can produce nitrotyrosine accumulation and lipid peroxidation in the skin (Radi, 2004; Terra *et al.*, 2012 A, B).

In the present study, hairless mice were treated with genistein (10 mg\kg or 15mg/Kg, i.p.) prior to UVB-irradiation, in order to investigate the anti-nitrosative effect of genistein. Compared to the UV-control group, the UV-GEN10 group showed tissue preservation, decreased lipid peroxide and nitrotyrosine formation, and low CAT activity. Furthermore, low-molecular-weight antioxidant defenses (shown by the TRAP test) were not mobilized, and NO levels and iNOS labeling remained high. The TRAP test results indicated that genistein in the UV-GEN10 group did not mobilize low-molecular-weight antioxidant defenses or reverse the reduction in CAT activity, but it prevented lipid peroxidation and nitrotyrosine formation, which indicated the antioxidant capacity of genistein. This finding indicates that genistein does not interfere with iNOS expression or act as an NO scavenger, but its H_2O_2 scavenging properties (Wei *et al.*, 2002; Huang *et al.*, 2008) prevent $ONOO^-$ formation, which reduce nitrosative skin injury. Thus, the probable mechanism of genistein photoprotection is the hindering of H_2O_2 accumulation and subsequent formation of $ONOO^-$.

In the UV-GEN10 treatment group, the reduction in lipid peroxides and nitrotyrosine was accompanied by upregulation of both PCNA and Ki67, which indicated that prevention of nitrosative skin injury promoted cell proliferation and DNA repair. Ki67 is a nuclear protein marker of cell proliferation (Urruticoechea *et al.*, 2005), and changes in its expression are related to PCNA levels in mouse skin after UV irradiation, and both are associated with elevated cell proliferation in the epidermis (El-Abaseri *et al.*, 2006). Moore *et al.*, (2006) also observed a decrease in PCNA inhibition with genistein, as well as decreased UVB-induced pyrimidine dimer formation in human reconstituted skin. The protective effect of genistein enabled monitoring of cell proliferation, which was confirmed by the reduction of p53 and apoptotic cell labeling in the UV-GEN10 group compared to that in irradiated mice. Ouhtit *et al.* (2000) showed that p53 labeling is upregulated in response to DNA damage in mouse skin 24 h after UV irradiation. When cell damage is mild,

p53 leads to cell cycle arrest through transcriptional activation of p21/Cip1 allowing DNA repair, and when the damage is severe, p53 induces apoptotic proteins (such as Fas/Apo-1, Bax, and DR5), and downregulate antiapoptotic proteins (such as cellular inhibitor of apoptosis protein 2 and bcl-2) (Ouhtit *et al.*, 2000; Mass *et al.*, 2003). Previously, we showed prevention of nitrosative events and modulation of cell proliferation by reducing NO levels with iNOS inhibitors (aminoguanidine and L-Name) in UVB-irradiated mouse skin (Terra *et al.*, 2012 A, B). In the present study, genistein also prevented nitrosative events, inhibited $ONOO^-$ formation, which leads to tissue protection and cell proliferation. This modulation is related to the maintenance of high NO levels, which indicates that $ONOO^-$ can interfere in these mechanisms.

Surprisingly, UV-GEN15 did not result in a greater protective effect compared to that with UV-GEN10. In the UV-GEN15 group, histological examination of the epidermis showed morphological alterations without efficient protection against lipid peroxide formation, as well as inhibition of PCNA, Ki67, and VEGF labeling, which suggested inhibition of cell proliferation. Labeling of p53 and apoptotic cells was lower in the UV-GEN10 group than in the UV-control group. Although, nitrotyrosine formation in the UV-GEN15 group was lower than that in the UV-Control, that in the UV-GEN10 was similar to that in the control group. These results suggest no additional protection by the higher concentration of genistein (15 mg/kg).

In vitro assays showed a pro-oxidant activity of genistein at the highest concentration. When HaCaT cells were pre-treated with genistein (3 μg/mL or 10 μg/mL) and submitted to UVB irradiation, only GEN10 diminished cellular viability in both tests (MTT and neutral red assays). Similar results were described by Chiu *et al.*, (2009). Despite the fact that genistein is normally considered an ROS-scavenging agent (Barnes, 1995; Wei *et al.*, 1996), other studies have shown that this isoflavone can induce ROS generation under a variety of conditions (Salvi *et al.*, 2002; Hwang *et al.*, 2005; Yeh *et al.*, 2007; Sánchez *et al.*, 2008).

In this study, we showed that genistein has an anti-nitrosative effect, which prevents UVB radiation-induced cell injury. To our knowledge, this is the first study, which shows that genistein can prevent nitrosative event and inhibit $ONOO^-$ formation, which leads to tissue protection and cell proliferation. These results help to elucidate the mechanisms underlying the photoprotective effect of genistein and reveal the importance of UVB radiation-induced nitrosative damage.

Materials and methods

Reagents

All chemicals used in this study were obtained from either Merck (Germany) or Sigma–Aldrich (USA).

Animals, UVB irradiation, and genistein treatment and tissue preparation

Hairless HRS/J mice weighing 20–25 g were obtained from the University of São Paulo (USP) and were given access to water and food *ad libitum*. The mice were treated in accordance with the National Institutional of Health guidelines for the welfare of experimental animals and with the approval of the Research Ethics Committee of the Londrina State University. The conditions of acute irradiation were previously described (Terra *et al.*, 2012 B).

Genistein was dissolved in dimethyl sulfoxide (DMSO) and intraperitoneally injected 30 min before UVB irradiation (Liang *et al.*, 2008). Treatment groups included a control (no UVB exposure), UV-control (irradiated, but not genistein-treated), UV-GEN10 (irradiated mice treated with genistein at 10 mg/kg), and UV-GEN15 (irradiated mice treated with genistein at 15 mg/kg). A 1-cm^2 patch of dorsal skin was removed from each mouse in the UVB irradiation treatment groups and was processed for subsequent analysis. Each group had 5–10 mice, and all parameters were measured in triplicate. Dorsal skin samples were removed after 24 h of irradiation and stored at -76°C until use. Homogenates from the dorsal skin of mice were prepared as described by Peres *et al.* (2011) and Terra *et al.* (2012 A, B).

Oxidative stress measurement

The *tert*-butyl hydroperoxide-initiated chemiluminescence (CL) reaction was performed using a GLOMAX TD/20 20 luminometer (Turner Designs, USA), with a response range of 300 to 650 nm, according to the method described by Gonzalez-Flecha *et al.* (1991), and according to a previously described

method for skin samples by Peres *et al.*, (2011) and Terra *et al.* (2012 A, B). The entire luminescence curve was used to determine the concentration of lipid peroxides present in the sample. Origin v. 7.5 data analysis software was used to determine the area under the curve (AUC). The results are expressed as relative light units/g tissue (RLU/g tissue).

Measurement of NO levels

NO levels were measured as described by Kikuchi *et al.* (1993 A, B), modified according to that by Terra *et al.* (2012 A, B), as previously described. The CL spectrum was recorded for 5 min using a GLOMAX TD/20 20 luminometer (Turner Designs, USA). Origin v. 7.5 data analysis software was used to determine the AUC. The results are expressed as NO RLU/g tissue.

Measurement of the total antioxidant capacity of skin

The total radical-trapping antioxidant parameter (TRAP) of the skin homogenate supernatant was measured using CL, according to the method by Repetto *et al.* (1996) and that previously described for skin samples by Peres *et al.* (2011) and Terra *et al.* (2012 A, B). The results are expressed in µM trolox.

Catalase activity

Catalase (CAT) activity was determined according to the method of Cohen, Dembiec, & Marcus (1970), modified according to Aebi (1984), and that previously described for skin samples by Peres *et al.* (2011) and Terra *et al.* (2012 A, B). The results are expressed as absorbance (ABS)/mg protein/min.

Protein concentration

Protein concentration was determined using the method of Lowry *et al.* (1951) modified according to Miller (1959). Both methods used bovine serum albumin (BSA) as a standard.

Histological assessment (PCNA, VEGF, and nitrotyrosine labeling)

The skin sample preparations and immunohistochemical analysis were performed as previously described by Terra *et al.* (2012 B). For nitrotyrosine and VEGF antibody labeling, positively-stained areas were quantified using a morphometric analysis system: 10 images were obtained using a light microscope at a magnification of 40×. Images were imported with image analysis software (Image J) and automatically merged. The total positive area was calculated as the sum of the area of all positive pixels. The immunolabeling percentage was evaluated by a ratio of unequivocal labeling located at nuclei (PCNA) for each of 100 counted epithelial cells.

Histological assessment (Ki67, p53, and iNOS labeling)

Endogenous peroxidase in 3-µm-thick formalin-fixed paraffin-embedded tissue sections was blocked using methanol and H_2O_2 solution (1:1). After antigen retrieval in a pressure cooker (0.1 M citrate buffer, pH 6.0, for 20 min), nonspecific protein binding was blocked by treatment for 30 min with 1% BSA (Sigma Chemical Company, St. Louis, MO, USA). Then, the sections were incubated overnight with primary antibodies against Ki-67, p53, and iNOS (Santa Cruz Biotechnology, Santa Cruz, CA, USA; dilution 1:200) at 4°C in a humidified chamber. After washing with 0.1 M PBS, the sections were incubated with reagent 1 and 2 of the Novo Link Polymer Detection System (Novocastra Laboratories, Newcastle Upon Tyne, UK) for 30 min each. Next, the sections were incubated with 3,3′-diaminobenzidine tetrahydrochloride (DAB; Sigma Chemical Company). The slides were counterstained using Harris hematoxylin, dehydrated, and mounted with Entellan (Merck KGaA, Darmstadt, Germany). The negative control specimens received the same treatment as that described above except incubation with primary antibody. Each marker was evaluated using 10 representative images of randomly selected high-power fields (400× magnification) and was calculated as the number of Ki67-positive epithelial cells with labeling of nuclei. The immunolabeling percentage was evaluated by a ratio of unequivocal labeling located at nucleus (p53) from each of 100 counted epithelial cells. ImageJ software was used to determine the percent area of iNOS immunolabeling.

Tunel assay

Paraffin-embedded skin sections were deparaffinized and incubated with 20 µg/mL proteinase K (Promega Corporation, Madison, USA). A DeadEnd peroxidase *in situ* apoptosis detection kit (DeadEnd TUNEL; Promega Corporation) was used for terminal deoxynucleotidyl transferase (TdT)-mediated dUTP-biotin nick-end labeling (TUNEL) staining. Briefly, the samples were treated with 3% H_2O_2 to quench endogenous peroxidase activity. After adding the equilibration buffer, the sections were treated with TdT-transferase and digoxigenin-dNTPs for 60 min at 37°C. Then, the specimens were treated with anti-digoxigenin-peroxidase for 30 min at 37°C, colorized with DAB, and counterstained with Mayer's hematoxylin. Finally, slides were rinsed, dehydrated, and mounted. A negative control was prepared by omitting the TdT-transferase enzyme to control for nonspecific incorporation of nucleotides or binding of enzyme-conjugate. TUNEL labeling was considered to be positive when distinct nuclear brown staining was homogenously present. The percentage of TUNEL-positive cells was obtained blindly, for each case, at a representative higher-power field (40×).

Cell culture assays

Human immortalized keratinocytes (HaCat cells) were seeded at a density of 1×10^5 cells/mL. The cells were cultivated in Dulbecco's modified Eagle's medium supplemented with 10% fetal bovine serum, and 1% penicillin/streptomycin mixture. Cultures were maintained in a humidified atmosphere with 5% CO_2 at 37°C (Sanyo CO_2 Incubator, Sanyo, Japan).

Cells were allowed to grow for 24 h in culture medium for cellular stabilization. For each experimental replicate, 2 plates were prepared: control (without UVB exposure) and UV exposure plates. Genistein was freshly dissolved in DMSO (maximum final concentration, 1%) and culture medium to obtain final concentrations of 3 µg/mL (UV-GEN3) and 10 µg/mL (UV-GEN3) (Chiu *et al.*, 2009). In addition, DMSO was added to control treatments at the same final concentration. For UVB exposure plates, cells were treated with genistein for 24 h before UVB exposure of 0.5 J/cm^2 (Chiu *et al.*, 2009) and incubated for another 24 h after exposure. For each plate, a control group without genistein treatment (DMSO alone) was also included (data not shown). Measurement of cell proliferation and cytotoxicity was determined using the MTT assay as previously described by Mosmann (1983). This assay is based on the conversion of

mitochondrial dehydrogenase by MTT into a purple formazan dye. Cells were incubated with MTT (0.3 mg/mL) for 4 h. The plates were read using a microplate spectrophotometer (Multiscan Go, Thermo Scientific, USA) at 550 nm. Absorbance values were converted to cell viability (% of control without UV exposure).Cellular toxicity was also evaluated using a neutral red retention test. In this test, viable cells take up the vital dye neutral red by active transport and incorporate the dye into lysosomes. After dye incorporation the cells are briefly washed, and the incorporated dye is released from the cells in an acidified ethanol solution according to the protocol provided by the Neutral Red-based In Vitro Toxicology Assay Kit (Sigma). For our experiments, the cells were allowed to incorporate the dye for 3 h, and the absorbance was measured at 540 nm. In addition, absorbance values were converted to cell viability (% of control without UV exposure).

Statistical analysis

The values obtained are presented as means ± standard error of mean (SEM). Histological assessments are reported as mean ± standard deviation (SD). One-way analysis of variance (ANOVA) and Bonferroni post hoc tests were used for statistical comparisons. Statistical analysis was performed using GraphPad Prism 4.0 and 5.0 (GraphPad, San Diego, CA). Probability values less than 0.05 were considered statistically significant.

DECLARATION OF INTEREST:

The authors state no conflict of interest. The authors alone are responsible for the content and writing of the paper.

ACKNOWLEDGMENTS: We thank Coordenação de Aperfeiçoamento de Pessoal de Nível Superior (CAPES) for financial support. The authors are grateful to J.A. Vargas and P.S.R.D. Filho for excellent technical assistance.

References

Aebi H. Catalase in vitro (1984). ***Methods in Enzymol*** 105 : 121-26.

Afaq, F, Mukhtar, H, (2006). Botanical antioxidants in the prevention of photocarcinogenesis and photoaging. ***Expl Dermatol*** 15, 678–84.

Afaq F, Syed DN, Malik A *et al* (2007). Delphinidin, an anthocyanidin in pigmented fruits and vegetables, protects human HaCaT keratinocytes and mouse skin against UVB-mediated oxidative stress and apoptosis. ***J Invest Dermatol*** 127: 222-32.

Aitken GR, Henderson JR, Chang SC, *et al* (2007). Direct monitoring of UV-induced free radical generation in HaCaT keratinocytes. ***Clin Exp Dermatol*** 32:722 – 27.

Armstrong BK, Kricker A, (2001).The epidemiology of UV induced skin cancer. ***J. Photochem Photobiol B*** 63:8–18.

Barnes S, (1995).Effect of genistein on in vitro and in vivo models of cancer. ***J Nutr*** 125:777S–83S.

Bickers DR, Athar M (2006). Oxidative Stress in the Pathogenesis of Skin Disease, ***J Invest Dermatol*** 126: 2565-75.

Birch-Machin MA, Swalwell H (2005). How mitochondria record the effects of UV exposure and oxidative stress using human skin as a model tissue, ***Mutagenesis*** 25:101–07.

Cao G, So"c E, Prior RL (1997). Antioxidant and prooxidant behavior of flavonoids: structure-activity relationships. ***Free Ral Biol Med*** 22:749–76.

Chiu T, Huang C-C, T-J, Fang J-Y, *et al* (2009). In vitro and in vivo anti-photoaging effects of an isoflavone extract from soybean cake. ***J Ethnopharmacol*** 126: 108–13.

Cohen G, Dembiec D, Marcus J (1970). Measurement of catalase activity in tissue extracts. ***Anal Biochem*** 34: 30-38.

Colado Simão AN, Suzukawa AA, Casado MF, *et al* (2005). Genistein abrogates pre-hemolytic and oxidative stress damage induced by 2,2'-Azobis (Amidinopropane). ***Life Sci*** 78:1202-10.

Deliconstantinos G, Villiotou V, Stavrides CJ, *et al* (1996). Increase of particular nitric oxide synthase activity and peroxynitrite synthesis in UVB-irradiated keratinocyte membranes, ***Bioche J*** 320: 997-1003.

El-Abaseri TB, Putta S,Hansen LA (2006). Ultraviolet irradiation induces keratinocyte proliferation and epidermal hyperplasia through the activation of the epidermal growth factor receptor. ***Carcinogenesis*** 27: 225-31

Gonzalez-Flecha B, Llesuy S, Boveris A, (1991). Hydroperoxide-initiated chemiluminescence: an assay for oxidative stress in biopsies of heart, liver, and muscle. ***Free Rad Biol Med*** 10: 93-100.

Grossman N, Schneid N, (1998). 780 nm low power diode laser irradiation stimulates proliferation of keratinocyte cultures: involvement of reactive oxygen species, ***Lasers Surg Medic*** 22:212-18.

Hakozaki T, Akira D, Yoshii T, *et al* (2008). Visualization and characterization of UVB-induced reactive oxygen species in a human skin equivalent model. ***Arch Dermatol Res*** 300: 1-56.

Holzbeierlein JM, McIntosh J, Thrasher J.B, (2005).The role of soy phytoestrogens in prostate cancer. ***Curr Opin Urol*** 15: 17-22.

Huang ZR, Hung CF, Lin YK, *et al*. (2008). In vitro and in vivo evalution of topical delivery and potential demal use of soy isoflavones genistein and daidzein. ***Int J Pharm***. 364:36-44.

Hwang JT, Park IJ, Shin JI, et al (2005). Genistein, EGCG, and capsaicin inhibit adipocyte differentiation process via activating. AMP-activated protein kinase. ***Biochem Biophys Res Commun*** 338:694–99.

Izzo AA, DiCarlo G, Borrelli F, *et al* (2005) Cardiovascular pharmacotherapy and herbal medicines: the risk of drug interaction. ***E Int J Cardiol*** 98: 1-14.

Kang S, Chung JH, Lee JH, *et al* (2003). Topical N-Acetyl Cysteine and Genistein Prevent Ultraviolet-Light-Induced Signaling That Leads to Photoaging in Human Skin in -vivo. ***J Invest Dermatol*** 120:835-41.

Kapiotis S, Herman M, Held I, *et al* (1997). Genistein, the dietary-derived angiogenesis inhibitor, prevents LDL oxidation and protects endothelial cells from damage by atherogenic LDL. ***Arteriosclerosis, Thrombosis and Vascular Biology*** 17:2868– 74.

Kikuchi K, Nagano T, Hayakawa H, *et al* (1993A). Detection of nitric oxide production from a perfused organ by a luminol-H_2O_2 system. ***Anal Chem*** 65: 1794-79

Kikuchi K, Nagano T, Hayakawa H, *et al* (1993B). Real time measurement of nitric oxide produced ex vivo by luminol-H_2O_2 chemiluminescence method. ***J Biol Chem*** **268**: 23106-110.

Kruszewski M, (2003). Labile iron pool: the main determinant of cellular response to oxidative stress, ***Mutat Res*** 531: 81-92.

Liang HW, Qiu SF, Shen J *et al* (2008). Genistein attenuates oxidative stress and neuronal damage following transient global cerebral ischemia in rat hippocampus. ***Neurosci Lett*** 438:116-20

Lowry OH, Rosenbrough NJ, Farr AL *et al* (1951). Protein measurement with the folin phenol reagent. ***J Biol Chem*** 193: 265-75.

Masaki H, Atsumi T, Sakurai H (1995). Detection of hydrogen peroxide and hydroxyl radicals in murine skin fibroblasts under UVB irradiation. ***Biochem Biophys Res Commun*** 206: 474-79.

Mass P, Hoffmann K, Gambichler T, *et al* (2003). Premature keratinocyte death and expression of marker proteins of apoptosis in human skin after UVB exposure. ***Arch Dermatoll Res*** 295:71–79.

Miller GL (1959). Protein determination for large number of samples. ***Anal Chem*** 31: 964.

Moore JO, Wang Y, Stebbins WG, *et al* (2006). Photoprotective effect of isoflavone genistein on ultraviolet B-induced pyrimidine dimer formation and PCNA expression in human reconstituted skin and its implications in dermatology and prevention of cutaneous carcinogenesis. ***Carcinogenesis*** 27:1627–35.

Mossmann T (1983). Rapid colorimetric assay for cellular growth an survival: application to proliferation and cytotoxicity assays. ***J Immunol Meth*** 65 : 55-63.

Mowbray M, McLintock S, Weerakoon R *et al* (2009). Enzyme-independent NO stores in human skin: quantificationand influence of UV radiation. ***J Invest Dermatol*** 129: 834-42.

Muramatsu S, Suga Y, Mizuno Y, *et al* (2005) Differentiation-specific localization of catalase and hydrogen peroxide, and their alterations in rat skin exposed to ultraviolet B rays. *J Dermat Sci* 37:151-58.

Noronha-Dutra AA, Epperlein MM, Woolf N (1993). Reaction of nitric oxide with hydrogen peroxide to produce potentially cytotoxic singlet oxygen as a model for nitric oxide-mediated killing. *FEBS Lett* 1:59-62.

Ouhtit A, Muller HK, Davis DW, *et al* (2000). Temporal events in skin injury and the early adaptive responses in ultraviolet-irradiated mouse skin. *Am J Pathol* 156:201–07.

Peres PS, Terra V.A, Guarnier FA, *et al* (2011). Photoaging and chronological aging profile: understanding oxidation of the skin, *J Photochem Photobiol B* 103: 93–97.

Radi R, Beckman JS, Bush KM, *et al* (1991). Peroxynitrite-induced membrane lipid peroxidation: the cytotoxic potential of superoxide and nitric oxide. *Arch Biochem Biophys* 288:481-87.

Radi R, (2004). Nitric oxide, oxidants, and protein tyrosine nitration. *Proc Natl Acad Sci* 101: 4003-08.

Repetto M, Reides C, Carretero MLG, *et al* (1996). Oxidative stress in blood of HIV infected patients. *Clin Chim Acta* 255: 107-17.

Salvi M, Brunati AM, Clari G, *et al* (2002). Interaction of genistein with the mitochondrial electron transport chain results in the opening of the membrane transition pore. *Biochim Biophys Acta* 1556:187–96.

Sanchez Y, Amran D, Fernandez C, (2008). Genistein selectively potentiates arsenic trioxide-induced apoptosis in human leukemia cells via reactive oxygen species generation and activation of reactive oxygen species-inducible protein kinases (p38-MAPK, AMPK). *Int J Cancer* 123: 1205–14.

Terra V.A, Souza-Neto FP, Pereira RC, *et al* (2012 A). Time-dependent reactive species formation and oxidative stress damage in the skin after UVB irradiation. *J Photochem Photobiol* B 109: 34–41.

Terra VA, Souza-Neto FP, Pereira RC, *et al* (2012 B). Nitric oxide is responsible for oxidative skin injury and modulation of cell proliferation after 24 hours of UVB exposures. *Free Radic Res* 46:872-82.

Urruticoechea A, Smith IE, Dowsett M (2005). Proliferation marker Ki-67 in early breast. Cancer J Clin Oncol. 23:7212-20.

Wang Y, Zhang X, Lebwohl M, *et al* (1998) Inhibition of ultraviolet B (UVB)-induced c-fos and c-jun expression in vivo by a tyrosine kinase inhibitor genistein. *Carcinogenesis* 19:649–54.

Wang L, Liu W, Parker SH, (2010). Nitric oxide synthase activation and oxidative stress, but not intracellular zinc dyshomeostasis, regulate ultraviolet B light-induced apoptosis. *Life Sci* **86**: 448–54.

Wei H, Cai Q, Rahn RO (1996). Inhibition of UV light- and Fenton reaction-induced oxidative DNA damage by the soybean isoflavone genistein. *Carcinogenesis*, 17, 73–7.

Wei H, Bowen R, Zhang X et al, (1998). Isoflavone genistein inhibits the initiation and promotion of two-stage skin carcinogenesis in mice. *Carcinogenesis*, 19, 1509–14.

Wei H, Zhang X, Wang Y, et al, (2002).Inhibition of ultraviolet light-induced oxidative events in the skin and internal organs of hairless mice by isoflavone genistein. *Cancer Letters* 185: 21-29.

Wu S, Wang L, Jacoby AM, *et al* (2010).Ultraviolet B light-induced nitric oxide/peroxynitrite imbalance in keratinocytes-implications for apoptosis and necrosis. *Photochem Photobiol* 86: 389– 96.

Yaar M, Gilchrest BA, (2007). Photoageing: mechanism, prevention and therapy. *Br J Dermatol* 157: 874–87

Yeh TC, Chiang PC, Li TK, *et al* (2007). Guh JH. Genistein induces apoptosis in human hepatocellular carcinomas via interaction of endoplasmic reticulum stress and mitochondrial insult. *Biochem Pharmacol* 73:782–92.

Yu X, Zhu J, Mi M, Wei Chen, (2010). Anti-angiogenic genistein inhibits VEGF-induced endothelial cell activation by decreasing PTK activity and MAPK activation. *Med Oncol* 29:349-57

Zhan S, Ho SC (2005). Meta-analysis of the effects of soy protein containing isoflavones on the lipid profile. *Am J Clin Nutr* 81: 397-408.

Fig. 1 Effect of genistein treatment (GEN, 10 mg/kg or 15 mg/kg) on oxidative stress in the skin of HRS/J hairless mice 24 h after ultraviolet B (UVB) irradiation. **(A)** Lipid peroxide formation was measured using *tert*-butyl hydroperoxide-induced chemiluminescence. Results are expressed as relative light units (RLU), and (B) the area under the curves were calculated for statistical analysis. **(C)** Antioxidant parameters were evaluated by total antioxidant capacity (TRAP μM trolox) and catalase activity (CAT ABS/mg protein) assays. Values are means ± standard error (SE). The superscript "a" and "b" letters represent statistical significance. ($p < 0.0001$).

Fig. 2 Effect of genistein treatment (GEN, 10 mg/kg or 15 mg/kg) on nitrosative stress in the skin of HRS/J hairless mice 24 h after ultraviolet B (UVB) irradiation. **(A)** Nitric oxide levels were quantified by luminol-H_2O_2-induced chemiluminescence and are expressed as relative light units (NO RLU). (B) The area under the curves were calculated for statistical analysis. Immunohistochemical analysis (percentage area positively immunolabeled) was used to evaluate inducible nitric oxide synthase (iNOS) expression **(C)** and nitrotyrosine formation **(E)** as illustrated in photomicrographs of skin sections labeled with iNOS (D) or

nitrotyrosine (F) antibody. Values are means ± standard error (SE). The superscript "a", "b," and "c" letters represent statistical significance. ($p < 0.0001$).

Fig. 3 Protective effect of genistein treatment (GEN, 10 mg/kg or 15 mg/kg) in the skin of HRS/J hairless mice 24 h after ultraviolet B (UVB) irradiation. **(A)** Histological sections of mouse skin (hematoxylin and eosin [H&E], 40×). Immunohistochemical analysis (percentage area positively immunolabeled) was used to evaluate p53 expression (B) and apoptotic cells (D), as illustrated in photomicrographs of skin sections labeled with p53 antibody (C) or TUNEL (E). Values are means ± standard error (SE). The superscript "a," "b," "c," and "d" letters represent statistical significance ($p < 0.0001$).

Fig. 4 Effect of genistein treatment (GEN, 10 mg/kg or 15 mg/kg) on cell proliferation in the skin of HRS/J hairless mice 24 h after ultraviolet B (UVB) irradiation. Immunohistochemical analysis was used to evaluate Ki67 expression (Ki67-positive epithelial cells/field) (A), PCNA-labeled cells (%) (C), and VEGF-labeled area (%) (D). (B) Photomicrographs of skin sections labeled with Ki67 antibody. Values are means ± standard error (SE). The superscript "a" and "b" letters represent statistical significance ($p < 0.0001$)

Fig. 5 Effect of genistein treatment (GEN, 3 µg/mL or 10 µg/mL) on viability in HaCat cells (density of 1×10^5 cells/mL) 24 h after either ultraviolet B (UVB) irradiation, or no irradiation (insert), evaluated by MTT assay (A) or neutral red retention test (B). Values are means ± standard error (SE). The superscript "a," "b," and "c" letters represent statistical significance. ($p < 0.0001$).

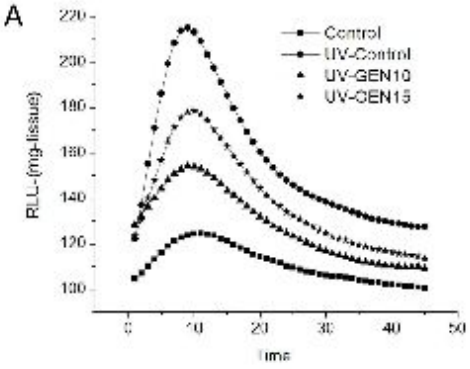

B

	Area under the curve ± SE (Number of animals)
Control	4679 ± 155.3 [a] (10)
UV-Control	6958 ± 527.7 [b] (8)
UV-GEN10	5712 ± 98.6 [a] (5)
UV-GEN15	6042 ± 257.1 [a] (5)

C

Group	TRAP (µM Trolox) (Number of animals)	CAT (ABS/mg protein) (Number of animals)
Control	1.988 ± 0.130 (5)	0.426 ± 0.048[a] (5)
UV Control	0.949 ± 0.071 (4)	0.291 ± 0.034[b] (4)
UV-GEN10	0.879 ± 0.053 (5)	0.325 ± 0.015[b] (5)
UV-GEN15	1.160 ± 0.190 (4)	0.370 ± 0.019[a] (4)

Fig. 1 Effect of genistein treatment (GEN, 10 mg/kg or 15 mg/kg) on oxidative stress in the skin of HRS/J hairless mice 24 h after ultraviolet B (UVB) irradiation. (A) Lipid peroxide formation was measured using tert-butyl hydroperoxide-induced chemiluminescence. Results are expressed as relative light units (RLU), and (B) the area under the curves were calculated for statistical analysis. (C) Antioxidant parameters were evaluated by total antioxidant capacity (TRAP µM trolox) and catalase activity (CAT ABS/mg protein) assays. Values are means ± standard error (SE). The superscript "a" and "b" letters represent statistical significance. ($p < 0.0001$).
86x152mm (300 x 300 DPI)

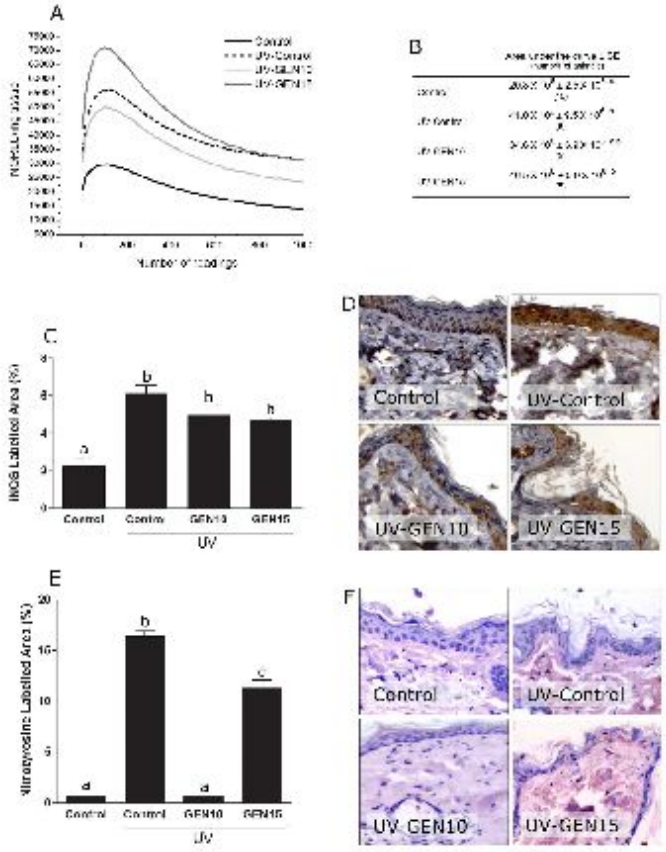

Fig. 2 Effect of genistein treatment (GEN, 10 mg/kg or 15 mg/kg) on nitrosative stress in the skin of HRS/J hairless mice 24 h after ultraviolet B (UVB) irradiation. (A) Nitric oxide levels were quantified by luminol-H2O2-induced chemiluminescence and are expressed as relative light units (NO RLU). (B) The area under the curves were calculated for statistical analysis. Immunohistochemical analysis (percentage area positively immunolabeled) was used to evaluate inducible nitric oxide synthase (iNOS) expression (C) and nitrotyrosine formation (E) as illustrated in photomicrographs of skin sections labeled with iNOS (D) or nitrotyrosine (F) antibody. Values are means ± standard error (SE). The superscript "a", "b," and "c" letters represent statistical significance. ($p < 0.0001$).
177x220mm (300 x 300 DPI)

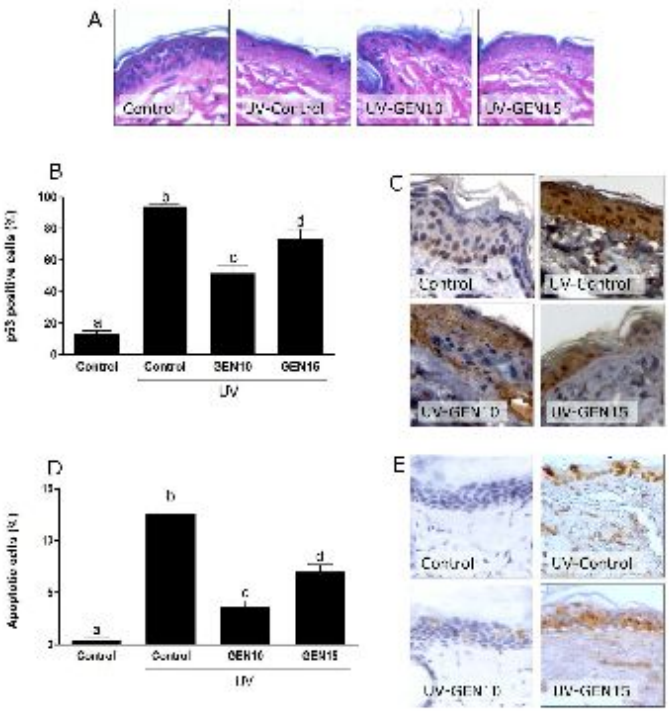

Fig. 3 Protective effect of genistein treatment (GEN, 10 mg/kg or 15 mg/kg) in the skin of HRS/J hairless mice 24 h after ultraviolet B (UVB) irradiation. (A) Histological sections of mouse skin (hematoxylin and eosin [H&E], 40I). Immunohistochemical analysis (percentage area positively immunolabeled) was used to evaluate p53 expression (B) and apoptotic cells (D), as illustrated in photomicrographs of skin sections labeled with p53 antibody (C) or TUNEL (E). Values are means ± standard error (SE). The superscript "a," "b," "c," and "d" letters represent statistical significance ($p < 0.0001$).
177x177mm (300 x 300 DPI)

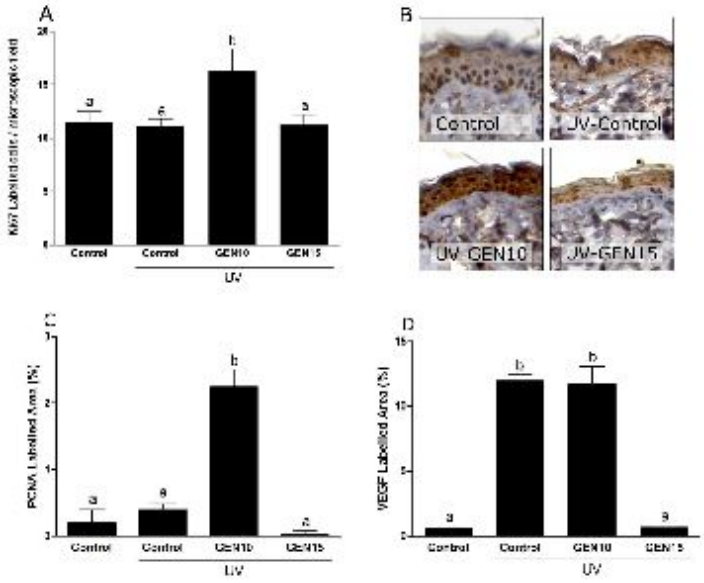

Fig. 4 Effect of genistein treatment (GEN, 10 mg/kg or 15 mg/kg) on cell proliferation in the skin of HRS/J hairless mice 24 h after ultraviolet B (UVB) irradiation. Immunohistochemical analysis was used to evaluate Ki67 expression (Ki67-positive epithelial cells/field) (A), PCNA-labeled cells (%) (C), and VEGF-labeled area (%) (D). (B) Photomicrographs of skin sections labeled with Ki67 antibody. Values are means ± standard error (SE). The superscript "a" and "b" letters represent statistical significance ($p < 0.0001$)
177x140mm (300 x 300 DPI)

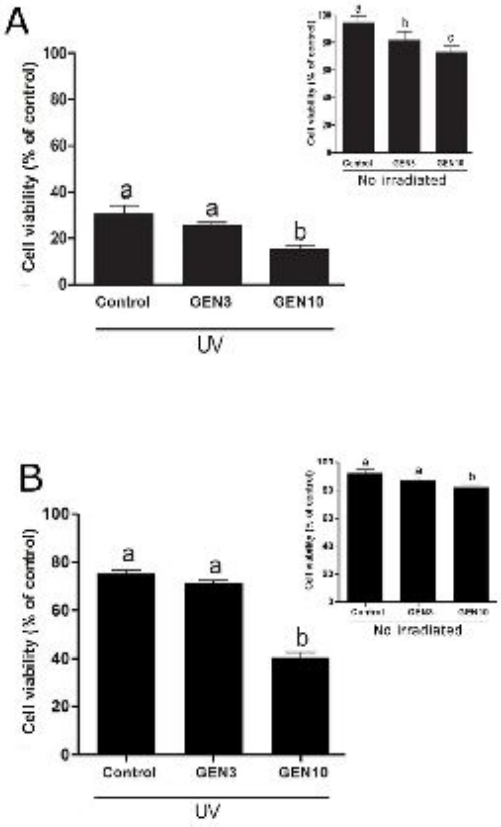

Fig. 5 Effect of genistein treatment (GEN, 3 µg/mL or 10µg/mL) on viability in HaCat cells (density of 1 × 105 cells/mL) 24 h after either ultraviolet B (UVB) irradiation, or no irradiation (insert), evaluated by MTT assay (A) or neutral red retention test (B). Values are means ± standard error (SE). The superscript "a," "b," and "c" letters represent statistical significance. ($p < 0.0001$).
86x114mm (300 x 300 DPI)

APÊNDICE 4 – Measurement of Nitric Oxide by a very sensitive luminol-H_2O_2 chemiluminescence technique in chemical systems and in fresh and frozen biological samples

Original article

Measurement of Nitric Oxide by a very sensitive luminol-H_2O_2 chemiluminescence technique in fresh and frozen biological samples.

Terra, VA[1]; Panis, C[2]; Saito, CAI[2]; Souza-Neto, FP[1], Luiz RC[1], Guarnier FA[2], Saito, AY[2]; Cecchini, R[2], Cecchni, AL[1]

[1] Laboratory of Molecular Pathology, State University of Londrina, Paraná State, Brazil.

[2] Laboratory of Patophysiology and Free Radicals, Department of General Pathology, State University of Londrina, Londrina, Paraná, Brazil.

***Corresponding author**

V. A. Terra

Department of General Pathology

[1]Laboratory of Molecular Pathology

Londrina State University, 86051-990 Londrina, Brazil

Phone (+55-43) 3371-4521

Fax (+55-43) 3371-4267

E-mail: vania.terra@uol.com.br

ABSTRACT

Luminol-H_2O_2 chemiluminescence (CL) has been used for real time Nitric oxide (NO) detection in physiopathological studies. The aim of this study was to apply this same CL method for NO detection in fresh or frozen biological samples. To validate NO detection we used well-established systems of NO donors (nitrite reduction at acid pH, KI-$NaNO_3$/H_2SO_4 or NPS systems), a specific NO scavenger (cPTIO), and free radical inhibitors (histidine, superoxide dismutase, mannitol). Our findings corroborated with the previous studies, reinforcing that NO is , in fact, the object of analysis in this study, and light-emitting species generated during the NO-luminol- H_2O_2 CL reaction are the same previously reported in literature. Once validated the CL reaction, we assessed NO levels in fresh and frozen biological samples (dorsal mice skin and gastrocnemius rat muscle). For biological samples, the addition of free radical inhibitors in the mixture reaction, promoted similar behavior on the CL curves compared to chemical systems. We conclude that this specific and sensitive method can be applied for the investigation of NO produced physiologically and pathologically, expanding the use of this method in fresh or frozen samples for different type of tissues and pathologies.

Keywords: nitric oxide, chemiluminescence, biological samples, chemical systems, skin, skeletal muscle, cachexia, ischemia-reperfusion.

INTRODUCTION

Nitric oxide (NO) is a ubiquitous gas with potent biological effects, hemostasis, including vasodilatation, neuronal signaling, and antimicrobial activity (Ignarro 1990; Stankevicius et al., 2003). NO and its metabolites, specially, peroxynitrite, have been implicated in several pathological conditions, including ischemia and muscle reperfusion injury (Khanna et al., 2005), cardiovascular diseases (Anaya-Prado et al., 2002), muscle wasting in cancer (Barreiro et al., 2005), and skin injury after UVB irradiation (Wang et al., 2010). In mammalian cells, NO is generated by the reaction of the NO synthases (NOS), with arginine as a substratum, presents three isoforms: two constitutive (cNOS and eNOS) and one inducible isoenzyme (iNOS). NO can also be generated by NOS-independent pathways at particular non-enzymatic conditions (Nagase et al., 1997, Mowbray et al., 2009).

NO instability under physiological tensions of oxygen and its high reactivity with biomolecules make its quantification a challenge, mainly in biological systems, (Archer et al., 1995). In biological tissues NO is easily oxidized to nitrite (Ignarro et al., 1993) and its half-life is very short (<6 seconds) (Kem et al., 1988), while in pure aqueous solution biologically active concentrations of NO (5 nM – 4 μM) has a half-time about 500 seconds (Laver, 2008).

Several direct and indirect methods are available to determine NO or its metabolites in a range of tissues and samples, including inhibitors of $^{\bullet}$NO synthesis (Knight et al., 1997; Zhang et al., 1997; Joneschild et al., 1999; Zimiani et al., 2005), $^{\bullet}$NO donors (Liu et al., 1998; Hallstrom et al.,2002), transgenic mice (Lefer et al., 1999; Barker et al., 2001; Ozaki et al., 2002), NO precursors (Cordeiro et al., 1998; Huk et al., 1998; Nanobashvili et al., 2004), detection of $^{\bullet}$NO oxidative degradation products

(Blebea et al. 1996; Nakamura et al., 2001), NOS mRNA (Messina et al., 2000), and nitrosyl-hemoglobin (Kozlov et al., 2001). However, all of these methods have shown limitations. The Griess assay, used for detection of nitrite and/or nitrate, both oxidation products of ˙NO, has shown low specificity because these substances are considered ubiquitous contaminants in water and common products of bacterial metabolism (Archer et al., 1995) and low sensibility (μM). Analogues of L-arginine containing nitro groups, such as some NOS inhibitors (LNAME, AG, and LNNA), have been suggested to interfere in Griess assay (Greenberg et al., 1961). Even the use of transgenic mice can produce controversial results due to compensatory mechanisms (Kanno et al., 2000).

Among them, chemiluminescence assay is considered a very useful method, due to its high sensitivity for detection of unstable radicals at low concentrations in physiological solutions, and allows attomolar/femtomolar-order detections (Tsukada et al., 2003; Laver et al., 2008). Kikuchi et al., (1993 A B) describes the specific reactivity of NO with luminol-H_2O_2 in chemiluminescence reaction, employing gaseous NO on solution as standard. NO is reported to react with H_2O_2 to form light-emitting species (Kikushi et al., 1993 A B; Radi et al., 1993, Noronha Dutra et al., 1993). Both, peroxynitrite ($ONOO^-$) (Kikuchi et al., 1993) and singlet oxygen ($^1O_2$) (Noronha-Dutra et al., 2003), were described as light-emitting species resulting from the reaction between NO and the luminol-H_2O_2 chemiluminescence system. Authors have employed NO chemical donors and specific inhibitors for reactive species, in order to determine the light-emitting specie formed by the reaction between the NO and luminol- H_2O_2 in chemiluminescence reaction. Kikuchi et al. (1993) demonstrated real time formation of $ONOO^-$ (in perfused kidney of rats) and also excluded the possibility of superoxide anion (O_2^-) as a precursor of $ONOO^-$, using manganese containing superoxide dismutase (Mn-SOD).

Noronha-Dutra et al. (2003) employed sodium nitroprusside (disodium nitroferricyanide) as a source of NO to demonstrate the reaction of NO with H_2O_2, giving rise to singlet oxygen ($^1O_2$), considered a strong reactive oxygen specie. In the same study, the authors used histidine ($^1O_2$ quencher) and mannitol (hydroxyl radical, $OH^{\bullet}$, quencher) to reveal $^1O_2$ formation and to exclude $OH^{\bullet}$ formation during the luminol- H_2O_2 chemiluminescence reaction.

NO-luminol- H_2O_2 CL is considered a very sensitive method to detect NO levels in biological, mainly used to real time evaluations. Using this method Tsukada et al. (2003) measured real time generation of NO in perfused rat heart, and calculated the NO concentrations (pmol/L) using a standard calibration curve constructed by NO formation by the reaction of nitrite reduction at acid pH (KI-NaNO3/H2SO4 system).

The aim of this study was to demonstrate the NO-luminol- H_2O_2 CL method as a fast, highly sensitive, specific and accurate technique to investigate the participation of NO in pathophysiological analyses in frozen and fresh biological samples. To validate the method, the results of biological analyses were compared with those obtained from well-established systems of NO donors, as well as those reported by other studies.

METHODS

1.0 Reagents - All the chemicals were obtained from Merck or Sigma laboratories.

2.0 INSTRUMENTATION: Analysis spectrophotometric were performed by Shimadzu detector. Two types of chemiluminescence detectors were used. Glomax™-20/20 Single tube luminometer (Promega, Madison, USA) was set to register 3000 numbers of readings (10 readings/second), during 5 minutes. For pathophysiological studies in muscle (Ischemia-reperfusion and cachexia protocols), TD 20/20 luminometer (Turner Designs, USA) with detection capacity of a wavelength range of 300-650 nm and 68.5% of sensibility with capacity of 1500 numbers of readings.

3.0 Chemical NO donnors

To validate the NO-luminol-H_2O_2 CL method we used two chemical NO donnors systems, as described above.

3.1 Nitrite reduction at acid pH – KI-$NaNO_3$/H_2SO_4 system

NO generates by nitrite (NO_2^-) reduction at acid pH, was described by Schmidt and Mayer (1997) and reproduced by Tsukada et al. (2003). In this reaction, were used 1.8mL of 0.1 M H_2SO_4 / 0.1 M KI and 7.2mL of 0.1 mM $NaNO_2$. The reaction immediately generates a solution of 400 pM NO at room temperature (Tsukada et al. 2003), on the following reaction of nitrite with iodide in sulfuric acid:

$$2KNO_2 + 2KI + 2H_2SO_4 = 2NO + I_2 + 2H_2O + 2K_2SO_4$$

This solution was diluted to final concentrations of 100 fM, 200 fM, 300 fM, 400 fM NO in 2 mM Na_2CO_3 buffer, pH 8.5, previously degassed by N_2. Chemiluminescence detection was performed as follow described.

3.2 Irradiation of NPS solution

Based on the sodium nitroprusside (NPS) photodegradation resulting in NO formation (Frank 1976; Arnold et al., 1984; Ederli 2009), aliquots of NPS 200µM diluted in Na_2CO_3 buffer (2 mM pH 8.5) were added to 1 mL microtubes and irradiated in a light-containing chamber at 30 cm of distance from the light source (commercial fluorescent lamp, Phillips). The aliquots of 30 min reaction were collected and immediately analyzed to determine NO levels (0 to 240 min) by photon emission as follow described (Relative Light Unities, RLU). The reactions with reactive species inhibitors were performed with 1 µM NPS solution.

4.0 Nitric Oxide quantification through Luminol-H_2O_2-induced chemiluminescence assay

NO detection was estimated employing chemiluminescence reaction as described by Kikuchi and collaborators (1993) with some modifications. Dissolved oxygen present in buffers, chemical and biological samples was removed by 20 min N_2 bubbling to avoid oxidative degradation of NO.

Equal volumes of 360 µM luminol/ 3 mM desferrioxamine (DFO) and 200mM H_2O_2 were mixed and incubated at room temperature under moderate agitation for 5min (reaction mixture). Desferrioxamine was added to remove interference of hemoglobin in luminol-H_2O_2 chemiluminescence reaction.

To initiate the chemiluminescence reaction, 50 µL of the reaction mixture were added automatically in the luminometer (Glomax™-20/20) containing 800 µL of biological system (mouse dorsal skin and rat gastrocnemius muscle) or chemical solutions (nitrite reduction at acid pH - KI-NaNO3/H2SO4 and NPS systems (sodium nitroprusside) as NO donors. For pathophysiological studies, 800 µL of muscle

homogenates were placed in a TD 20/20 luminometer. After 1min 20 µL of the reaction mixture were added – using an accurate syringe (Hamilton, USA) - to initiate CL reaction.

Glomax™-20/20 Single tube luminometer (Promega, Madison, USA) was set to register 3000 numbers of readings (10 readings/second), during 5 minutes. TD 20/20 luminometer (Turner Designs, USA) with detection capacity of a wavelength range of 300-650 nm and 68.5% of sensibility with capacity of 1500 numbers of readings. Results were expressed in relative light units (NO RLU). The luminometers were connected to a microcomputer through Spreadsheet Interface v. 1.0 program to record chemiluminescence emission. The Origin v.8.0 software was used to plot chemiluminescence curves.

5.0 Free radicals inhibitors

In chemical and biological analyses, 2-(4-carboxyphenyl)-4,4,5,5-tetramethylimidazoline-1-oxyl-3-oxide (cPTIO) 10 to 200 µM was used as specific NO scavenger (Ederli et al. 2009). Superoxide dismutase (SOD) 1UI to 20UI (Kikuschi et al., 1993) was employed as superoxide scavenger. Mannitol, from 2 to 200 mM (Noronha-Dutra et al., 1993) as hydroxyl radical scavenger and histidine from 1 to 20 mM (Noronha-Dutra et al., 1993) as singlet oxygen scavenger. All chemicals were added immediately before quantification of light emission.

6.0 Biological samples

Hairless mice HRS/J, weighing 20-25g, were obtained from University of São Paulo (USP). Adult male Wistar rats, weighing 200-250g were obtained from the Animal House of Centro de Ciências Biológicas / Universidade Estadual de Londrina,

with access to water and food ad libitum. The animals were treated in accordance with the National Institutional of Health Guidelines for the welfare of experimental animals and with the approval of the Universidade Estadual de Londrina Animal Experimentation Ethics Committee. Biological samples (mouse dorsal skin and rat gastrocnemius muscle) were homogenized (5mg/ml) for 45s using an Ultraturrax homogenizer (Marconi, Brazil). This procedure was performed under N_2 bubbling to ensure O_2 free medium in 2 mM Na_2CO_3 buffer, at pH 8.5, previously degassed by N_2. The homogenates (5% w/v, 5mg of tissue/ml) were centrifuged (10500 x g, - 4ºC, 10 minutes). The supernatants were used on a 0.250% (w/v) concentration for all experiments. Biological samples were used in fresh (homogenized immediataly after the surgical procedure for removal of organs) and frozen (stored until three months at low temperatures (-80ºC).

7.0 Pathophysiological studies:

7.1 Ischemia-reperfusion protocol - Muscle injury was induced in rats using an ischemia-reperfusion protocol, as previously described (Concannon et al., 1992; Zamiani et al., 2005). Briefly, male Wistar rats were anesthetized by inhalation of ether ethilic and the left hindlimb was exsanguinated using a Penrose drain prior to apply a nylon tourniquet at the limb root for ischemia induction, After 4h ischemia, the tourniquet was removed and the limb was reperfused for 4h. Sham control animals were anesthetized without the ischemia induction and further handled in the same manner as the experimental ones. Gastrocnemius muscles were excised, homogenized at 0.05% (w/v) in 2mM Na_2CO_3 buffer, pH 8.5, previously degassed by N_2, through 45s period of homogenization using an Ultraturrax homogenizer (Marconi, Brazil) followed by muscle

homogenates 20 times dilution with the same buffer before the luminol-H_2O_2-induced chemiluminescence assay.

7.2 Cachexia protocols - Muscle injury was induced in rats using a protocol of Walker-256 tumor-induced cachexia, as previously described (Guarnier et al., 2010). Briefly, male Wistar rats were inoculated subcutaneously with 0.5 mL of PBS or $8x10^7$ tumor cells suspended in 0.5 mL of the same buffer, at the right flank. A sham group (Control) of animals inoculated with PBS and fed in a similar manner to experimental ones was also performed. Five days after PBS or tumor inoculation, left gastrocnemius muscles were excised and homogenized at 0.05% (w/v) in 2 mM Na_2CO_3 buffer, at pH 8.5, previously degassed by N_2, through 45s period of homogenization using an Ultraturrax homogenizer (Marconi, Brazil) followed by muscle homogenates 20 times dilution with the same buffer before the luminol-H_2O_2-induced chemiluminescence assay.

8.0 Quantification of nitrite levels by Griess reaction of NPS solutions.

NO levels released from NPS solution were also evaluated by Griess reaction, based on the measurement of nitrite levels (Griess, 1879). Equal volumes of NPS solution and Griess reagent (Reagent I: 50 mg of N-naphthylethylenediamine in 250 mL of distilled water; reagent II: 5 g of sulfanilic acid in 500 mL of 3 M HCl) were used for Griess reaction. To determine nitrite concentration, calibration curve was prepared by dilution of $NaNO_2$ (ranging from 250μM to 0). The absorbance was determinated at 550 nm in a microplate reader.

Statistical analysis

All experiments were made in triplicate with three repetitions. Figures represent reproducible data obtained from triplicates. Chemiluminescent curves were obtained

after data treatment in the software Origin Lab (version 8.0, USA). Analysis of regression was performed using Spearman´s test in GraphPad Prism Software (version 5.0, USA). Probability values less than 0.05 were considered statistically significant.

RESULTS

NO levels were measured by the CL curves generated by light emission (RLU). The CL curves were analyses by area under the curves (AUC). Figure 1 (A, B) NPS-derived NO was measured by CL and Griess reaction and the results showed a time-dependent linear increased of NO levels (AUC) and nitrite concentrations, respectively. The results showed a linear and significant correlation (r^2 0.7331 P=0.0133) between nitrite concentrations and NO levels (AUC) (1 C). NO levels obtained from KI-$NaNO_3/H_2SO_4$ system demonstrated a linear correlation between AUC of the CL curves and NO concentrations (100 fM to 400 fM) (r^2 = 0.9579 P= 0.0037) (1 D). Additionally, to verify the specificity of the CL reaction to NO-luminol- H_2O_2 system, cPTIO, a specific scavenger of NO was added in mixture reaction. The chemical systems showed a dose-dependent inhibition of emission pattern by cPTIO addition in CL mixture (Figures 2 A, B). Superoxide dismutase (SOD) was added in chemical systems in order to verify the implication of $O_2^{\cdot-}$, during NO chemiluminescence reaction. Both NPS and KI-$NaNO_3/H_2SO_4$ systems (Figure 2 C and D) presented an enhancement of light emission when treated with SOD at 1 UI/mL and 10 UI/mL.

When histidine ($^1O_2$ quencher) 10 mM was added to NPS solution and KI-$NaNO_3/H_2SO_4$ system we observed a complete inhibition of light emission (Figure 3A and B). The use of Mannitol 20mM, as hydroxyl scavenger, showed partial inhibition of

light emission generated by NO (NPS) donor (Figure 3A), while the KI-$NaNO_3$/H_2SO_4 system demonstrated a discrete reduction in CL curves (Figures 3B).

In biological analyses, skin and muscle (fresh or frozen – 0.25mg tissue/ml) in the NO luminol-H_2O_2 CL reaction, generates similar curves (Figure 4 A, B). Figure 4 C shows a linear increase of NO levels (RLU) with increasing concentrations of the skin homogenate (0.05 to 0.5mg tissue/ml). Concentrations higher than 1 mg of tissue/ml showed quencher property. The biological samples (0.25mg tissue/ml) showed a dose-dependent inhibition of light emission by cPTIO addition in CL reaction (Figures 5 A, B). SOD addition to the mixture reaction resulted in mild reduction of photon emission at the initial portion of the curve (Figures 5 C, D), however, during the course of the light emission we detected that SOD increased the photon emission (data not shown). Histidine promoted partial inhibition of light emission (Figures 6 A, B). Finally, mannitol demonstrated a discrete reduction of curve peaks (Figures 6 A, B).

Figure 7 A, B presents chemiluminescence curves of pathophysiological studies in ischemia-reperfusion protocol (fig. 7 A) and cachexia protocol (fig. 7B). Based on RLU, the NO levels were marked increased in IR4 and in tumor groups compared to respective control groups.

DISCUSSION

In this study we reproduced a CL method based on a specific reaction of NO with luminol-H_2O_2 that generates light emission species. The use of NO-luminol-H_2O_2 CL in chemical and biological systems *in real time*, was proposed by Kikuchi et al. (1993) to measure the continuous NO release from isolated perfused kidney and further reproduced by Tsukada et al. (1993), Kojima et al., (1997) and Yavuz et al. (2003). In comparison with these previous reports, in this study we validated the NO-luminol-H_2O_2 CL in aqueous chemical NO donor systems and applied this method for the first time to fresh and frozen biological samples.

NO is described as a very reactive and instable molecule in physiological conditions in the presence of oxygen (Ignarro 1990). In this condition, NO has a short half-life of 5 s or less (Archer 1993, Bates 1992, Nathan 1992), but Wink et al. (1993) reported a half-life of 500s for NO, in 0.01–1μM aqueous solutions. Hakim et al. (1996), demonstrated that the NO concentration fell slowly over 20 min with a half-life of 445 s, through monitoring biological concentrations of NO (< 1.5 μM) in aqueous solutions (prepared from authentic gas; PO_2 = 40 mmHg). An increase on NO stability was reported in absence of haemoglobin (Archer, 1993), and oxygen (Archer, 1993; Clancy et al., 1990).Therefore, the uses of chemical aqueous systems that ensure NO stability consist in a reliable strategy to measure NO by NO-luminol-H_2O_2 CL.

In this study the first used chemical NO donor was NPS aqueous system. All solutions of chemical NO donors were degasified by N_2 bubbling to eliminate the oxygen presence and avoid its reaction with NO. During our study we observed NO release when NPS aqueous solution was exposed to white fluorescent commercial light, resulting in enhanced chemiluminescence detected on a response range of 300-650 nm.

Arnold et al., (1984) showed that NPS photodegradation generates linear NO release, and also small quantities of aquapentacyanoferrated. Additionally, the authors demonstrated that 100% of NPS photodegradation resulted in 10% of NO release. Rauhala et al. (1998) showed the iron moiety of breakdown products of NPS, can also generate $OH^{\bullet}$ radicals, via the Fenton reaction. Other study discuss that NPS is a source of nitrosonium anion (NO^{+}), a nitrosating electrophilic specie (Al-Sa' Doni and Ferro, 2000).

NO present in NPS aqueous solution was also evaluated in this study by measuring nitrite levels in Griess reaction. The time-dependent linear increase of nitrite concentrations obtained from NPS system (measured by Griess reaction) was previous described by Arnold et al. (1984). This is the first time we describe a time-dependent linear increase of NO levels obtained from NPS system using Luminol-H_2O_2 CL reaction, and it is also the first study showing a linear correlation between nitrite levels (Griess method) and NO-based photon emission (NO-luminol-H_2O_2 by CL reaction).

The second used chemical NO donor was KI-$NaNO_3$/H_2SO_4 system. This pure chemical system was first described by Schmidt and Mayer (1997). Tsukada et al. (2003) reproduced this method and used this reaction to build a NO standard calibration curve between 1 and 400 pM. Using this same procedure, in this study we were able to detect fM levels of NO, revealing the sensibility and specificity of this CL reaction for NO detection. To ensure that the object of analysis was in fact NO and provide additional evidences of NO-luminol-H_2O_2 by CL reaction specificity, we used cPTIO, a specific NO scavenger (Ederli et al., 2009). The injection of cPTIO in the reaction mixture promoted a dose-dependent decrease on the light emission.

In fact, this reaction is NO dependent, but other reactive species can be involved in the photon emission. In this study, the use of free radicals scavengers in chemical NO

donors, was a strategy to ensure that our results were similar to previous reported and validated that this method based on the reaction NO-luminol-H_2O_2 was reproduced here.

To verify the generation of the light emission species resulting of the NO-luminol-H_2O_2 CL, the uses of free radicals inhibitors in the mixture reaction consist in a reliable strategy to ensure that our results were similar to previous reported by other authors (Noronha Dutra et al., 1993; Kikuchi et al., 1993 A B; Kikuchi et al., 1993; Tsukada et al. 1993). Kikushi et al. (1993), Radi et al. (1993) and validated that this method based on the reaction NO-luminol-H_2O_2 was reproduced here.

Noronha Dutra et al. (1993), Kikushi et al. (1993) and Mascio et al. (1994) described that other light-emitting species formed during the reaction of NO in luminol-H_2O_2 system - such as singlet oxygen ($^1O_2$) and peroxynitrite ($ONOO^-$) - are responsible for photon emission. Radi et al. (1993) showed that neither NO, nor O_2^- are capable of directly inducing significant luminol chemiluminescence.

In this study, further experiments using free radical inhibitors, were performed to reveal if CL curves generates by NO-luminol-H_2O_2 system presented similar behavior of light emission as previous described in literature. Our data showed that the injection of histidine in both chemical NO donors inhibited light emission, indicating that $^1O_2$ is a light emission specie which results from the reaction of NO-luminol-H_2O_2, as previous described by Noronha Dutra et al. (1993).

Kikuchi et al. (1993) report that the light emission specie resulted from NO-luminol-H_2O_2 system is peroxinitrite. To exclude the participation of O_2^- as a precursor of $ONOO^-$, the authors used manganese containing superoxide dismutase (Mn-SOD). Our results showed that SOD increased light emission observed in CL curves generates by NO-luminol-H_2O_2 system, as previous observed by Noronha-Dutra et al. (1993). This

behavior can be explained by a reversible conversion of nitroxyl anion (NO^-) to NO by superoxide dismutase (Murphy and Sies, 1991). These findings reinforce that the light emission of NO-luminol-H_2O_2 system is dependent on NO levels.

In addition, we examined the possibility of involvement of $OH^\bullet$ in this CL system by using its inhibitor (mannitol). For the NO donnor KI-$NaNO_3$/H_2SO_4 system, the injection of mannitol were not able to decrease photon emission, proving that $OH^\bullet$ is not generated in this case during NO-luminol-H_2O_2 by CL reaction, as discussed by other authors (Noronha-Dutra et al., 1993; Kikushi et al., 1993). On the other hand, we observed a significant inhibition of light emission using mannitol in NPS system. Probably part of the light emission of NPS is due the $OH^\bullet$ formation during the NPS photo-degradation (Rauhala et al., 1997). Thus, these data corroborates that the KI-$NaNO_3$/H_2SO_4 system produces specifically NO, while the NPS system, beyond NO, gives raise, the $OH^\bullet$.

Our results confirmed that NO-luminol-H_2O_2 by CL reaction is a fast, sensitive and specific method to measure NO levels in chemical analyses, since our results are similar to those from previous studies, corroborating that the detected specie in the luminol-H_2O_2 system is NO, resulting in other light emission species as previous described by Kikushi et al. (1993), Radi et al. (1993), Noronha Dutra et al. (1993), and Di Mascio et al. (1994).

Based on these characteristics we applied this technique to evaluate NO levels in fresh and frozen biological samples (mouse dorsal skin and rat gastrocnemius muscle).

Degasification with N_2 for biological samples demonstrated to be an important step, as it is associated to sample stability. In muscle homogenates, only 60 minutes after the degasification with N_2 bubbling (during 10 minutes) was observed significant reduction (55%, data not showed) of light emission in CL curves generates by NO-

luminol-H_2O_2 system. On the other hand, when muscle homogenates were saturated with oxygen the photon emission immediately decreased (almost 87%, data not showed), this result was similar to previous reported by Archer et al. (1995). Although the apparent stability supplied by N_2, all experiment we performed immediately after degasification.

In biological analyses, we conclude that NO can be measure by NO luminol-H_2O_2 CL method in either fresh or frozen (skin, muscle samples) once it generates similar curves profiles. The photon emission curves profile for biological samples were similar to that presented by Kikuchi et al. (1993) using NO gas (1μM). For skin samples, we observed a linear photon emission increase according to tissue concentration in the sample solution (range 0.05 – 0.5 mg/ml).Concentrations higher than 1 mg of tissue/ml presented a quencher response, inhibiting the light emission (seem as a lower curve profile) due the excessive NO, a known quenching specie (Kikuchi et al., 1993 A).

The same inhibitors previous used were employed in biological samples aiming to verify if the NO-luminol-H_2O_2 should present the same behavior observed in the chemical systems. All data obtained from reactive species inhibitors reinforces that photon emission in biological samples originates from NO. Histidine added to the biological samples inhibited partially the light emission indicating the involvement of $^1O_2$, while for both NO donors was observed a complete inhibition of light emission. When SOD was used, biological samples exhibited mild reduction of photon emission at the initial portion of the curve. Our data is similar to that reported by Kikuchi et al. (1993 A), when the basal level of chemiluminescence by luminol-H_2O_2 was slightly lowered by SOD. However, during the course of the light emission we detected that SOD increased the photon emission to biological samples (data not shown), as observed

in the NO chemical donors in this study. The use of mannitol in biological samples also revealed the absence of $OH^{\bullet}$ participation in CL reaction, as observed for NO donor KI-$NaNO_3/H_2SO_4$. For O_2^{-} and $OH^{\bullet}$, similar results were reported by Kikuchi et al. (1993).

This work used for the first time in the NO- luminol-H_2O_2 CL system the specific NO scavenger cPTIO, reported as an efficient NO quencher by Ederli et al 2009. cPTIO inhibited photon emission from biological samples in a dose dependent manner, as observed for chemical donors. This result confirms that the object of analysis in luminol-H_2O_2 CL system is in fact NO, even for biological samples. This specificity was previous reported by Kikushi et al. (1993), when the authors related that nitrogen-containing compounds (organic nitrite, organic nitrate, and thio-nitroso compounds), and endothelium-derived compounds do not interfere in the reaction. We did not detect any emission in nitrite containing solution using the luminol-H_2O_2 CL system (data not shown).

In the present study we showed the application of this technique in the pathophysiological experimental models (ischemia-reperfusion and cachexia), using fresh and frozen rat gastrocnemius muscle samples. In these studies we observed differences in NO levels when the experimental groups were compared to respective controls. These differences can be associated with inflammatory process that is involved in both experimental models (Zamiani et al. 2005; Guarnier et al. 2010). Previously, using the same CL system, our group were able to identify significant differences in NO levels of the skin samples from mice submitted to UVB irradiation, returning to control levels when animals were treated (i.p) with NOS inhibitors (Terra et. al., 2012 A; Terra et. al., 2012 B).

In conclusion, the measure of NO levels in biological samples by a specific and sensitive NO- H_2O_2-luminol CL method presents important advantages, such as a short time of execution, and ability to detect NO level from small amounts of samples at very low NO concentrations. The most important contribution of our work is to show that this CL system can be used to NO detection in fresh and frozen samples from different tissues, expanding the use of this method for the investigation of NO pathophysiological role in different type of samples and diseases.

Acknowledgements

The authors are grateful to Jesus Antonio Vargas for his excellent technical assistance and CAPES and Fundação Araucária for providing the financial support.

References:

Anayda-Prado R, Toledo-Pereira L, Lentsch AB, Ward PA. Ischemia/reperfusion injury. J. Sur. Res. (2002), 105, 248-258.

Archer S. Measurement of nitric oxide in biological models FASEB J. (1993) 7 349–60.

Archer SL, Shultz PJ, Warren JB, Hampl V, Demaster EG. Preparation of standarts and measurement of nitric oxide, nitroxyl and related oxidation products. Methods 7 (1995) 21-34.

Arnold WP, Longnecker DE, Epstein RM. Photodegradation of sodium nitroprusside: biologic activity and cyanide release. 61(3) (1984) 254-60

Al-Sa'doni H, Ferro A. S-Nitrosothiols: a class of nitric oxide-donor drugs. Clin Sci (Lond). 98 (5) (2000) 507-20.

Barreiro E, De La Puente B, Busquets S, Lopes-Soriano FJ, Gea J, Argiléz JM. Both oxidative and nitrosative stress are associated with muscle wasting in tumour-bearing rats. FEBS Letters. 529 (7) (2005)1646-1652.

Barker JE, Knight KR, Romeo R, Hurley JV, Morrison WA, Stewart AG. Targeted disruption of the nitric oxide synthase 2 gene protects against ischemis/reperfusion injury to skeletal muscle, J. Pathol. 194 (2001), 109-115.

Bates J N. The study of biological nitric oxide Neuroprotocols 1 (1992) 99–107.

Blebea J, Bacik B, Strothman G, Myatt L. Decreased nitric oxide production following extremity ischemia and reperfusion, Am. J. Surg. 172 (1996), 158-161.

Clancy R M, Miyazaki Y, Cannon PJ. Use of thionitrobenzoic acid to characterize the stability of nitric oxide in aqueous solutions and in porcine aortic endothelial cell suspensions Anal. Biochem. 191 (1990) 138–43

Concannon MJ, Kester CG, Welsh CF. Patterns of free radical production after tourniquet ischemia: implications for the hand surgeon, Plast. Reconstr. Surg. 89 (1992), 846-852.

Cordeiro P.G, Santamaria E, Hu QY.Use of a nitric oxide precursor to protect pig myocutaneous flapsfrom ischemia-reperfusion injury, Plast. Reconstr. Surg. 102 (1998), 2040-2049.

Ederli L, Reale L, Madeo L et al. NO release by nitric oxide donors in vitro and in planta. Plant Physiol Biochem 47 (2009) 42-48.

Frank MJ, Jhnson JB, Rubin SH: Spectrophotometric determination os sodium nitroprusside and its photodegradation products. J. Pharm. Sci. 65 (1976) 44-8.

Guarnier FA, Cecchini AL, Suzukawa AA, et al., Time course of skeletal muscle loss and oxidative stress in rats with Walker 256 solid tumor, Muscle Nerve 42 (2010) 950–958.

Griess, P. Bemerkungen zu der abhandlung der H.H. Weselsky und Benedikt. "Ueber einige azoverbindungen." Chem. Ber. 12 (1879) 426–8. 4.

Greenberg SS, Xie J, Spitzer JJ, Wang JF, J, Lancaster J, Grisham MB, Powers DR, Giles TD. Nitro containing L-arginine analogs interfere with assays for nitrate and nitrite, Life Sciences 57 (1995), 1949-1961.

Hakim T.S.; Sugimori K.; Camporesi E.M.; Anderson G. Half-life of nitric oxide in aqueous solutions with and without haemoglobin. Physiol. Meas. **1996**, 17, 267–277.

Hallstrom S, Gasser H, Neumayer C, Fugl A, Nanobashvili J, Jakubowski A, Huk I, Schlag G, Malinski T. S-nitroso human serum albumin treatment reduces ischemia/reperfusion injury in skeletal muscle via nitric oxide release, Circulation 105 (2002), 3032-3038.

Huk I, Nanobashvili J, Orljanski W. L-arginine treatment in ischemia/reperfusion injury, Cas. Lek. Cesk. 137 (1998), 496-499.

Ignarro LJ. Biosynthesis and metabolism of endothelium-derived nitric oxide. Annu. Rev. Pharmacol. Toxicol. 30 (1990) 535-560.

Ignarro L J, Fukuto J M, Griscavage J M, Robers N E and Byrns R E 1993 Oxidation of nitric oxide in aqueous solution to nitrite but not nitrate: comparison with enzymatically formed nitric oxide from L-arginine Proc.Natl. Acad. Sci., USA 90 8103–07.

Khanna A, Cowled PA, Fitridge RA. Nitric oxide and skeletal muscle reperfusion injury: current controversies. Research Review, J. Surg. Res. 128 (2005) 98-107.

Kikuchi K, Nagano T, Hayakawa H et al. Detection of nitric oxide production from a perfused organ by a luminol-H202 system. Anal Chem, 65 (1993 A) 1794-99.

Kikuchi K, Nagano T, Hayakawa H et al. Real time measurement of nitric oxide produced ex vivo by luminol-H202 chemiluminescence method. J Biol Chem, 268 (1993 B) 23106-110.

Kozlov AV, Sobhian B, Costantino G, Nohl H, Redl H, Bahrami S. Experimental evidence suggesting that nitric oxide diffuses from tissue into blood but not from blood into tissue, Biochim. Biophys. Acta 1536 (2001), 177-184.

Kanno S, Lee PC, Zhang Y, Ho C, Griffith BP, Shears LL 2nd, Billiar TR. Attenuation of myocardial ischemia/reperfusion injury by superinduction of inducible nitric oxide synthase, Circulation 101 (2000), 2742-2748.

Kojima H, Kikuchi K, Hirobe M, Nagano T. Real-time measurement of nitric oxide production in rat brain by the combination of luminol-H_2O_2 chemiluminescence and microdialysis, Neurosci. Lett. 233 (1997) 157-159.

Knight KR, Zhang B, Morrison WA, Stewart AG. Ischemia-reperfusion injury in mouse skeletal muscle is reduced by N-omega-nitro-L-arginine methyl ester and dexamethasone, Eur. J. Pharmacol. 332 (1997), 273-278.

Joneschild ES, Chen LE, Seaber AV, Frankel ES, Urbaniak JR. Effect of a NOS inhibitor, L_NMMA, on the contractile function of reperfused skeletal muscle, J. Reconstr. Microsur. 15 (1999), 55-60.

Lefer DJ, Jones SP, Girod WG, Baines A, Grisham MB, Cockrell AS, Huang PL, Scalia R. Leucocyte-endothelial cell interactions in nitric oxide synthase-deficient mice, Am. J.Physiol. 276 (1999), H1943-H1950.

Liu K, Chen L-E, Seaber AV, Urbaniak JR. S-nitroso-N-acetylcysteine protects skeletal muscle against reperfusion injury, Microsurgery 18 (1998), 299-305.

Laver J.R., Stevanin T.M., Read R. Chemiluminescence quantification of NO and its derivatives in Liquid Samples. Methods in Enzymology, 436 (2008), 113-127.

Di Mascio P, Bechara EJH, Medeiros MHG, Briviba K, Sies H. Singlet molecular oxygen production in the reaction of peroxynitrite with hydrogen peroxide. FEBS LETT, 355 (1994), 287-289.

Messina A,Knight KR, Dowsing BJ, Zhang B, Phan LH, Hurley JV, Morrison WA, Stewart AG. Localization of inducible nitric oxide synthase to mast cells during ischemia/reperfusion injury of skeletal muscle, Lab. Invest. 80 (2000), 423-431.

Mowbray M, McLintock S, Weerakoon R et al. Enzyme-independent NO stores in human skin: quantification and influence of UV radiation. J Invest Dermatol, 129 (2009) 834-842.

Murphy ME, Sies H. Reversible conversion of nitroxyl anion to nitric oxide by superoxide dismutase. Proc Natl Acad Sci USA, 88 (1991) 10860-10864.

Nanobashvili J, Neumayer C, Fuegl A, Punz A, Blumer R, Mittlbock M, Prager M, Polterauer P, Dobrucki LW, Huk I, Malinski T. Combined L-arginine and antioxidative vitamin treatment mollifies ischemia-reperfusion injury of skeletal muscle, J. Vasc. Surg. 39 (2004), 868-877.

Nakamura K, Yokoyama K, Itoman M. Changes in nitric oxide, superoxide, and blood circulation in rabbit rectus femoris muscle. Scand. J. Plast. Reconstr. Surg. Hand Surg. 35 (2001), 13-18.

Nagase S, Takemura K, Ueda A, Hirayama A, et al. A novel nonenxymatic pathway for the generation of nitric oxide by the reaction of hydrogen peroxide and D- or L-arginine, 233 (1997) 150-153.

Nathan C. Nitric oxide as a secretory product of mammalian cells FASEB J. 6 (1992) 3051–64

Noronha-Dutra AA, Epperlein MM, Woolf N. Reaction of nitric oxide with hydrogen peroxide to produce potentially cytotoxic singlet oxygen as a model for nitric oxide-mediated killing. FEBS Lett; 1 (1993) 59-62.

Ozaki M, Kawashima S, Hirase T, Yamashita T, Namiki M, Inoue N, Hirata Ki K, Yokoyama M. Overexpression of endothelial nitric oxide synthase in endothelial cells is protective against ischemia-reperfusion injury in mouse skeletal muscle, Am. J. Pathol. 160 (2002), 1335-1344.

Radi R, Cosgrove T, Beckman JS, et al. Peroxynitrite-induced luminol chemiluminescence. Biochem J; 290 (1993): 51-57.

Rauhala P, Khild A, MohanaKumar P, Chiurn CC. Apparent role of Hydroxyl radicals in oxidative brain injury by sodium nitroprusside. Free Rad. Biol. Med. 24 (1998) 1066-1073, 1998.

Stankevicius E, Kevelaitis, E, Vainorius E, et al. Role of nitric oxide and other endothelium-derived factors. Med, 39 (2003) 4.

Terra VA, Souza-Neto FP, Pereira RC, Silva TNX, Costa ACC, Cecchini R, Cecchini AL. Time-dependent reactive species formation and oxidative stress damage in the skin after UVB irradiation. J. Photochem. Photob. B. 109 (2012 A) 34–41.

Terra VA, Souza-Neto FP, Pereira RC, Silva TNX, Ramalho LNZ, Cecchini R, Cecchini AL. Nitric oxide is responsible for oxidative skin injury and modulation of cell proliferation after 24h of UVB exposure. Free Rad. Res. 46 (2012 B) 872-82.

Tsukada Y, Yasutakea M, Jiab D et al. Real-time measurement of nitric oxide by luminol-hydrogen peroxide reaction in crystalloid perfused rat heart. Life Sci, 72 (2003) 989–1000.

Yavuz D, Kuçukkaya B, Haklar G, et al. Effects of captopril and losartan on lipd peroxidation, protein oxidation and nitric oxide release in diabetic rat kidney. Prostaglandins, Leukot. Essent. Fatty Acids. 69 (2003) 223-227.

Wang L, Liu W, Parker SH, Wu S. Nitric oxide synthase activation and oxidative stress, but not intracellular zinc dyshomeostasis, regulate ultraviolet B light-induced apoptosis. Life Sci, 86 (2010) 448–54.

Wink D A, Darbyshire J F, Nims R W, Saavedra J E, Ford P C. Reactions of the bioregulatory agent nitric oxide in oxygenated aqueous media: determination of the kinetics for oxidation and nitrosation by intermediates generated in the NO/O2 reactions Chem. Res. Toxicol. 6 (1993) 23–7.

Zhang B, Knight KR, Dowsing B, E. Guida E, Phan LH, Hickey MJ, Morrison WA,Stewart AG, Timing administration of dexamethasone or the nitric oxide synthase inhibitor, nitro-L-arginine methyl ester, is critical for effective treatment of ischaemia-reperfusion injury to rat skeletal muscle, Clin. Sci. 93 (1997), 167-174.

Zimiani K, Guarnier FA, Miranda H.C, Watanabe MAE, Cecchini R. Nitric oxide mediated oxidative stress injury in rat skeletal muscle subjected to ischemia/reperfusion as evaluated by chemiluminescence. Nitric Oxide Volume 13, Issue 3, November 2005, Pages 196–203

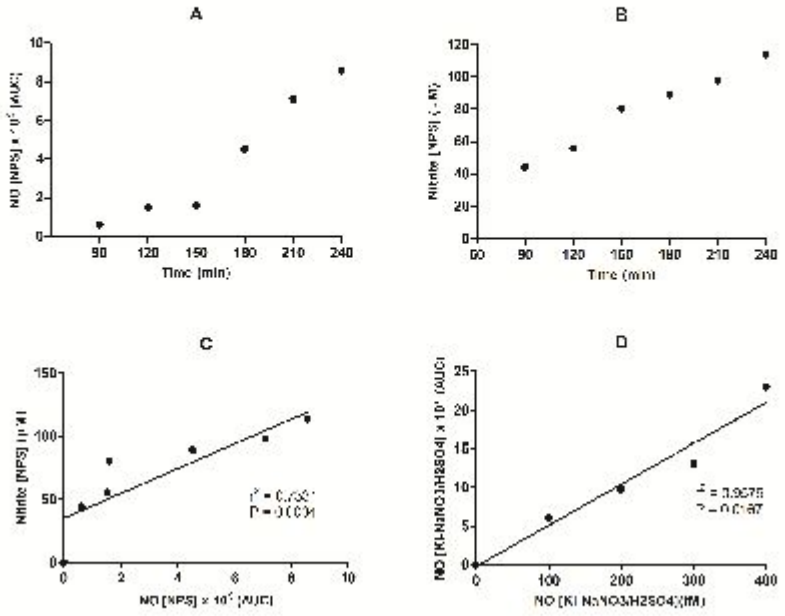

Fig. 1

Figure 1 – Samples of NPS 200 µM solution irradiated during 240 minutes and aliquots collected at each 30 minutes. (A) NO levels by NO-luminol-H_2O_2 chemiluminescence (CL) reaction estimated by area under the CL curves (AUC). (B) Nitrite concentrations (µM) were estimated by Griess reaction. (C) Correlation between nitrite concentration (µM) and area under the CL curves (AUC) (r^2=0.7331). (D) Linear correlation between NO concentration (100fM to 400 fM) by NO-luminol-H_2O_2 CL reaction and AUC of the CL curves (r^2 = 0.0167). Pearsons'correlation. P<0.05.

25

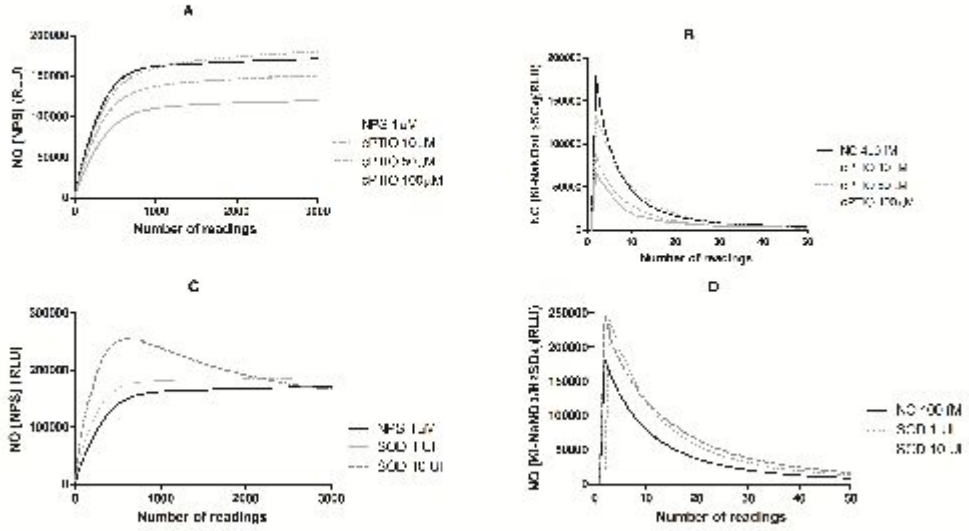

Fig.2

Figure 2 – Chemical systems (NPS and KI-$NaNO_3$/H_2SO_4 systems), of NO by luminol-H_2O_2- induced chemiluminescence. Effect of NO inhibitor (cPTIO 10uM 50uM 100uM) (A, B) and the SOD (10UI 20UI) on NO production (C, D). Relative light units (RLU). Results are mean of three replicates.

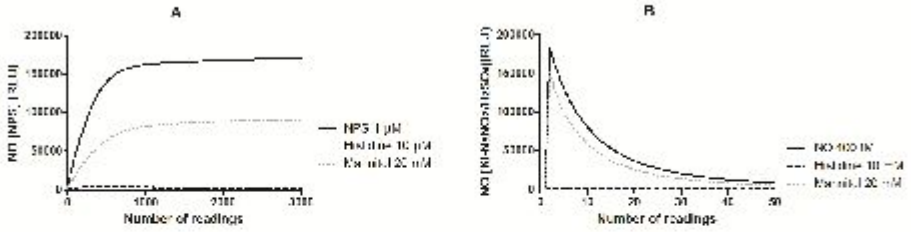

Fig. 3

Figure 3 – Chemical analysis (NPS and KI-$NaNO_3$/H_2SO_4 systems) of NO by luminol-H_2O_2-induced chemiluminescence. (A, B) Effect of singlet oxygen scavenger (histidine) and hydroxyl radical scavenger (mannitol) on NO production. Relative light units (RLU). Results are mean of three replicates.

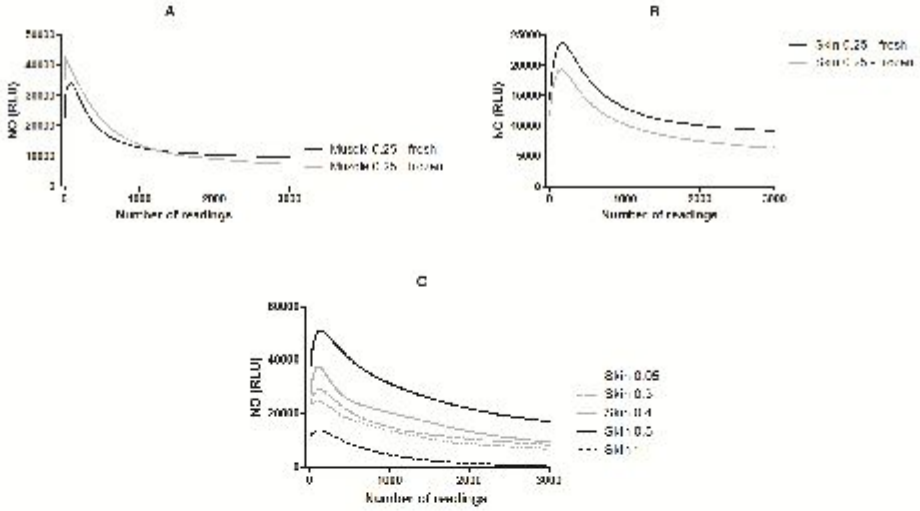

Fig. 4

Figure 4 (A B) NO levels by luminol-H_2O_2-induced chemiluminescence in fresh and frozen biological samples (mouse dorsal skin and rat gastrocnemius muscle – 0.25 mg tissue/ml). (C) Linear increases of light emission (RLU) in skin samples (0.05 to 0.5 mg tissue/ml). Concentrations higher than 1 mg of tissue/ml not showed linear increases of light emission (RLU). Results are mean of three replicates.

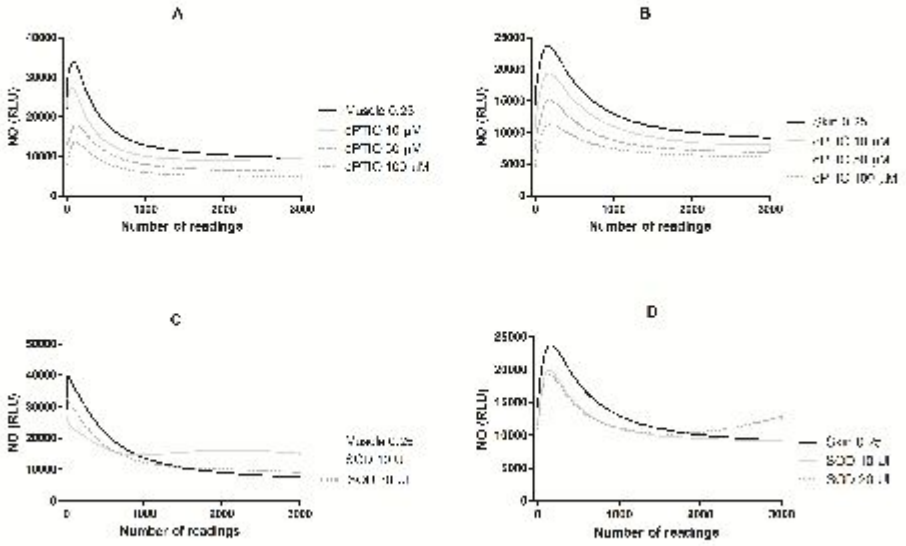

Fig. 5

Figure 5 (A) Biological analysis (mouse dorsal skin and rat gastrocnemius muscle) of NO by luminol-H_2O_2-induced chemiluminescence. Effect of NO inhibitor (cPTIO 10uM 50uM 100uM) (A, B) and the SOD (10 UI, 20 UI) on NO production (C, D). Relative light units (RLU). Results are mean of three replicates.

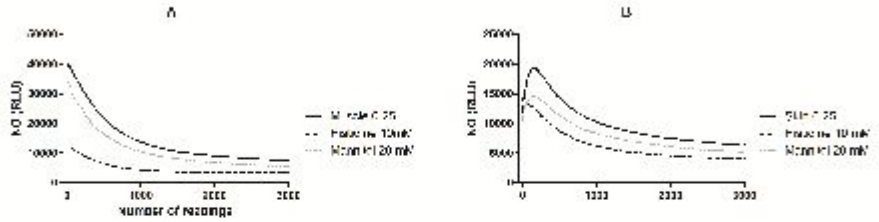

Fig. 6

Figure 6 Biological analysis (mouse dorsal skin and rat gastrocnemius muscle) of NO by luminol-H_2O_2-induced chemiluminescence. (A, B) Effect of singlet oxygen scavenger (histidine) (A, B) and hydroxyl radical scavenger (mannitol) on NO production. Relative light units (RLU). Results are mean of three replicates.

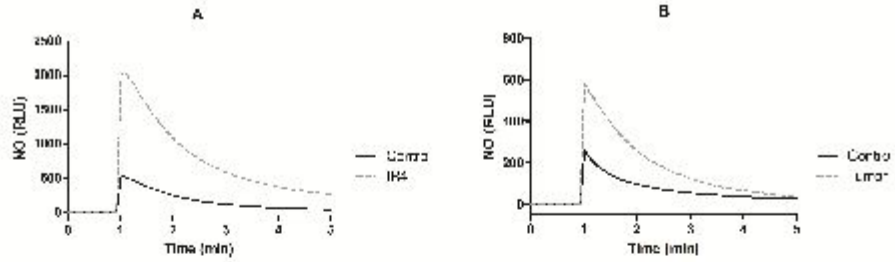

Fig. 7

Figure 7 NO levels by luminol-H_2O_2-induced chemiluminescence in pathophysiological studies. (A) Comparison of chemiluminescence curves obtained from muscle homogenates of control (sham group) and IR4 group (4h ischemia following 4h reperfusion). Control (n = 9), IR4 (n = 15). (B) Comparison of chemiluminescence curves obtained from muscle homogenates of control (sham group) and tumor (Walker-256 tumor-induced cachexia). Control (n=6); Tumor (n=9). RLU: Relative light unit.